SOFT-SWITCHED DC-DC CONVERTER CONFIGURATIONS FOR LED LIGHTING APPLICATIONS

A Thesis

Submitted in partial fulfilment of the requirements

for the award of the degree of

DOCTOR OF PHILOSOPHY

IN

ELECTRICAL ENGINEERING

by

Ch Kasi Ramakrishnareddy

(Roll No. 714117)

Supervisor

Dr. S Porpandiselvi

Assistant Professor

Co-Supervisor

Dr. N Vishwanathan

Professor

DEPARTMENT OF ELECTRICAL ENGINEERING

NATIONAL INSTITUTE OF TECHNOLOGY

WARANGAL – 506004, TELANGANA STATE, INDIA

MARCH-2019

APPROVAL SHEET

This Thesis entitled "**Soft-Switched DC-DC Converter Configurations for LED Lighting Applications**" by **Ch Kasi Ramakrishnareddy** is approved for the degree of Doctor of Philosophy

Examiners

_____

_____

_____

Supervisor

Dr. S Porpandiselvi
Assistant Professor
EED, NIT Warangal

Co-Supervisor

Dr. N Vishwanathan
Professor
EED, NIT Warangal

Chairman

Dr. S Srinivasa Rao
Professor & Head,
EED, NIT Warangal

Date: _____

DEPARTMENT OF ELECTRICAL ENGINEERING
NATIONAL INSTITUTE OF TECHNOLOGY
WARANGAL – 506 004

DEPARTMENT OF ELECTRICAL ENGINEERING

NATIONAL INSTITUTE OF TECHNOLOGY WARANGAL

CERTIFICATE

This is to certify that the thesis entitled **"Soft-Switched DC-DC Converter Configurations for LED Lighting Applications"**, which is being submitted by **Mr. Ch Kasi Ramakrishnareddy** (Roll No. 714117), is a bonafide work submitted to National Institute of Technology, Warangal in partial fulfilment of the requirement for the award of the degree of **Doctor of Philosophy** in Department of Electrical Engineering. To the best of my knowledge, the work incorporated in this thesis has not been submitted elsewhere for the award of any degree.

Co-Supervisor

Dr. N Vishwanathan
Professor
Department of Electrical Engineering
National Institute of Technology
Warangal – 506004

Supervisor

Dr. S Porpandiselvi
Assistant Professor
Department of Electrical Engineering
National Institute of Technology
Warangal – 506004

DECLARATION

This is to certify that the work presented in the thesis entitled "**Soft-Switched DC-DC Converter Configurations for LED Lighting Applications"** is a bonafide work done by me under the supervision of **Dr. S Porpandiselvi and Prof. N Vishwanathan**, Department of Electrical Engineering, National Institute of Technology, Warangal, India and was not submitted elsewhere for the award of any degree.

I declare that this written submission represents my ideas in my own words and where others ideas or words have been included; I have adequately cited and referenced the original sources. I also declare that I have adhered to all principles of academic honesty and integrity and have not misrepresented or fabricated or falsified any idea/data/fact/source in my submission. I understand that any violation of the above will be a cause for disciplinary action by the institute and can also evoke penal action from the sources which have thus not been properly cited or from whom proper permission has not been taken when needed.

Signature:

Name: **Ch Kasi Ramakrishnareddy**

Roll.No: **714117**

Date:

Place: Warangal

ACKNOWLEDGEMENTS

It gives me immense pleasure to express my deep sense of gratitude and thanks to my supervisors **Dr. S Porpandiselvi,** Assistant Professor and **Prof. N Vishwanathan,** Professor, Department of Electrical Engineering, National Institute of Technology Warangal, for their valuable guidance, support and suggestions. Their knowledge and guidance helped me to become a capable researcher. They have shown me the interesting side of this wonderful and potential research area. Their encouragement helped me to overcome the difficulties encountered in my research.

I am very much thankful to **Prof. S Srinivasa Rao**, Head, Department of Electrical Engineering for his constant encouragement and support.

I wish to express my sincere thanks to **Prof. N V Ramana Rao**, Director, NIT Warangal for his support and encouragement.

I take this privilege to thank all my Doctoral Scrutiny Committee members, **Dr. B L Narasimha Raju**, Associate Professor, Department of Electrical Engineering, **Dr. A Kirubakaran,** Assistant Professor, Department of Electrical Engineering and **Dr. V Venkata Mani**, Associate Professor, Department of Electronics and Communication Engineering for their constructive suggestions and advices during the progress of this research work.

I also appreciate the encouragement from teaching, non-teaching members, and fraternity of Department of Electrical Engineering of NIT Warangal.

I convey my special thanks to Research Scholars Mr. U Ramanjaneya Reddy, Mr. T Kiran, Mr. M Hareesh, Mr. T Ratna Rahul, Mr. M Santhose, Mr. B Kiran Babu, Mr. K Vijaybabu, Miss. D Mounika, Mr. M Vishnu Prasad, Mr. B Anil Kumar, Mr. B Durga Harikiran, Mr. O V S R Vara Prasad, Mr. Venu Sonti, Mr. V V K Satyakar, Mr. K Hemasundar Rao, Mr. A Pranay Kumar, Mr. and B Srinivasa Reddy (Mechanical).

I acknowledge my gratitude to all my teachers and colleagues at various places for supporting and co-operating me to complete the work.

My heartfelt gratitude and indebtedness are due to my parents Shri. Ch Onnur Reddy & Smt. Ch Venkata Subbamma, my wife Ch Vasantha and my children Ch Joshika & Ch Chatvik for their sincere prayers, blessings, constant encouragement, shouldering the responsibilities

and moral support rendered to me throughout my life, without which my research work would not have been possible. My heartily gratitude to my brother Siva Kasireddy Ch and my sister Sharada K. I heartily acknowledge all my relatives for their love and affection towards me.

Above all, I express my deepest regards and gratitude to "**ALMIGHTY**" whose divine light and warmth showered upon me the perseverance, inspiration, faith and enough strength to keep the momentum of work high even at tough moments of research work.

Kasi Ramakrishnareddy Ch

ABSTRACT

Globally, about 19 % of total electrical energy produced is used for lighting applications. Hence lighting loads have significant potential for improving energy efficiency and cost savings. In view of this, energy efficient lighting sources need to be developed. The light emitting diode (LED) is becoming a promising lighting source over conventional lighting sources for a future generation due to its various advantages such as high luminous efficacy, long life, solid state characteristic, compactness, ease of controllability and eco-friendliness etc.

LED lighting systems require constant current regulators to produce constant illumination. These regulators must provide the features such as high efficiency, LED load current regulation, dimming control, compact size, high reliability etc. Despite the availability of several converter configurations and control techniques, there is enough scope for further research in making a compact LED power driver with reduced component count, high efficiency and dimming control to suit various application needs. This thesis work focuses on soft-switched DC-DC converters for LED lighting applications.

This thesis proposes four LED driver circuit configurations. The objectives are to provide high power conversion efficiency, reduced device current, powering of multiple lighting loads with dimming, zero-voltage switching, reduced size of reactive elements, driving LED lamps of different power ratings, regulation of LED lamp current against input voltage variations and configurations suitable for high power lighting application.

The first proposed converter configuration comprises of a full-bridge topology with soft switching inductor. It is powering four LED lamps of same rating. Regulation of LED lamp current against input voltage variations is achieved using a buck-boost topology at the input side. This configuration also provides PWM dimming control of all the LED lamps. It offers zero voltage switching in devices of the bridge circuit. In this configuration, switches of the bridge circuit carry a small current which is almost independent of LED lamp currents. Hence conduction losses are reduced. This configuration provides high efficiency at both full illumination and during dimming operation. It provides an efficiency 93.88% at full illumination level. This configuration also provides reduced components count per lamp and hence reduction in cost. This configuration can be extended to multiple LED lamps by addition of legs in bridge. This configuration is suitable for street lighting as well as domestic lighting applications.

The second proposed converter configuration consists of a full bridge topology with multi-phasing technique for ripple free current. It powers two LED lamps of same rating. It provides ripple free currents through two LED lamps. In this configuration, power processed through bridge circuit is less and hence the losses are reduced. This configuration provides current cancellation, which reduces current stress of the devices. This further reduces the conduction losses. Zero-voltage switching is obtained in bridge circuit devices. This configuration provides high efficiency at both full illumination and during dimming operation. It provides an efficiency of 94.26% at full illumination level. This configuration can be extended to multiple LED lamps by addition of legs in bridge. This configuration is suitable for street lighting as well as domestic lighting applications. This configuration allows use of small value of inductor and hence reduces size and cost. This configuration also provides PWM dimming operation and regulation of LED lamp current.

The third proposed converter configuration consists of a three leg resonant converter. This configuration is powering two LED lamps of different power ratings. In this configuration, two series resonant circuits with different resonant frequencies are used to power two LED lamps. This circuit operates simultaneously at two different frequencies. This configuration provides regulation of LED lamp currents and independent PWM dimming control of LED lamps. It also provides ZVS operation. This configuration provides high efficiency at both full illumination and during dimming operation (>91%).

The fourth proposed converter configuration consists of a full bridge resonant converter. This configuration is powering single LED lamp of high power rating. In this configuration, LED lamp is powered by two voltages of different magnitudes derived from series resonant converter. In this configuration, only small controlled power is used for regulating the lamp current which increases the efficiency. This configuration provides ZVS operation and PWM dimming control. This configuration provides high efficiency at both full illumination and during dimming operation (>92%). This topology is suitable for applications where lamp voltages are smaller than supply voltages like dc micro grid applications.

All the above four proposed LED driver configurations provide LED current regulation, low or zero ripple in LED lamp currents, PWM dimming control, ZVS operation and high efficiency. All these proposed configurations are analysed, simulated and experimentally validated.

Contents

List of Figures

List of Tables

Abbreviations

AC	Alternating current
AM	Amplitude modulation
BCM	Boundary conduction mode
BDC	Bi-directional converter
CCM	Continuous conduction mode
CEA	Central electricity authority
CMC	Current mode control
DC	Direct current
DCM	Discontinuous conduction mode
DPWM	Double pulse width modulation
EMI	Electromagnetic interference
ESR	Equivalent series resistance
FFT	Fast fourier transform
GWh	Giga watt-hours
HB	High brightness
HID	High-intensity discharge
HF	High frequency
HFAC	High-frequency alternating current
LED	Light emitting diode
LCD	Liquid crystal display
LF	Low frequency
MOSFET	Metal-oxide-semiconductor field-effect transistor
PCM	Pulse-code modulation
PDS	Power distribution system
PF	Power factor
PFC	Power factor correction
PSBCM	Phase shifted boundary conduction mode
PV	Photovoltaic
PWM	Pulse width modulation
S-type	Switched mode
S1	Single-stage

S2	Two-stage
S2A	Two-stage type-A
S2B	Two-stage type-B
S3	Three-stage
THD	Total harmonic distortion
UV	Ultraviolet
VI	Variable inductor
ZCS	Zero current switching
ZVS	Zero voltage switching

List of symbols

α_h	Phase angle in HF resonant circuit
α_l	Phase angle in LF resonant circuit
Δi_{L1}	Ripple current in inductor (L_1)
Δi_{L2}	Ripple current in inductor (L_2)
Δi_{L3}	Ripple current in inductor (L_3)
C_{r1}	High frequency resonant capacitor
C_{r2}	Low frequency resonant capacitor
C_{01}	Output filter capacitor-1
C_{02}	Output filter capacitor-2
D	Duty ratio of S_1-S_4
f_h	High switching frequency
f_l	Low switching frequency
f_s	Switching frequency
f_0	Resonant frequency
$f_{0,1}$	High resonant frequency
$f_{0,2}$	Low resonant frequency
i_{d1}	Switch (S_1) current
i_{d2}	Switch (S_2) current
i_{d3}	Switch (S_3) current
i_{d4}	Switch (S_4) current
i_{Laux}	Auxiliary inductor current
$i_{Laux(peak)}$	Peak current in auxiliary inductor
i_{Lr}	Inductor (L_r) current
$i_{Lr\text{-}pk}$	Peak current in inductor (L_r)
i_{L1}	Inductor (L_1) current
i_{L2}	Inductor (L_2) current
i_{L3}	Inductor (L_3) current
i_{L4}	Inductor (L_4) current
i_r	Resonant frequency
i_{r1}	High resonant frequency
i_{r2}	Low resonant frequency

I_0	Lamp output current
I_{01}	Lamp-1 output current
I_{02}	Lamp-2 output current
I_{03}	Lamp-3 output current
I_{04}	Lamp-4 output current
L_{aux}	Auxiliary inductor
L_{r1}	High frequency resonant inductor
L_{r2}	Low frequency resonant inductor
L_0	Output filter inductance
n	Turns ratio
Q	Quality factor of resonant circuit
Q_1	Quality factor of HF resonant circuit
Q_2	Quality factor of LF resonant circuit
R_{ac}	Equivalent ac resistance
R_{ac1}	Equivalent ac resistance-1
R_{ac2}	Equivalent ac resistance-2
R_{LED}	Resistance offered by LED lamp
R_{LED1}	Resistance offered by LED lamp-1
R_{LED2}	Resistance offered by LED lamp-2
S_{dim}	PWM dimming signal
S_{dim1}	PWM dimming signal-1
S_{dim2}	PWM dimming signal-2
t_d	Dead time
T	Switching period
T_h	High switching period
T_l	Low switching period
T_R	Switching period of switch (S_R)
v_{ds1}	Drain to source voltage of S_1
v_{ds2}	Drain to source voltage of S_2
v_{ds3}	Drain to source voltage of S_3
v_{ds4}	Drain to source voltage of S_4
v_{Lr}	Voltage across inductor (L_r)
v_{L1}	Voltage across inductor (L_1)

v_{L2}	Voltage across inductor (L_{2})
v_{L3}	Voltage across inductor (L_{3})
V_C	Buck-boost converter output voltage
V_{DC}	Input DC voltage
V_{DC1}	Input DC source voltage-1
V_{DC2}	Input DC source voltage-2
V_f	Forward voltage drop
V_{gB}	Gate to source voltage of S_B
V_{gd}	Gate to source voltage of S_d
V_{gR}	Gate to source voltage of S_R
V_{gs1}	Gate to source voltage of S_1
V_{gs2}	Gate to source voltage of S_2
V_{gs3}	Gate to source voltage of S_3
V_{gs4}	Gate to source voltage of S_4
V_{gs5}	Gate to source voltage of S_5
V_{gs6}	Gate to source voltage of S_6
V_h	High frequency voltage signal
V_{in}	Bridge input voltage
V_{th}	Threshold voltage
V_1	DC voltage source-1
V_2	DC voltage source-2
V_0	Lamp output voltage
V_{01}	Lamp-1 output voltage
V_{02}	Lamp-2 output voltage
V_{03}	Lamp-3 output voltage
V_{04}	Lamp-4 output voltage

Chapter 1

Introduction

Chapter 1

Introduction

Sustainable development of a nation needs technology and industrial growth which demand energy sources. To meet the energy demand, the governments are prompting the technology developers for promoting the ways for sustainable energy sources. One of the viable solution for energy sustainability is energy saving, which can be achieved by efficient use of electrical energy. Electric lighting is one of the major applications of high energy consumption. The importance of energy efficient lighting sources, drawbacks of conventional lighting sources, LED technology, overview of driver circuits for LED lighting systems, motivation and objectives, contributions of this thesis are presented in this chapter.

1.1 Need for Development of Energy Efficient Lighting Sources

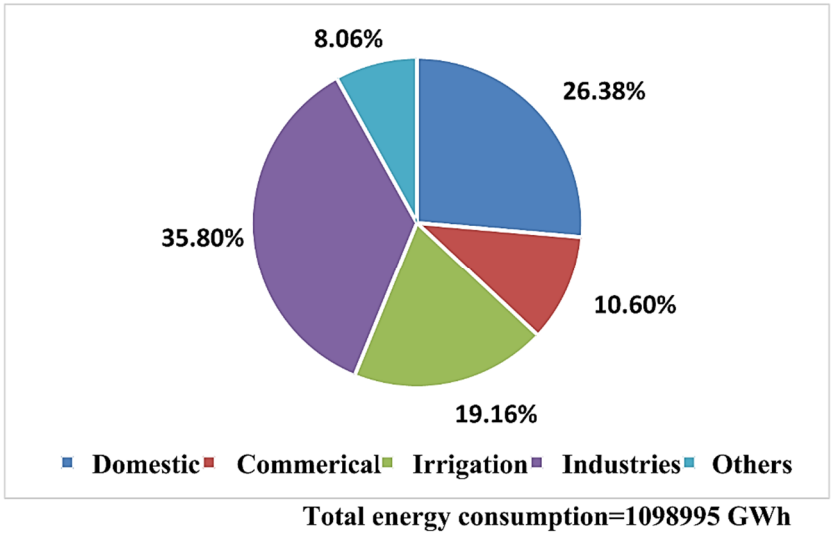

Figure 1.1 Total estimated electricity consumption in 2016-17 in India

Globally, about 19 % of total electrical energy produced is used for lighting applications [1]-[3]. Figure 1.1 depicts the total estimated electricity consumption in 2016-17 in India as per 18th electric power survey which was conducted by central electricity authority (CEA) of India. According to the survey, public lighting consumes about 10,021 GWh and domestic sector electricity consumption is about 2,89,924 GWh, out of it 26 % is accounted for lighting systems. Hence lighting loads have significant potential for improving energy efficiency and cost savings. Energy savings can be achieved either by improving the energy conservation of traditional lighting sources or by reducing the capacity of lighting devices using efficient

products. Usage of efficient products helps in reducing significant amount of energy. In view of this, energy efficient lighting sources need to be developed.

1.2 Conventional Lighting Sources

The first and most common light source is incandescent lamp. It produces light when an electric current is passed through a filament. Incandescent lamps produce yellow color due to the temperature of the filament. They can be turned on and off instantly without additional circuit. These lamps utilize only 10% of electrical energy supplied and remaining is converted into heat, hence surface temperature of incandescent lamps is high. The limitations of incandescent lamps are low luminous efficacy (4-18 lm/W) and short life span (750-2000 hrs).

Fluorescent lamps produce light based on different mechanisms. They use electricity to ionize mercury vapor which emits ultraviolet (UV) light. The phosphor which is coated inside the lamp absorbs UV light and emits visible light. To produce visible light, fluorescent lamps require an additional circuit called ballast. However, luminous efficacy (50-80 lm/W) and life span (5000-8000 hrs) are high compared to incandescent lamps. Further heat produced inside the fluorescent tube is less. The limitation of the fluorescent lamps is that they are not eco-friendly due to the presence of toxic gas.

High-intensity discharge (HID) lamps produce light by means of arc discharge in arc tube which contains electrodes, starting gas, and metal. They are classified as high pressure mercury, metal halide, ceramic metal halide, and high pressure sodium discharge lamps based on the type of gas and metal used in arc tube. HID lamps require current limiting ballast due to negative resistance characteristic of arc discharge. The luminous efficacy (45-150 lm/W) and operating life (20000-30000 hrs) of HID lamps are higher than incandescent and fluorescent lamps. Like fluorescent lamps, HID lamps contain toxic gases.

Conventional lighting sources have less potential to save energy consumption and cost which limit their wide range of potential applications due to their own drawbacks and limitations. Lighting industry needs clean and energy efficient lighting sources to increase energy savings. To make significant developments in the lighting industry, researchers have been putting their contribution to develop alternate lighting sources. In the following section, light emitting diode (LED) technology which is one of this kind is explained in detail.

1.3 LED Technology

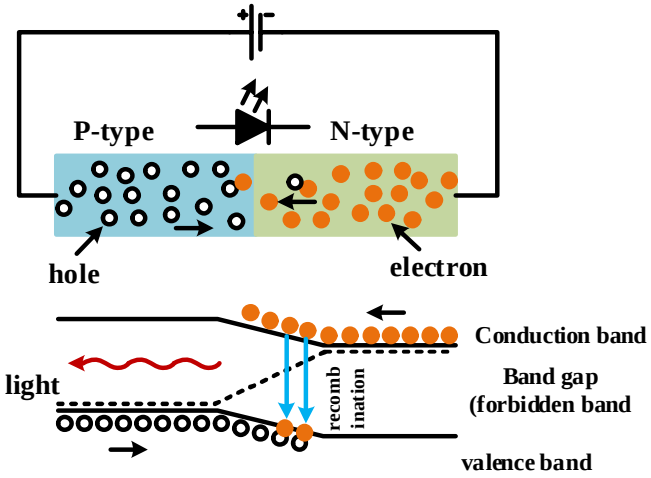

Figure 1.2 Light emission in LED

Light emitting diode (LED) is a semiconductor device which emits light due to electroluminescence. To generate light from an LED, it is fabricated as normal p-n junction diode. The light emission in LED is shown in Figure 1.2. When the LED junction is forward biased, the electrons from n-side cross the junction and recombine with holes. This recombination produces photons. If the wavelength of emitted photons is in visible spectrum, the exposed semiconductor area emits light. The light output from LED depends on the amount of forward current through it. The current rating of high-brightness (HB) or power LEDs ranges from 20 mA to 1500 mA based on illumination level of fabrication technologies used. Power LEDs can be available in two different packages which are single LED fragment and multiple LEDs fragments on single chip. LED transforms more than 90% of electrical energy into light energy when it is forward biased and operation of reverse biased LED is not generally recommended. The materials used in the fabrication of LED determines the emitted light colour. The representation and electrical model of an LED are discussed in the following section.

1.3.1 Equivalent Model of LED

The symbolic representation and its equivalent electrical model of an LED are shown in Figure 1.3. The LED is a device that emits light when a forward dc voltage is applied. The electrical characteristics of an LED are similar to p-n junction diode. Hence Shockley diode equation can be applied to study the electrical characteristics of an LED. According to Shockley diode model, current in LED increases exponentially when the voltage across it is greater than threshold voltage. The typical values of threshold voltage of LED is 2 V to 4 V which depends

on wavelength of emitted light. In high power LEDs ranging from 350 mA to 1500mA, the internal parasitic resistance of LEDs should be considered in modelling of LEDs. Thus an LED is represented by a series connection of a dynamic resistance r_d, an equivalent voltage V_{th} and an ideal diode [4]. The forward voltage across an LED when it conducts is given by

$$V_F = V_{th} + I_F r_d \quad (1)$$

Where V_F is the forward voltage drop across LED, V_{th} is the threshold voltage of LED, r_d is the dynamic resistance of LED, I_F is forward current through LED.

LEDs are current controlled or current driven devices as their forward voltage is almost constant for wide current variations. Since the power output from LED is proportional to current flowing through LED, they must be powered from constant current switching power supplies to get constant illumination. In the following sections, the attractive features of LEDs which make them prominent light sources [5]-[7] and their applications [8]-[10] are discussed.

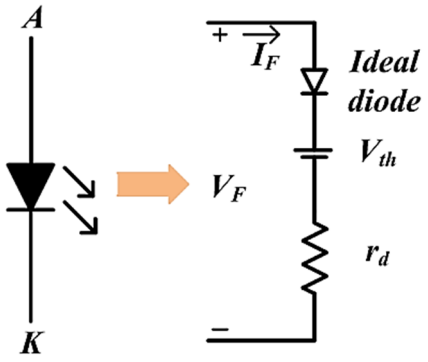

Figure 1.3 Symbol and electrical equivalent model of LED

1.3.2 Advantages and Disadvantages of LED

LED lighting offers advantages and disadvantages:

Advantages:

i. LEDs are energy efficient lighting sources as compared to conventional lighting sources.
ii. The average operating life of LED is around 50,000 hrs. to 1, 00,000 hrs.
iii. LEDs are more reliable due to their solid state characteristic.
iv. They can emit light of different color without using color filters.
v. They do not produce heat.

vi. LEDs are green light sources due to their pollution-free lighting and their emission do not contain harmful substances like in conventional lights.
vii. LEDs can turn ON/OFF instantly and frequent on-off cycling doesn't affect the operation of LEDs. Whereas, the instant switching of conventional lighting system reduces the operating life.
viii. LEDs are compact which reduces the size of lighting equipment.
ix. They can provide wide range of brightness control which further improves energy saving.
x. Sun phantom effect in LEDs is eliminated.
xi. Operation of LEDs requires a very low dc voltage source. Thus, LED based lighting can be powered without using utility ac mains supply also. They can be supplied from the battery or solar PV, and hence suitable for wide range of commercial and industry lighting applications.

LEDs suffer from some limitations also. They are listed as below:

Disadvantages:

i. The initial cost of LEDs is much higher than that of conventional lighting sources and hence LED based lighting systems are more expensive.
ii. LEDs require an efficient driver circuit.
iii. LEDs need proper heat sinks due to temperature dependent characteristics.

1.3.3 Applications of LEDs

LEDs are suitable for wide range of applications due to their several advantages like; energy efficient, high operating life, high brightness, environment friendly nature, and compactness. The applications of LED based lighting are listed as follows.

i. General illumination
ii. Residential lighting
iii. Automotive applications
iv. Street Lighting
v. Signal lighting
vi. Decorative lighting
vii. Liquid crystal display (LCD) panels
viii. Agriculture

ix. Communication applications

x. Biomedical applications

Due to promising features of LED lighting technology, it can make energy sector stronger, reduce greenhouse gas emissions and change global economy. Therefore development of energy efficient LED lighting systems is a current interest of research area in lighting industry. In the following section, the need of driver circuit and different configurations for LED lighting applications are discussed.

1.4 Driver Circuits for LED Lighting

LEDs produce light output when they are forward biased. They require dc voltage sources to produce light output. LEDs are equivalent to constant voltage load. Light output from LEDs is related to their forward current. To get steady illumination, LEDs current must be constant. Hence a constant current regulator must be connected between LED load and the driving source. The current regulator and LED load together is generally called as LED driver circuit which is shown in Figure 1.4. Several types of driver circuits for LED lighting applications have been proposed by different researchers based on the availability of driving sources, such as AC fed LED drivers [11]-[36], DC fed LED drivers [37]-[64] etc. The requirements of AC fed LED drivers and DC fed LED drivers are different. However, high efficiency, LED load current regulation, dimming control, compact size, high reliability etc., are the main requirements to be met by LED driver circuit irrespective of the driving source.

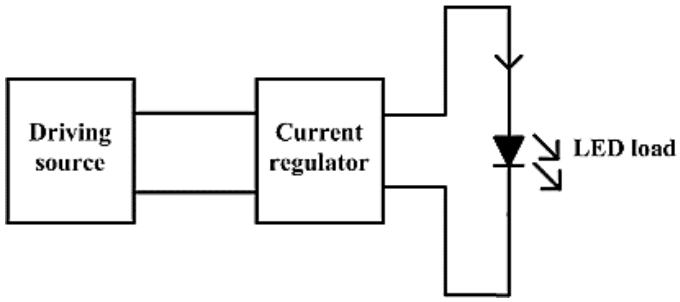

Figure 1.4 Schematic view of LED driver

In AC fed LED drivers, the required constant current is supplied by the utility ac mains supply. They are classified as passive LED drivers and switched mode LED drivers. Passive LED drivers consists of only passive components such as capacitors and inductor. LED loads are supplied with high ac ripple without active control. Hence they are simple, highly reliable, cost-effective and they produce low electromagnetic interference (EMI) [11]-[14]. However,

low power factor (PF), lack of precise current regulation, high source current total harmonic distortion (THD), usage of large electrolytic capacitors and large size of inductors are the limitations of passive LED drivers. On the contrary, switched mode LED drivers overcome the limitations of passive LED drivers due to their high frequency operation. Due to active control of switched mode LED drivers, they achieve high PF, low THD, precise LED load current regulation, high efficiency, dimming control, compactness, isolation between LED load and input etc [15]-[36]. Switched mode LED drivers are further classified as single-stage LED drivers [15]-[24], two-stage LED drivers [25]-[32] and three-stage LED drivers [33]-[36]. In single-stage LED drivers, both PFC and LED load current regulation are achieved with single dc-dc converter. Due to less components, single stage drivers are used in low and medium power lighting applications (<50 W). In two-stage LED drivers, PFC function and LED load current control are performed separately using two dc-dc converters. The performance of two stage drivers is better than single stage drivers. However, two stage drivers are complex and are costly. Hence two stage drivers are applicable for medium and high power lighting applications. In three-stage switched mode LED drivers, stage-1 and stage-2 perform PFC and dc-dc regulation respectively and stage-3 is a post regulator which features dimming control and current equalization in LED strings. Since each stage performs a single function, three stage drivers are mainly suitable for high power lighting applications (>100 W).

In DC fed LED drivers, driving source itself is dc voltage which can be obtained from PV, battery or dc grid. Since the driving input is dc source, PFC stage is not required. In addition, DC fed LED drivers are efficient and more reliable. In DC fed drivers, LED loads are supplied from either linear or switched mode dc-dc converters. The efficiency of switched mode dc-dc converters is high and are more preferred for LED drivers [37]-[39]. Basic isolated and non-isolated dc-dc converters are used for powering LED lighting loads [40]-[52]. Recently, usage of soft-switching converters in LED lighting applications is increasing due to their high efficiency, compactness and low EMI [53]-[64].

1.5 Motivation and Objectives of the Thesis

From the literature review on driver circuits for light emitting diode (LED) lighting applications, the following observations are drawn.

i. Some of the configurations are not capable of providing soft switching feature.
ii. Some of the driver circuits are having high device current or voltage stress.
iii. The size of reactive elements in some of the circuits is high.
iv. Some configurations do not provide regulation of LED lamp current against input voltage fluctuations.
v. Some of the LED drivers are not able to drive multiple lighting loads
vi. Only few circuits are having independent regulation and dimming feature.
vii. Some of configurations are not able to drive LED lamps of different power ratings.
viii. Some of the LED drivers described in literature have certain limitations such as low power conversion efficiency, absence of pulse width modulation (PWM) dimming, regulation of LED lamp current, lack of constant duty operation at constant frequency and not able to support high power LED applications.

Despite the availability of several converter configurations and control techniques, there is enough scope for further research in making a compact LED power driver to suit various application needs.

The proposed research work aims at design and development of DC-DC converter configurations for LED lighting applications with objectives to provide high power conversion efficiency, reduced device current stress, powering multiple lighting loads with dimming, zero-voltage switching, reduction in the size of reactive elements, driving LED lamps of different power ratings, regulate LED lamp current against input voltage variations, design for high power lighting application.

1.6 Contributions

This research work focuses on high efficiency DC-DC converter configurations with low voltage or current stress on switching devices, dimming control and current regulation for LED lighting applications. This necessitates use of soft-switching technique in DC-DC Converter configurations. Four different LED driver configurations have been proposed. These configurations and their features are listed below:

1. **Soft Switched Full-bridge Light Emitting Diode Driver Configuration for Street Lighting Application**

   Features:

   i. High power conversion efficiency
   ii. Reduced device current stress
   iii. Multiple LED lamps with dimming
   iv. Zero-voltage switching
   v. Regulation of LED lamp current against input voltage variations

2. **An Efficient Ripple Free LED Driver with Zero-Voltage Switching for Street Lighting Application**

   Features:

   i. Ripple free current through LED lamp
   ii. ZVS operation
   iii. Reduced device current stress
   iv. Reduction in size of reactive components
   v. High efficiency at full load and dimming operation
   vi. Regulation of LED lamp current against input voltage variations

3. **A Three-leg Resonant Converter for Two Output LED Lighting Application with Independent Control**

   Features:

   i. Capability of driving LED lamps of different power ratings
   ii. Independent lamp current regulation
   iii. Independent illumination control
   iv. High efficiency with zero-voltage switching

4. **An Efficient Full-Bridge Resonant Converter for LED Lighting Application with Simple Current Control**

   Features:

   i. High power conversion efficiency with zero-voltage switching
   ii. Regulation of LED lamp current against input voltage variations
   iii. Dimming operation
   iv. Constant duty cycle operation at constant switching frequency
   v. Possibility of operation from large DC voltage source

1.7 Organization of the Thesis

This thesis is structured into seven chapters. The work presented in the following chapters is summarized as follows.

In Chapter 2, review of the existing LED driver converter topologies and dimming control techniques are presented. The relative merits and demerits of these topologies are also discussed. This motivates for the research work presented in this thesis.

In Chapter 3, soft-switched full bridge configuration has been proposed for LED street lighting application. The circuit operation, analysis and design procedure are explained. Dimming control and current regulation are demonstrated. Simulation and experimental results are presented. Efficiency characteristic is presented.

In Chapter 4, an efficient ripple free LED driver with zero-voltage switching for street lighting application has been proposed. The circuit operating principle, analysis, design considerations, dimming and regulation features are explained. Simulation and experimental results obtained from the prototype are presented. An extension of proposed driver to multiple LED lamps is also presented. Efficiency characteristic is presented

In Chapter 5, a three leg resonant converter has been proposed to drive two LED lamps of different power ratings. Working principle and analysis of proposed configuration are explained. LED lamp current regulation and independent dimming operations are explained. Simulation and experimental results are discussed. Efficiency characteristics are presented.

In Chapter 6, an efficient full-bridge resonant converter with simple current control has been proposed. The circuit operation, analysis and its design procedure are presented. Dimming

control and regulation of lamp are explained. Simulation and experimental results are presented. Efficiency characteristic is presented.

Chapter 7 presents the main conclusions of the thesis and scope for future work in this research area.

Chapter 2

Review of LED Driver Circuits

Chapter 2

Review of LED Driver Circuits

LEDs are being used in number of applications due to their performance indices such as high efficacy, high operating life, solid state characteristic and eco-friendliness. LEDs are dc operated devices and have non-linear voltage-current characteristics like a diode. The illumination level of an LED directly depends upon the forward current through it. In addition, they behave like a constant voltage load with small dynamic resistance. LED output characteristics clearly indicates that a small variation in its output voltage causes significant current variation which changes the lumen output. The variation or fluctuation in the lamp illumination is undesirable. To ensure uniform light output from an LED, it must be powered from constant current regulator which is called as LED driver. This chapter presents an overview of AC fed LED drivers [11]-[36], DC fed driver circuits for LED lighting applications [37]-[64] and LED illumination control methods [68]-[75].

2.1 Classification of LED Driver Circuits

Driver circuits for LED applications can be classified based on the type of the input source namely: 1) AC fed LED drivers and 2) DC fed LED drivers.

2.1.1 AC fed LED drivers

LED lighting loads require regulated constant DC current for producing uniform brightness. In AC fed LED drivers, constant DC current is derived from AC utility line. These drivers are classified as passive LED drivers [11]-[14] and switched mode LED drivers [15]-[36].

2.1.1.1 Passive LED drivers

Passive LED drivers consist of passive components (resistor, capacitor, and inductor/transformer) and diodes. The block diagram representation of passive LED driver is shown in Figure 2.1. They do not have semiconductor switches, associated gate driver and linear or active regulators. Without active control, they supply required dc current for LED load with large ac ripple. In these drivers, output current control function is realized either by lossy or lossless impedance at line frequency or double-line frequency. The limitations of passive LED drivers are low PF, high THD in source current, requirement of large filter capacitor to avoid

flickering due to 100Hz ripple in LED load, large size of inductors, lack of precise output current control against input voltage variations etc. However, high reliability, simple structure, low cost and less electromagnetic interference (EMI) due to absence of high switching frequency operation are key features of passive LED drivers. They are suitable for applications where high priority is given to reliability such as outdoor lighting applications.

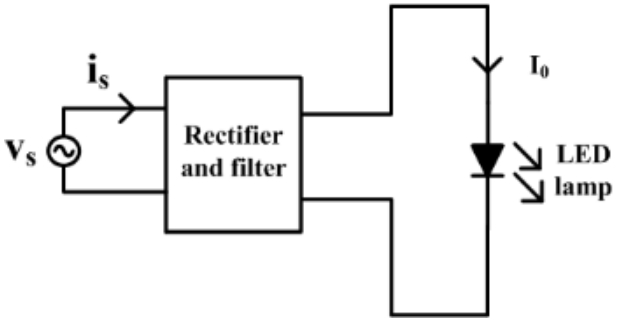

Figure 2.1 Passive LED driver

2.1.1.2 Switched mode LED drivers

Switched mode (*S-type*) LED drivers contain active switches and active switching regulators. Due to high switching frequency operation of *S- type* LED drivers, they overcome the limitations of passive LED drivers. *S-type* LED drivers use power factor correction (PFC) converter to attain high PF and low THD in source current. Active control of DC-DC switching converter in *S-type* LED drivers provide precise current control, high efficiency, and compactness. The features of *S-type* LED drivers such as good PF, ability to regulate LED load current against input voltage and load variations, dimming operation, isolation between LED load and input, and protection in all aspects make them suitable for wider range of applications in lighting industry. Good number of *S-type* LED drivers are available in literature to explore key issues of lighting systems [15]-[36]. *S-type* LED drivers are further classified based on power processing stages and applications such as single-stage (*S1*) LED drivers [15]-[24], two-stage (*S2*) LED drivers [25]-[32] and three-stage (*S3*) LED drivers [33]-[36].

Single-stage (*S1*) LED drivers have only one power processing stage. The schematic representation of *S1* LED drivers is shown in Figure 2.2. In these LED drivers, ac is converted into unregulated dc output by diode bridge rectifier which is given as input to dc-dc converter. With suitable high frequency operation of switches in dc-dc converter topology, PFC and output current control are realized simultaneously. The filter or energy storage capacitor C_0 can be connected either on low frequency side or on the frequency side which does not affect its size.

They have less component count due to single power conversion stage and are applicable for low and medium power lighting applications (<50 W). Conventional topologies based on buck [15], boost [16], buck-boost [17], SEPIC [19], flyback [20], half-bridge [23], push-pull [24] converters can be used as *S1* LED drivers. However it is difficult to achieve good PF, high energy efficiency, high step-down conversion and constant output current simultaneously in *S1* LED drivers.

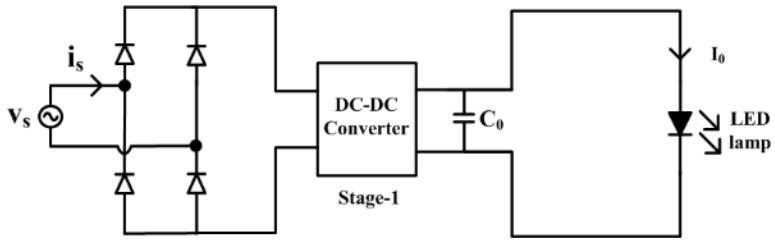

Figure 2.2 Single stage LED driver

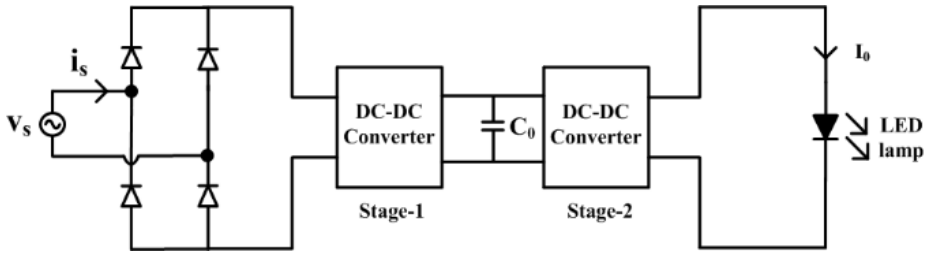

(a)

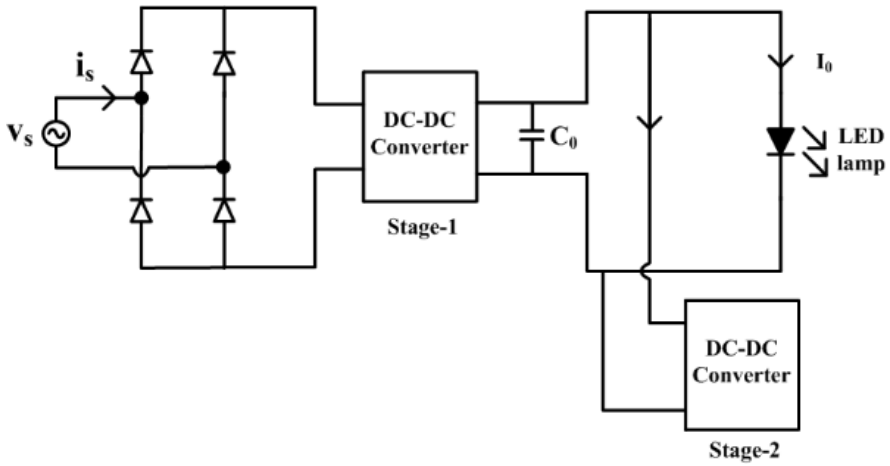

(b)

Figure 2.3 (a) Two stage type-A LED driver (b) Two stage type-B LED driver

Two-stage (*S2*) LED drivers contain two power processing stages. As each stage is designed for specific function, *S2* driver's performance is better as compared to *S1* drivers in terms of PFC, LED load current regulation, ac ripple and reliability. However, *S2* drivers have some limitations such as low efficiency, high cost and require two isolated control circuits. The

S2 drivers are suitable for medium and high power lighting applications, where the LED load current regulation and reliability issue are major priority than that of cost and size of lighting system. Depending on stage-2 configuration, the *S2* drivers are further classified as two-stage type-A (*S2A*) drivers and two-stage type-B (*S2B*) drivers as shown in Figure 2.3(a) and (b). In *S2A* drivers, stage-1 performs PFC operation, whereas stage-2 which is a high step-down dc-dc converter performs dc-dc regulation [25]-[29]. Both stage-1 and stage-2 are connected in cascaded structure with LED load. Generally, boost converter in discontinuous conduction mode (DCM) is used to achieve good PF in stage-1. The major drawback of *S2A* drivers is that they require large size filter capacitor. In *S2B* drivers, stage-1 performs both PFC and output current regulation. And stage-2 which is connected in parallel with LED load extracts double-line frequency power from dc-link to minimize flickering effect in LED load [30]-[32]. The size of filter capacitor in *S2B* drivers can be reduced by allowing large voltage variations.

Three-stage (*S3*) switched mode LED drivers have three power processing stages as shown in Figure 2.4. The function of stage-1 and stage-2 is same as the *S2A* drivers. And stage-3 comprises a current post regulator that provides dimming operation and current equalization among the parallel connected LED strings [33]-[35]. Current post regulator can be linear or switched type depending upon lighting application. Since each stage is optimized for a single function, *S3* drivers are used for high power lighting applications (>100 W). Further soft-switching topologies are preferred in stage-2 to increase the efficiency of whole lighting system. The cost and component count of *S3* LED drivers often increases for multi LED string application. To reduce the lighting system cost, single input multi output topologies are employed in stage-2 which eliminates current post regulator [36].

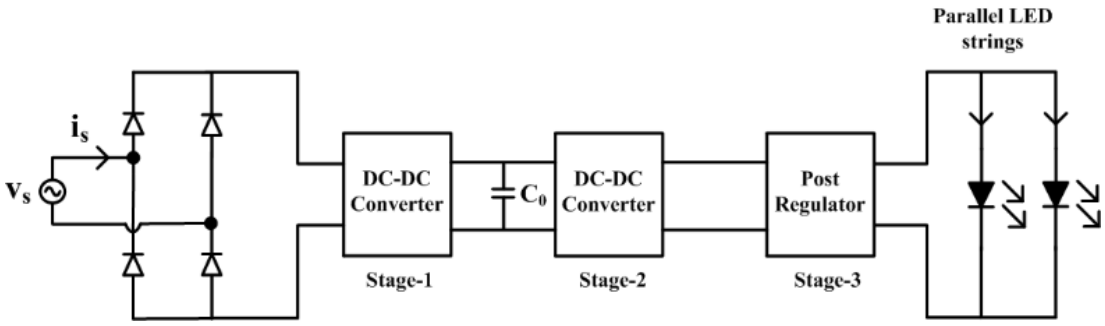

Figure 2.4 Three stage switched mode LED driver

2.1.2 DC fed LED drivers

In dc fed LED drivers, dc input is obtained from PV or battery or dc grid. The advantages of dc fed LED driver are: PFC stage elimination, non-requirement of electrolytic capacitor, simplified converter design aspects, improved efficiency and reliability. The requirements of LED driver circuit are different for each application. However, high power conversion efficiency, regulation of LED load current, dimming operation, less component count, high operating life, simple structure, reliability etc., are the basic objectives of LED driver circuit. As the available input is dc source, LED lighting loads can be powered from either linear or switched mode dc-dc converters. Switching converters are more preferred due to their high efficiency [37]-[39]. These dc-dc converter topologies are classified according to the electrical isolation between input and output. The basic isolated dc-dc converter topologies are Flyback, Forward, Push-pull, Half-bridge, and Full-bridge converters. Similarly, basic non-isolated topologies are Buck, Boost, Buck-Boost, Cuk, SEPIC, and Zeta converters. Based on the available input voltage and required output voltage for LED lighting loads, both isolated and non-isolated topologies have been used for driving LED loads for all lighting applications [40]-[52]. Some of the converters used in *S2* and *S3* LED drivers in second stage can also be used for dc fed LED driver circuit configurations. Recently, soft-switching converters have gained significant popularity in LED lighting applications [53]-[64]. High power conversion efficiency and high frequency operation of soft switching converter makes the LED driver system compact with good dynamic response, which is desirable when PWM dimming is applied.

As this thesis work focuses on the development of dc operated LED drivers, this section describes the literature related to the different dc operated driver circuit configurations for LED based lighting applications.

Jorge Garcia et al have proposed an interleaved buck converter as an LED driver circuit to overcome the limitations of standard buck converter [40]. The circuit and operating waveforms are shown in Figure 2.5 (a) and (b). In this interleaved buck converter, two sets of switches S_1 and S_2, diodes D_1 and D_2, and inductors L_1 and L_2 are connected with LED lamp. Phase shifted boundary conduction mode (PSBCM) peak current control is employed in this driver. In this control, the gate voltages of switches S_1 and S_2 are 180^o out of phase with equal duty ratio at constant switching frequency. When S_1 is on, L_1 is energized and L_2 is freewheeled linearly through LED lamp. Similarly, when S_2 is on, L_2 is energized and L_1 is freewheeled linearly through LED lamp. Hence LED lamp current I_0 is the sum of inductor currents i_{L1} and

i_{L2}. Since inductors are operated in PSBCM, both peak current and ripple current in each inductor are I_0. If duty ratio of switches is set to 0.5, a perfect ripple free current flows through LED lamp. Due to more ripple current in inductors, their size reduces significantly. This helps in using higher PWM dimming frequencies. This BCM in inductors also helps in achieving zero-current switching (ZCS) in devices which improves the efficiency. In addition, LED lamp current is regulated against input voltage variations by changing the duty of both switches simultaneously. The selected ripple current in LED lamp limits the input voltage swing.

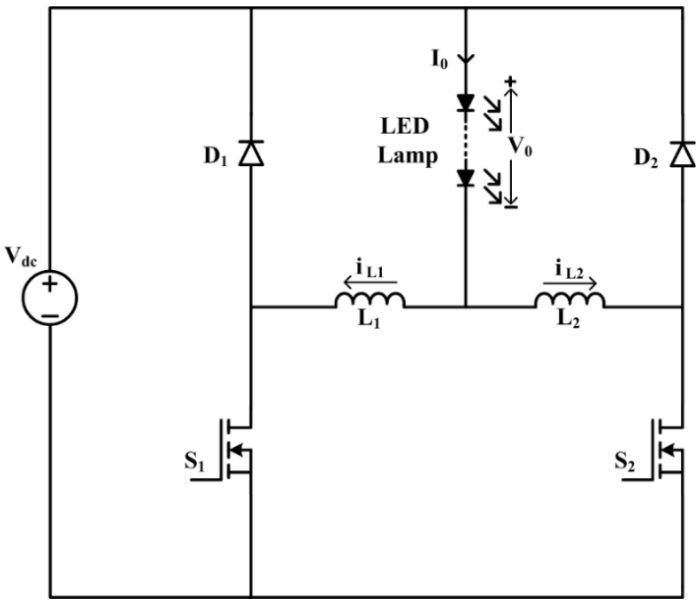

(a)

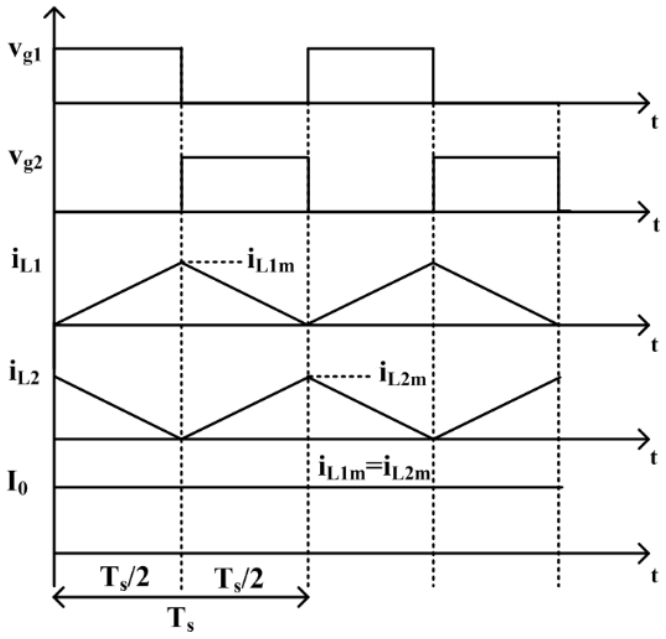

(b)

Figure 2.5 (a) Interleaved buck converter (b) Operating waveforms

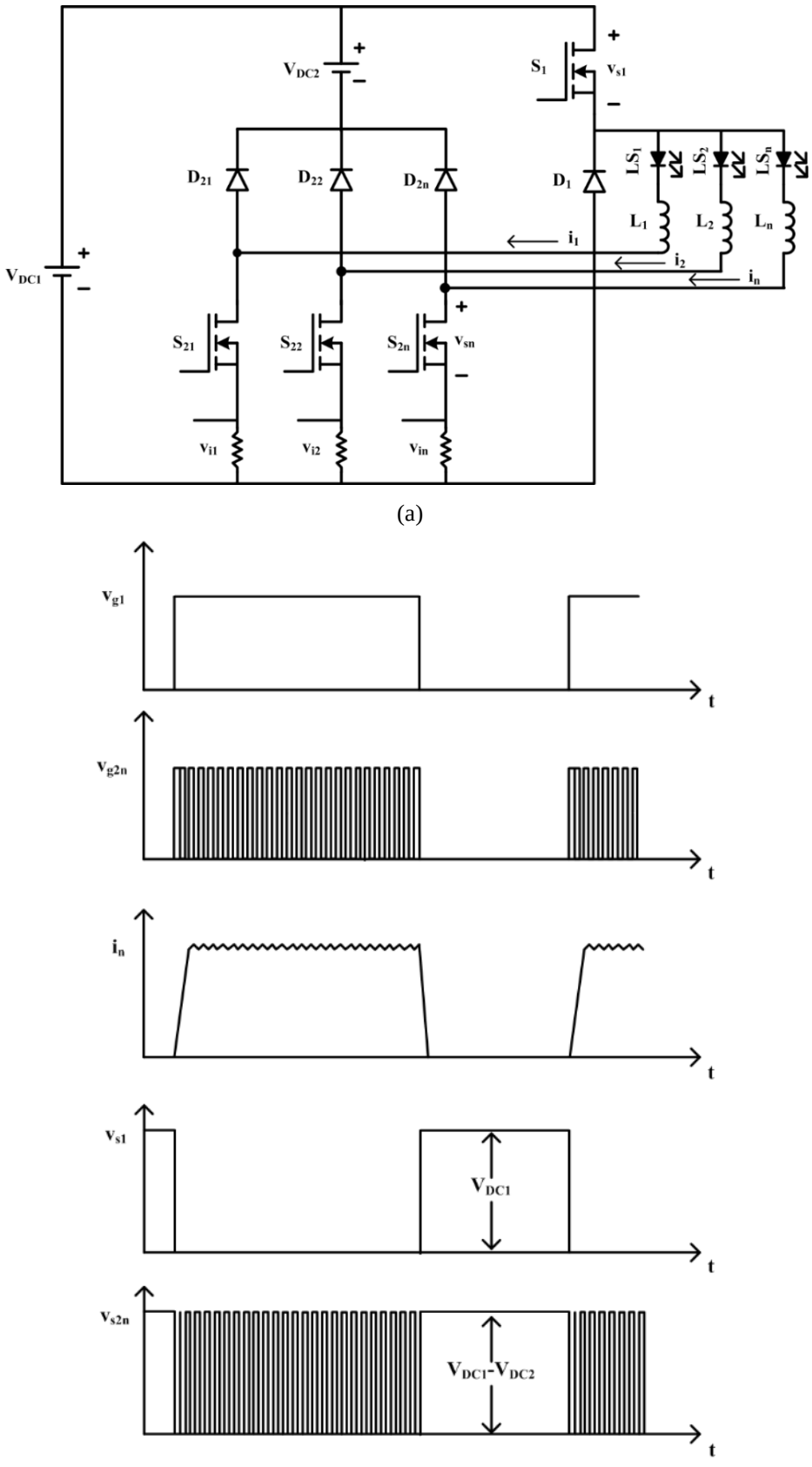

Figure 2.6 (a) Twin bus based LED driver (b) Operating waveforms

W Yu et al have developed a two-input buck converter to drive *n*-string LEDs using (*n* + 1) active switches [41]. The circuit configuration and its operating waveforms are shown in Figure 2.6 (a) and (b). This converter contains two input voltages, V_{DC1} and V_{DC2}, (n + 1) power MOSFETs, S_1 and S_{21}–S_{2n}, freewheeling diodes, D_1 and D_{21}–D_{2n}, and *n*-number of the output inductors, L_1–L_n. The switch S_1 is operated at low frequency which controls the illumination of all LED strings simultaneously. Switch S_{2n} and freewheeling diode D_{2n} operate at high switching frequency to power the LED string, LS_n. Due to two input voltages, the voltage stress across S_{2n} and D_{2n} is only $V_{DC1} - V_{DC2}$. Hence conduction and switching losses incurred in this driver are greatly reduced if the V_{DC2} is close to V_{DC1} which helps in achieving high efficiency. This also decreases the size of inductors that improves the dimming range of proposed LED driver. Moreover, each LED string current can be regulated.

Anne Pollock et al have proposed a high efficiency driver circuit for automotive LED lighting applications [42]. The block diagram of high efficiency LED driver is shown in Figure 2.7 (a). It comprises two LED lamps. Lamp-1 is powered by dc-dc converter and lamp-2 is connected in series with input dc source. Lamp-2 is powered without conversion and it is regulated due to the operation of dc-dc converter. Lamp-1 is regulated by dc-dc converter. The dc-dc converter can be replaced with any type of switching converter. In this LED driver, dc-dc converter is implemented with standard buck converter as shown in Figure 2.7 (b). The input supply V_S supplies only Lamp-1 power through buck converter and Lamp-2 is powered directly. Hence the losses associated with buck converter are reduced which increases the overall efficiency of the driver circuit. However dc link capacitor C_1 in the proposed driver circuit causes high inrush current problems.

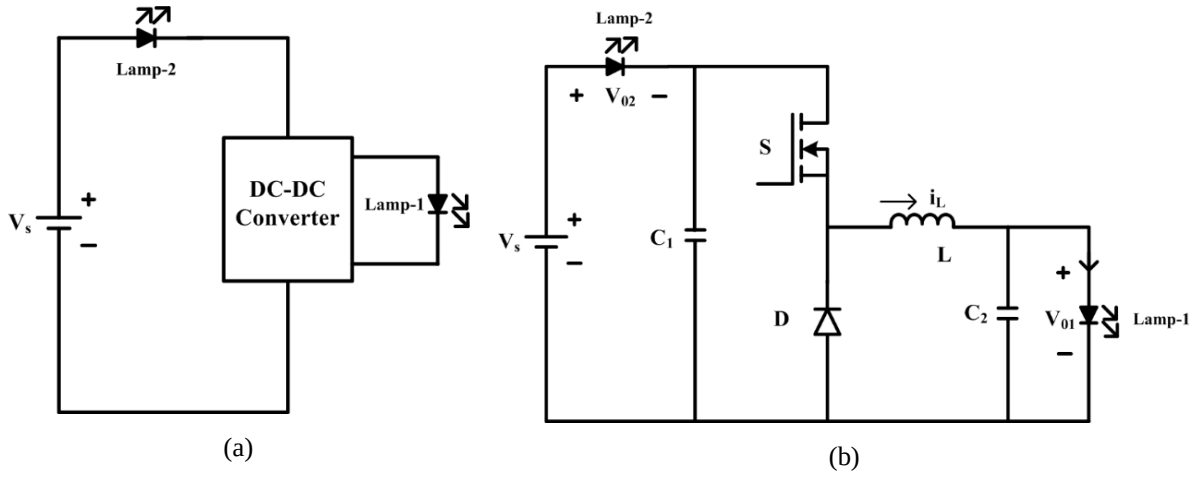

Figure 2.7 (a) Block diagram of high efficiency LED driver (b) High efficiency LED driver using buck converter

K I Hwu and W Z Jiang have developed a two-phase interleaved driver circuit for LED lighting applications with current balancing [43]. This driver is a step-up converter whose gain is higher than conventional boost converter and is shown Figure 2.8 (a). Gate control voltages of switches Q_1 and Q_2 are shifted by 180^o and their duty ratio is greater than 0.5. The operating waveforms are shown in Figure 2.8 (b). The converter is operated in continuous conduction mode (CCM). Both inductor currents i_{L1} and i_{L2} and two LED string currents are balanced due to charge balance in capacitor C_b. The input current ripple (i_{L1} + i_{L2}) is also reduced with this control. LED currents can be balanced even with different counts in each LED string in this driver. The input voltage variations are compensated by changing the duty ratio of switches. Due to high voltage gain, it is suitable for low input voltage applications. This driver can be used in LED display applications. An efficiency of 91.7% is obtained at rated load of 24 W. Due to interleaved control, ripple current in output capacitors C_{01} and C_{02} is considerably high.

C Zheng et al have proposed a three level boost converter with single switch for PWM dimming LED lighting applications [44]. This converter is shown in Figure 2.9. The switch S_1 is operated with a gate voltage which is a combination of high switching frequency and low PWM dimming frequency. Inductor L_r limits the switch inrush current during on-state. When the switch is in off-state, capacitors C_1 and C_2 are naturally balanced and charged to $0.5V_0$. Hence switch voltage stress is reduced which reduces the losses in the converter. The proposed topology reduces the switch count and its associated gate driver compared to conventional three level boost converter. Also, it has solved dimming issues encountered in two level boost LED drivers. Both current regulation and dimming operation are achieved with high efficiency through single switch. This converter can be applied for automotive lighting applications.

E E Santos Filho et al have presented a switched capacitor based driver circuit for LED lighting applications [54]. Figure 2.10 (a) shows the switched capacitor LED driver. The switches S_1 and S_2 are operated alternately with equal duty ratio as shown in Figure 2.10 (b). This driver utilizes an inductor L_0 which allows complete charging and discharging of C_s and it operates in DCM. The stored energy in capacitor C_s is supplied to LED lamp. The power delivered to LED lamp is independent of its forward voltage which improves the efficiency of driver. Due to DCM operation, ZCS is achieved in switches S_1 and S_2. Frequency modulation is used to control the illumination and to compensate input voltage variations. The obtained efficiency of this LED driver circuit is very low.

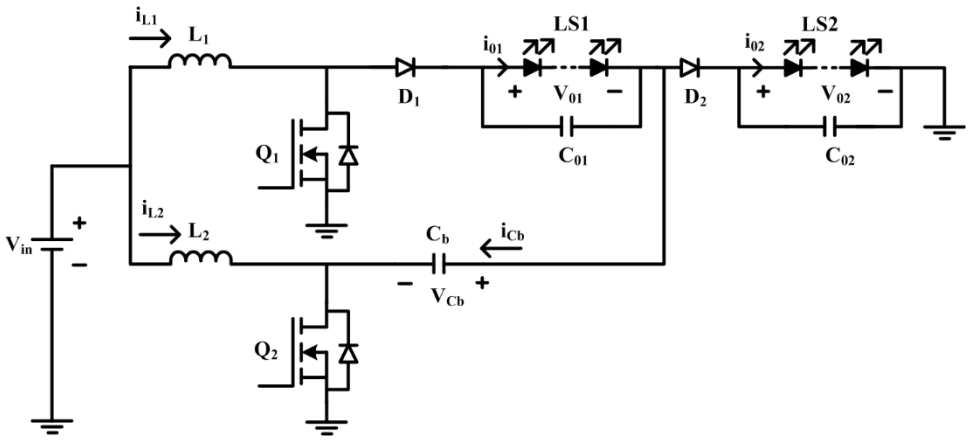

(a)

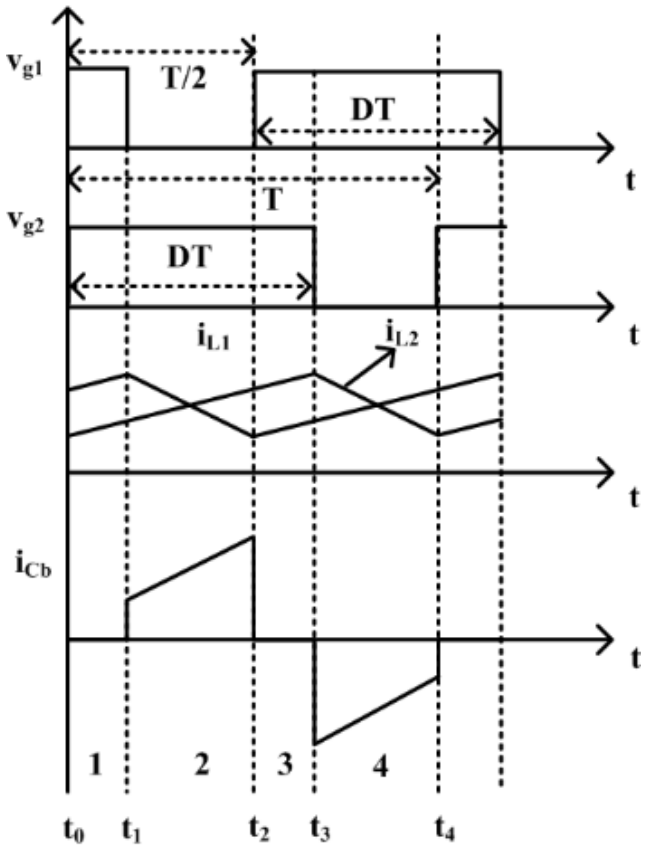

(b)

Figure 2.8 (a) Two-phase interleaved LED driver (b) Operating waveforms

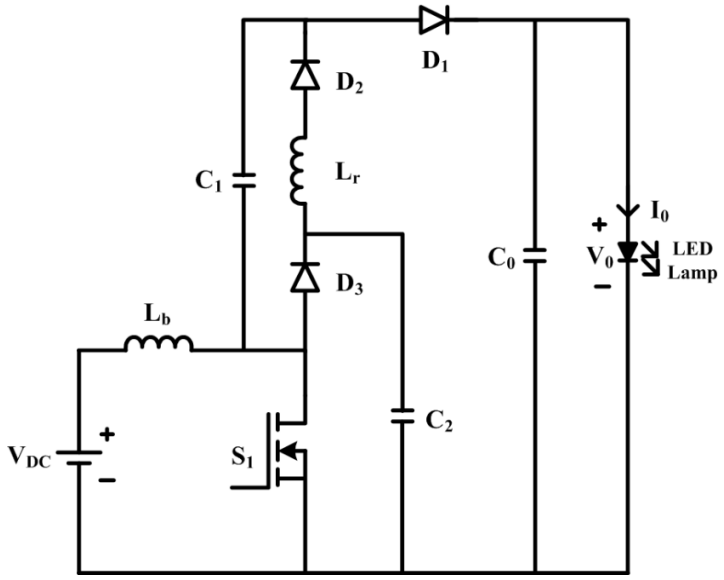

Figure 2.9 Single switch three level boost converter based LED driver

Jose Marcos Alonso et al have explained a variable inductor (VI) based LED driver circuit for dc grid lighting applications [59]. This driver uses a half-bridge inverter, a variable inductor and a center tapped diode rectifier. Figure 2.11 (a) and Figure 2.11 (b) show the schematic representation and operating waveforms of proposed driver respectively. Both regulation against input voltage and load variations and dimming operations are accomplished through variable inductor. This driver offers constant frequency operation, zero-voltage switching (ZVS) operation in the half-bridge switches, zero-current switching (ZCS) in center tapped rectifier diodes, inherent short-circuit and open-circuit protection. In addition, this configuration can supply multiple LED lamps with independent current control and can be suitable for high-end smart lighting applications. The limitations of this driver are: it requires an auxiliary winding with a driver to create variable inductor and offers low efficiency of 85% at full illumination level.

J Liu et al have presented a driver circuit for vehicle LED lighting applications using high-frequency alternating current (HFAC) power distribution system (PDS) [60]. The schematic diagram of HFAC PDS in vehicle is shown in Figure 2.12 (a). The HFAC bus is created by using resonant inverter and it distributes power to different loads through suitable converters. LED based lighting has become popular in automotive sector due to its high energy conservation and long life time. Using HFAC bus, a driver circuit is developed for vehicle LED lighting application as shown in Figure 2.12 (b). This topology has an input transformer for making the input voltage suitable for LED strings, bidirectional ac-switch, full-bridge diode

rectifier to converter high frequency (HF) ac into dc voltage, valley-fill circuit to achieve high input PF with low THD, and an inductor L_0 to filter HF harmonics. Current balancing and dimming operation of parallel LED strings are accomplished by pulse-density modulation control through ac-switch. The operating life time of this driver is high due to absence of electrolytic capacitor. In addition, ZCS is achieved in bidirectional ac-switch. An efficiency of greater than 91% is obtained from a prototype at distribution frequency of 50 kHz and peak voltage of 30 V.

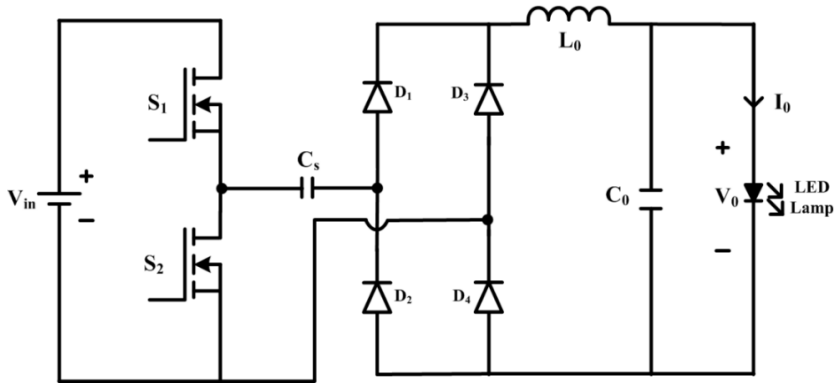

(a)

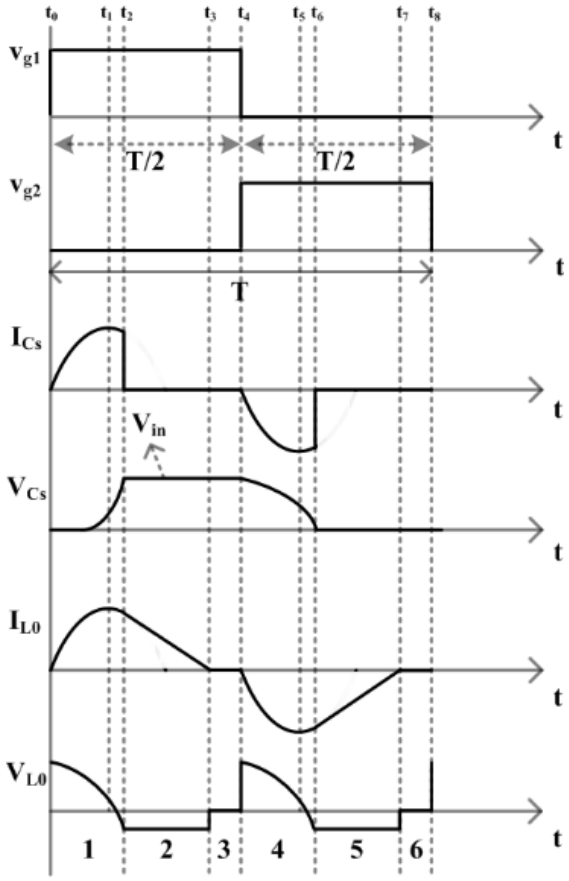

(b)

Figure 2.10 (a) Switched capacitor based LED driver (b) Operating waveforms

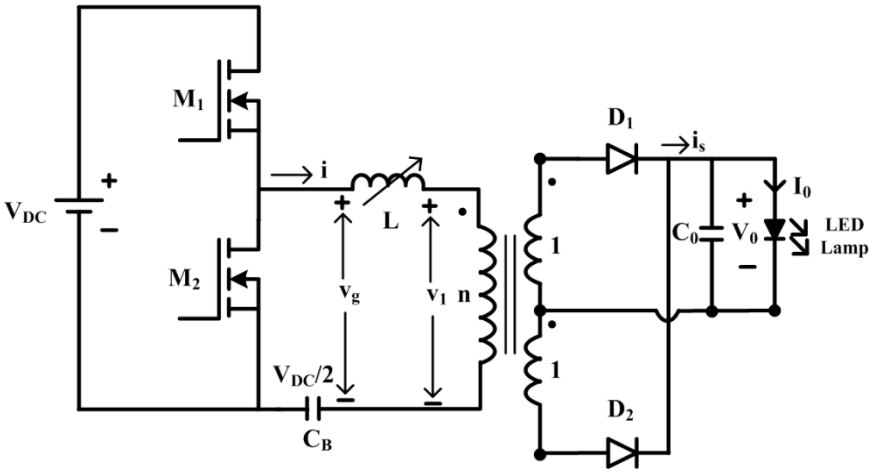

(a)

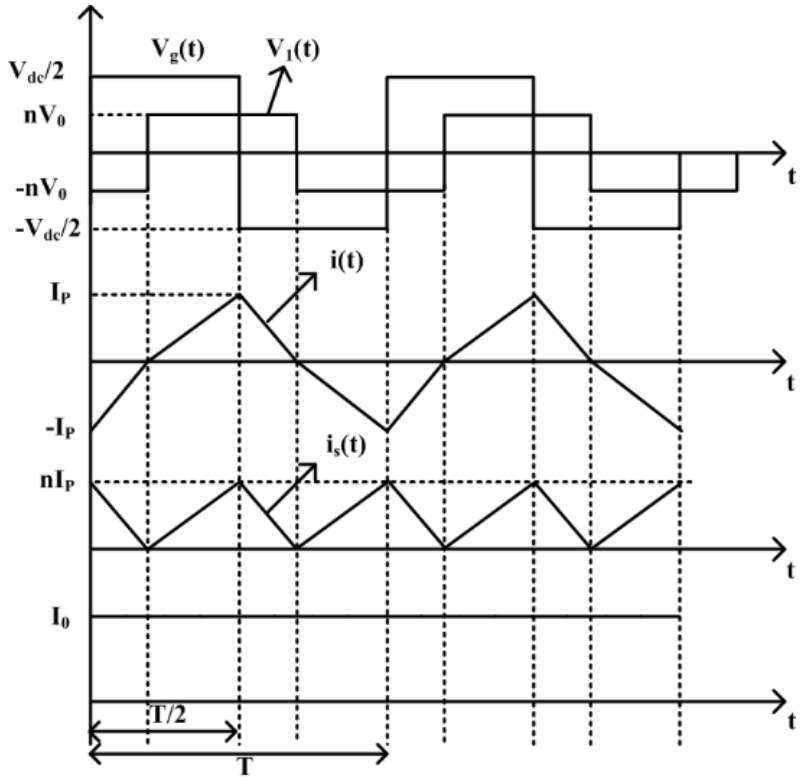

(b)

Figure 2.11 (a) VI based LED driver (b) Operating waveforms

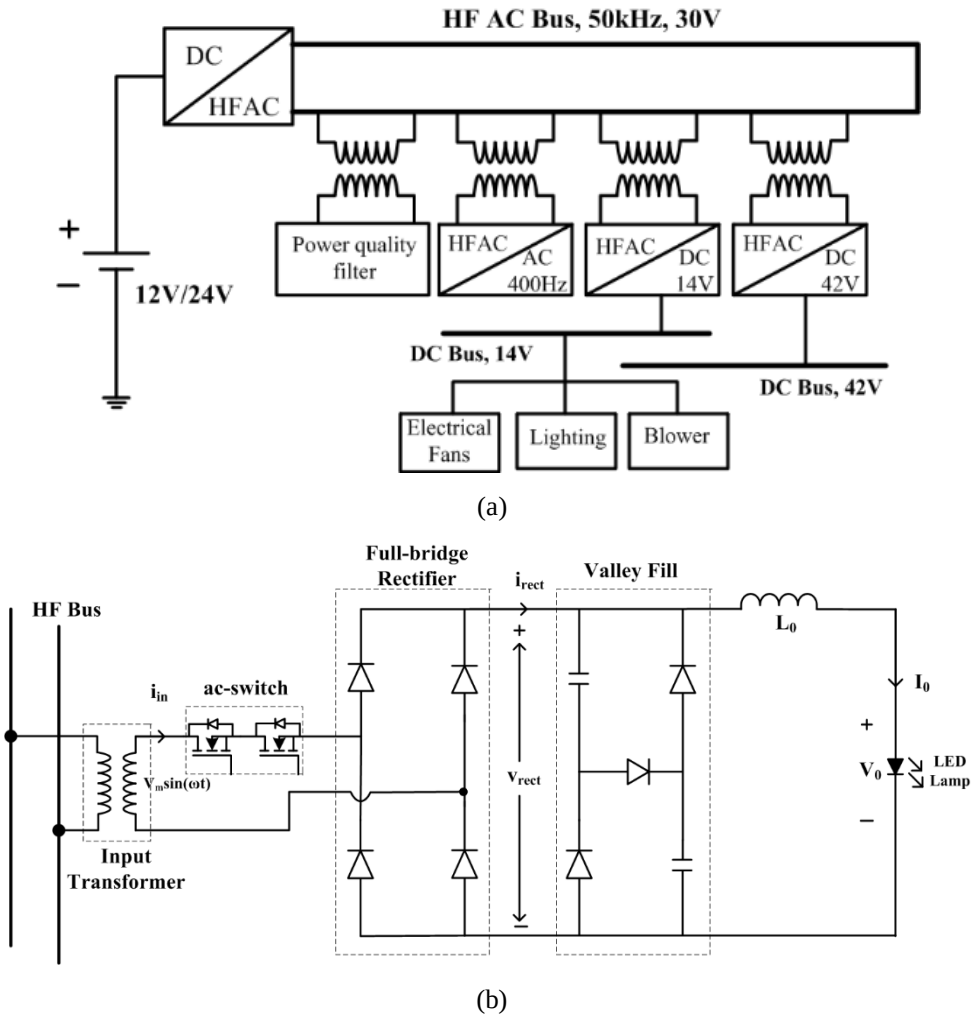

Figure 2.12 (a) Schematic representation of HFAC PDS in electric vehicle (b) LED driver using HFAC bus

2.2 Control Techniques for LED Lighting Systems

The adjustable illumination from an LED is called dimming. It is an important requirement for LED lighting applications. Dimming operation in LED driver saves good amount of power which further reduces the consumption of energy. Dimming can be achieved by Amplitude Modulation (AM) or Pulse-Width Modulation (PWM) schemes. In AM, dimming is attained by controlling the dc current through LED strings [68], [69]. As LED current is varied, AM dimming causes chromaticity variations which are undesirable for sensitive lighting applications. Also, AM dimming does not provide a wide dimming range due to non-linear current–voltage characteristics of LED. PWM dimming methods have been widely used to overcome the limitations of AM [70]-[75]. In PWM dimming, the average current through LED strings is controlled by turning on and off the LED strings at a low frequency at nominal current. It offers high dimming range without chromaticity variations and provides smooth dimming.

Several PWM dimming schemes like turning on and off the LED strings through a series connected controlled switch [70], turning on and off the input voltage to the driver circuit [71], multi-phase PWM [72], pulse-code modulation (PCM) [73], double pulse width modulation (DPWM) [74], bi-level driving [75], etc., have been reported in literature.

2.3 Conclusions

In this chapter, an overview of AC fed LED driver circuits has been presented. In section 2.1.2, DC fed LED drivers for single and multi-output LED based lighting applications have been discussed. Different illumination or dimming control methods have been explained in section 2.2.

The number of soft switched converters in the literature with reduced current stress for multiple LED lighting applications are less in number in the literature. Converters with ripple free LED current, soft switching, dimming operation, ability to power multiple LED lamps and LED current regulation are also few. Also, some of configurations are not capable to drive LED lamps of different power ratings with independent dimming and regulation. Some of the LED drivers described in literature are not suitable for high power LED applications.

Hence there is sufficient scope for further research in development of driver circuits with soft switching, reduced current stress, current regulation, independent dimming control, ability to drive multiple LED lamps and high efficiency for LED based lighting applications. With this objective, four different converter configurations have been proposed in this thesis.

In the next four chapters, proposed converter configurations for LED based lighting applications are explained in detail.

Chapter 3

Soft Switched Full-Bridge LED Driver Configuration for Street Lighting Application

Chapter 3

Soft Switched Full-Bridge LED Driver Configuration for Street Lighting Application

This chapter presents an LED driver circuit topology based on full-bridge configuration. Principle of operation, analysis and design procedure of the proposed circuit configuration are explained in detail and it is validated through simulated and experimental results on the 145 W experimental prototype with dimming control.

3.1 Principle of Operation of Proposed LED Driver

Figure 3.1 (a) shows the circuit diagram of the proposed LED driver. This circuit uses a full-bridge configuration consisting of four power metal-oxide-semiconductor field-effect transistors (MOSFETs) S_1, S_2, S_3, and S_4. $D_1 - D_4$ are the intrinsic body diodes of power MOSFETs and $C_1 - C_4$ indicate either the output capacitances of power MOSFETs or external capacitors. Series connection of LEDs and an inductor is in parallel with each switch. Each LED lamp represents a dc load and can be considered as one street light lamp. In proposed circuit, four LED lamps are present. The number of LED lamps can be increased by addition of more legs. Figure 3.1 (b) shows an extension of proposed configuration to multiple LED lamps. The inductors L_1, L_2, L_3 and L_4 are designed to provide continuous current through lamp-1, lamp-2, lamp-3, and lamp-4 respectively. The inductor L_r is used to obtain (ZVS) in all the four switches. The switches S_1 and S_2 are alternately turned on and off at a switching frequency $f_s = 1/T$ with 50% duty ratio. Similarly, S_3 and S_4 are alternately turned on and off at the same switching frequency with 50% duty ratio. To avoid short circuit across the dc power supply, a dead time is provided between the gate voltages of switches in each leg. As the dead times are very small, the lamp currents and inductor current i_{Lr} are assumed to be constant during dead time. The switch S_d incorporates dimming feature by using a low frequency gate signal. Input voltage V_{in} to the bridge is obtained from three dc voltages V_{DC1}, V_{DC2}, and V_C. V_{DC2} is input voltage to the buck-boost converter and V_C is its output voltage. V_{DC1} must be far greater than the summation of remaining dc voltages i.e., ($V_{DC2} + V_C$) to reduce the power handled by buck-boost converter. The dc voltage sources V_{DC1} and V_{DC2} can be obtained from rechargeable batteries. For any variations in supply voltage, input voltage V_{in} is controlled to be constant by the buck-boost converter.

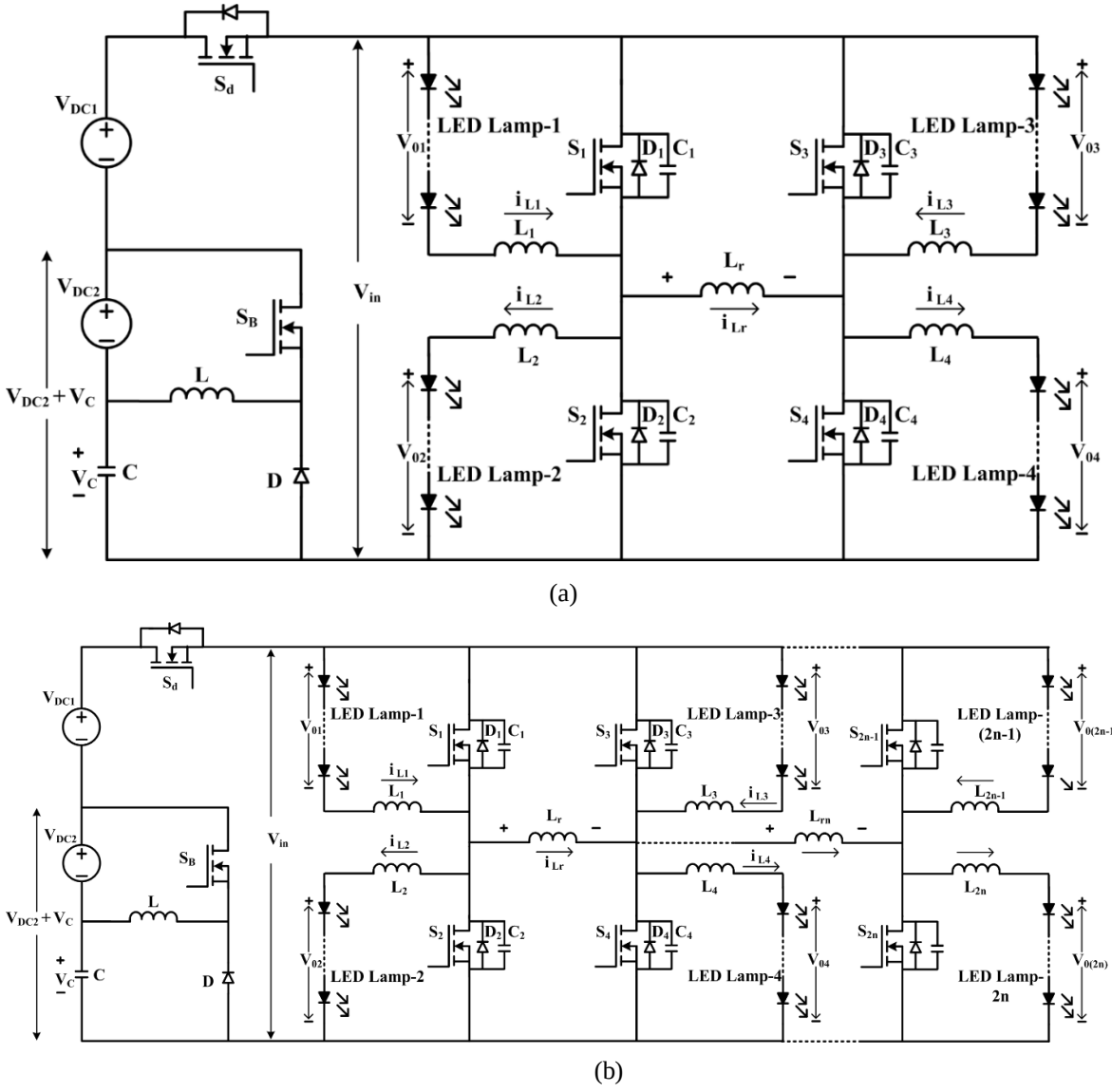

Figure 3.1 (a) Proposed LED driver (b) Extension to multiple LED lamps

To understand the working principle of the proposed LED driver, the simplified circuit diagram shown in Figure 3.2 is considered, where the input voltage V_{in} is represented by a voltage source. Figure 3.3 shows the operating waveforms of the proposed LED driver. The different working modes in a switching cycle are explained in this section.

3.1.1 Mode I: (t_0-t_1)

At time instant t_0, switches S_1 and S_4 are turned on at zero voltage. LED lamp-2 and lamp-3 are powered by input voltage V_{in}. LED lamp-1 and lamp-4 are supplied by energy stored in inductors L_1 and L_4 respectively. Due to the nature of inductor L_r, the current i_{Lr} linearly increases through the switches S_1 and S_4. Currents through lamp-2 and lamp-3 increase and

currents through lamp-1 and lamp-4 decrease linearly. As all LED lamps are identical, average lamp current values are equal. Difference of i_{L2} and i_{L1} which is of a small value flows through S_1. Similarly, difference of i_{L3} and i_{L4} flows through S_4. Hence devices are conducting only a small value of current. This reduces device current stress and conduction losses. This mode ends when inductor current i_{Lr} becomes zero. The equivalent circuit of mode-I is shown in Figure 3.4 (a).

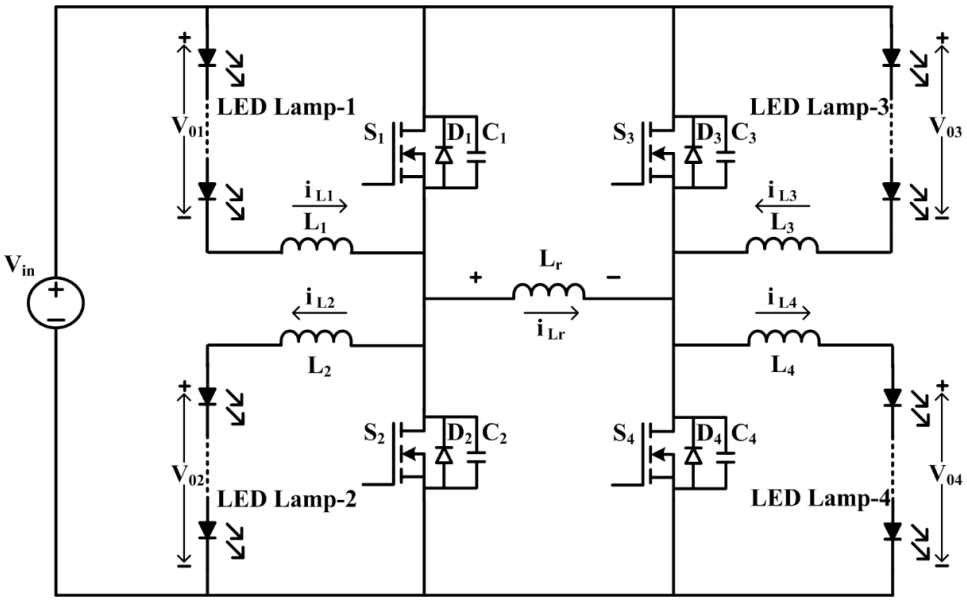

Figure 3.2 Simplified circuit diagram

3.1.2 Mode II: (t_1-t_2)

The explanation in mode I is valid for this mode also except that the current i_{Lr} increases from zero to positive maximum through the switches S_1 and S_4. This mode ends at t_2. Figure 3.4 (b) shows equivalent circuit of mode-II.

3.1.3 Mode III: (t_2-t_3)

This mode begins after removing gate signals for switches S_1 and S_4, which are carrying positive currents. Switches S_1 and S_4 are turned off at zero voltage. During t_2 to t_3 none of the switches are conducting. Current $(i_{Lr} + i_{L2} - i_{L1})/2$ charges the capacitor C_1 and discharges the capacitor C_2. Similarly, $(i_{Lr} + i_{L3} - i_{L4})/2$ charges the capacitor C_4 and discharges the capacitor C_3. After this, D_2 and D_3 start conducting. Now the switches S_2 and S_3 may be turned on with zero voltage switching. This mode ends when capacitors C_2 and C_3 are discharged from V_{in} to

zero or C_1 and C_4 are charged from zero to V_{in}. The equivalent circuit of mode-III is shown in Figure 3.4 (c).

3.1.4 Mode IV: (t_3-t_4)

Figure 3.5 (a) shows the equivalent circuit of mode-IV. At time instant t_4, switches S_2 and S_3 are turned on at zero voltage. LED lamp-1 and lamp-4 are powered by input voltage V_{in}. LED lamp-2 and lamp-3 are supplied by energy stored in inductors L_2 and L_3 respectively. Due to the nature of inductor L_r, the current i_{Lr} decreases through the switches S_2 and S_3. Currents through lamp-1 and lamp-4 increase and current through lamp-2 and lamp-3 decrease linearly. Difference of i_{L1} and i_{L2} flows through S_2 and difference of i_{L4} and i_{L3} flows through S_3. As the device current is less, device current stress and conduction losses are reduced. This mode ends when current i_{Lr} becomes zero.

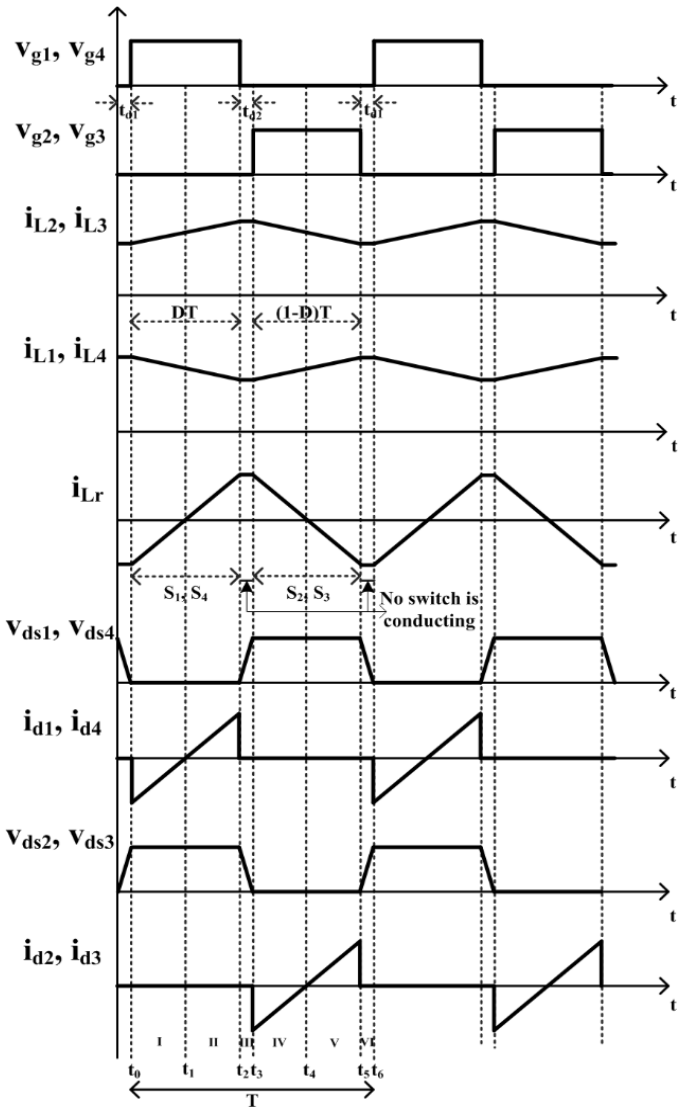

Figure 3.3 Operating waveforms

3.1.5 Mode V: (t_4-t_5)

The explanation in mode IV is valid for this mode also except that the current i_{Lr} decreases from zero to negative maximum through the switches S_2 and S_3. This mode ends at t_5 and its equivalent circuit is shown in Figure 3.5 (b).

3.1.6 Mode VI: (t_5-t_6)

This mode begins after removing gate signals for switches S_2 and S_3, which are carrying positive currents. The process of turning off of switches S_2, S_3 and turning on of switches S_1, S_4 with zero voltage is similar to that in mode III. The equivalent circuit of this mode is shown in Figure 3.5 (c). This mode ends when capacitors C_1 and C_4 are discharged from V_{in} to zero or C_2 and C_3 are charged from zero to V_{in}.

3.2 Analysis of the Proposed LED Driver

The analysis of the proposed LED driver is carried out by considering the following assumptions.

i. The proposed converter is operating in steady state
ii. The circuit components are ideal
iii. All four LED lamps are identical
iv. The voltage across each LED lamp is constant

The switches are operated with fixed duty cycle at fixed frequency. Each switch is on for 50% duty cycle and off for remaining period. To calculate the voltage across each LED lamp, it is essential to examine the inductor currents and voltages. As the LED lamps and their operating currents are identical, the analysis is shown for a single LED lamp, i.e LED lamp-2. When the switches S_1 & S_4 are ON and S_2 & S_3 are OFF, the LED lamp-2 is supplied by input dc voltage V_{in} through the inductor L_2. The corresponding equivalent circuits are shown in Figure 3.4 (a) and (b).

3.2.1 Mode-I and Mode-II (t_0-t_2)

The voltage across inductor L_2 is expressed as

$$v_{L2} = V_{in} - V_{02} = L_2 \frac{di_{L2}}{dt} \qquad t_0 \le t < t_2 \tag{3.1}$$

The current through the inductor L_2 is

$$i_{L2}(t) = \frac{1}{L_2}\int_{t_0}^{t} v_{L2}(t)\,dt + i_{L2}(t_0) = \frac{V_{in} - V_{02}}{L_2}(t - t_0) + i_{L2}(t_0) \qquad t_0 \le t < t_2 \qquad (3.2)$$

where $i_{L2}(t_0)$ is the initial current in the inductor L_2 at time $t = t_0$. At $t = t_2$, $i_{L2}(t)$ reaches maximum value, which is

$$i_{L2}(t_2) = \frac{V_{in} - V_{02}}{L_2}(t_2 - t_0) + i_{L2}(t_0) \qquad (3.3)$$

The duration $(t_2 - t_0)$ is the ON period of switches S_1 and S_4. Hence (3.3) can be written as

$$i_{L2}(t_2) = \frac{V_{in} - V_{02}}{L_2} DT + i_{L2}(t_0) \qquad (3.4)$$

where D is duty ratio of switches S_1 and S_4 and T is the switching period.

From (3.4), the ripple current in inductor L_2 is expressed as

$$\Delta i_{L2} = i_{L2}(t_2) - i_{L2}(t_0) = \frac{V_{in} - V_{02}}{L_2} DT \qquad (3.5)$$

During this interval, voltage across L_r is V_{in}. The current through it increases linearly and is expressed as

$$i_{Lr}(t) = \frac{V_{in}}{L_r}(t - t_0) + i_{Lr}(t_0) \qquad t_0 \le t < t_2 \qquad (3.6)$$

3.2.2 Mode-IV and Mode-V ($t_3 - t_5$)

When the switches S_1 & S_4 are switched-off and S_2 & S_3 are switched-on, the LED lamp-2 is supplied by the stored energy in the inductor L_2. The corresponding equivalent circuits are shown in Figure 3.5 (a) and (b)

The voltage across inductor L_2 is

$$v_{L2} = -V_{02} = L_2 \frac{di_{L2}}{dt} \qquad t_3 \le t < t_5 \qquad (3.7)$$

The current through the inductor L_2 is expressed as

$$i_{L2}(t) = \frac{1}{L_2}\int_{t_3}^{t} v_{L2}(t)\,dt + i_{L2}(t_3) = \frac{-V_{02}}{L_2}(t - t_3) + i_{L2}(t_3) \qquad t_3 \le t < t_5 \qquad (3.8)$$

where $i_{L2}(t_3)$ is the initial current in the inductor L_2 at time $t = t_3$. At $t = t_5$, $i_{L2}(t)$ reaches minimum value and is given by

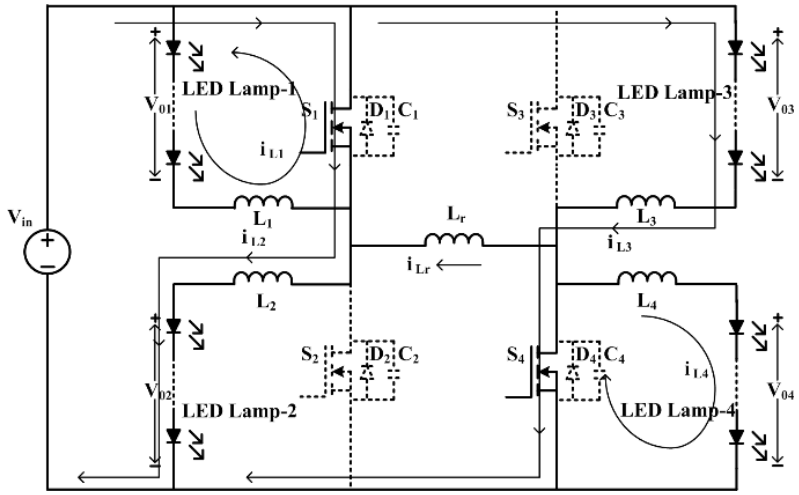

(a) Mode I

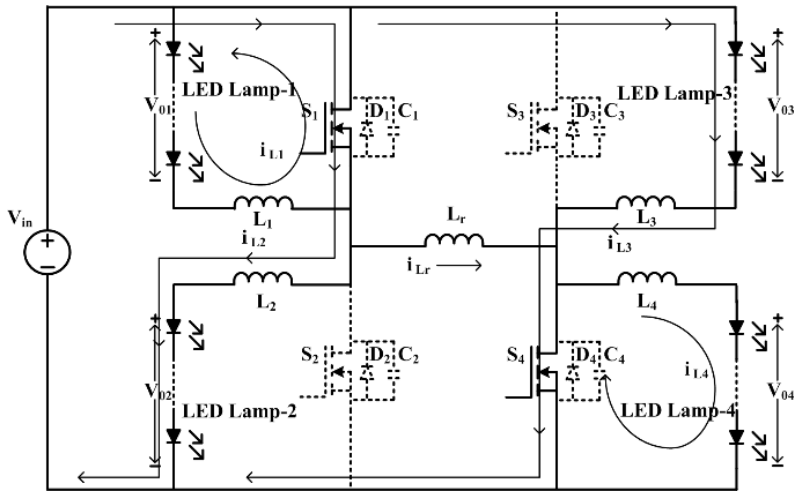

(b) Mode II

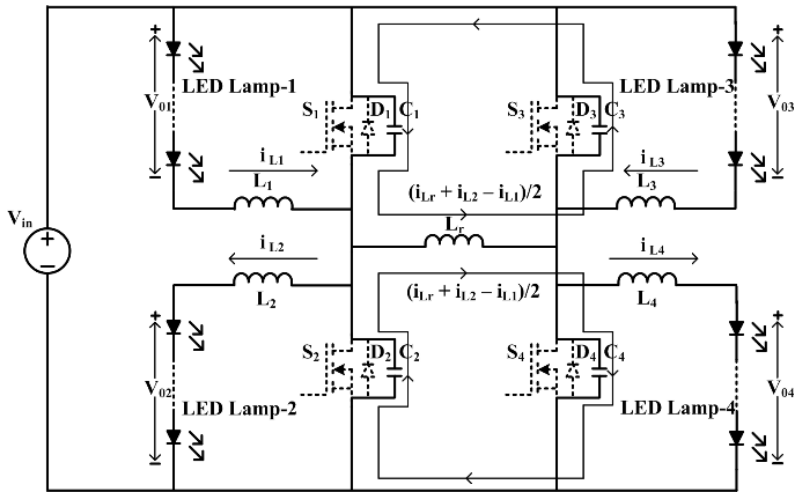

(c) Mode III

Figure 3.4 Equivalent circuits of proposed LED driver when S1 and S4 are ON

$$i_{L2}(t_5) = \frac{-V_{02}}{L_2}(t_5 - t_3) + i_{L2}(t_3) \tag{3.9}$$

Assuming that dead time t_{d1} and t_{d2} are negligible, the duration $(t_5 - t_3)$ is the OFF period of switches S_1 and S_4. (3.9) can be written as

$$i_{L2}(t_5) = \frac{-V_{02}}{L_2}(1-D)T + i_{L2}(t_3) \tag{3.10}$$

From (3.10), the ripple current in inductor L_2 is expressed as

$$\Delta i_{L2} = i_{L2}(t_5) - i_{L2}(t_3) = \frac{-V_{02}}{L_2}(1-D)T \tag{3.11}$$

During this interval, voltage across L_r is $-V_{in}$. The current through it decreases linearly and is given by

$$i_{Lr}(t) = -\frac{V_{in}}{L_r}(t - t_3) + i_{Lr}(t_3) \quad t_3 \le t < t_5 \tag{3.12}$$

Under steady state operation, the net change in current through inductor L_2 is zero over the time period T. Hence from (3.5) and (3.11)

$$[i_{L2}(t_2) - i_{L2}(t_0)] + [i_{L2}(t_5) - i_{L2}(t_3)] = 0 \tag{3.13}$$

$$\Rightarrow \quad \frac{V_{in} - V_{02}}{L_2} DT - \frac{V_{02}}{L_2}(1-D)T = 0 \tag{3.14}$$

$$\Rightarrow \quad V_{02} = DV_{in} \tag{3.15}$$

Hence the voltage across LED lamp V_{02} is D times the input voltage V_{in}. The analysis for other LED lamps is similar to the aforementioned analysis. (3.5), (3.11), and (3.15) are applicable to other LED lamps also. Hence the ripple current through each LED lamp and voltage across each LED lamp are given by

$$\Delta i_{Lk} = \frac{V_{in} - V_{0k}}{L_k} DT = \frac{-V_{0k}}{L_k}(1-D)T \text{ , where } k = 1, 2, 3, 4 \tag{3.16}$$

$$V_{0k} = DV_{in}, \text{ where } k = 1, 2, 3, 4 \tag{3.17}$$

The value of inductor for specified current ripple can be determined from (3.16) under continuous current.

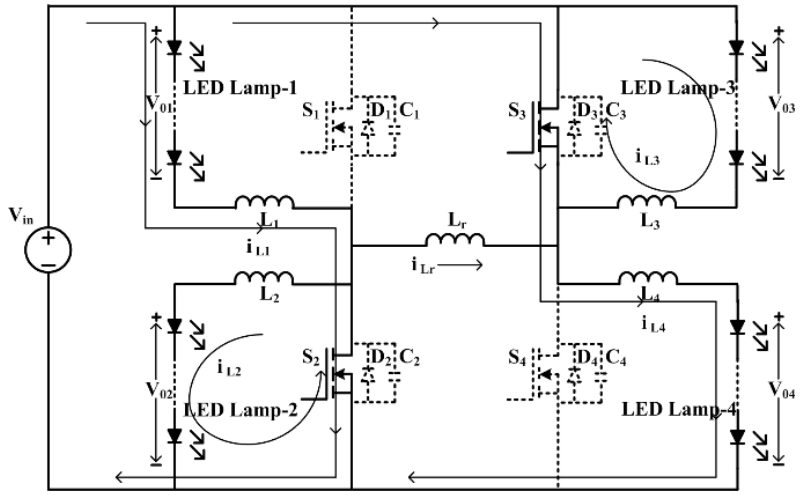

(a) Mode IV

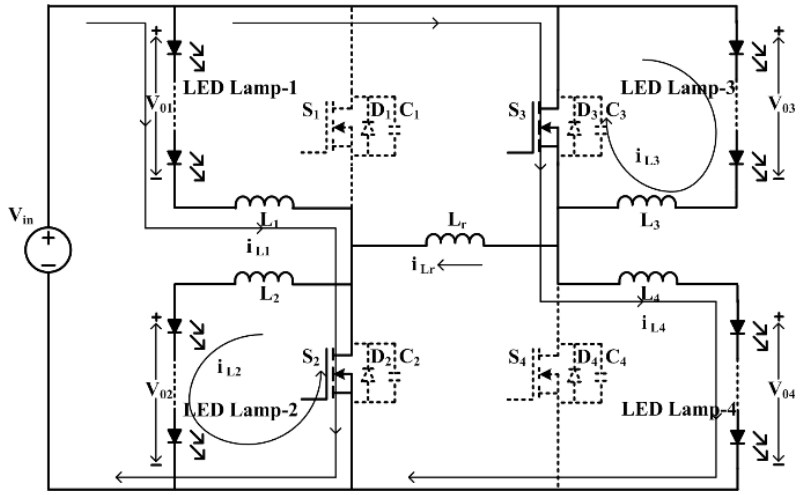

(b) Mode V

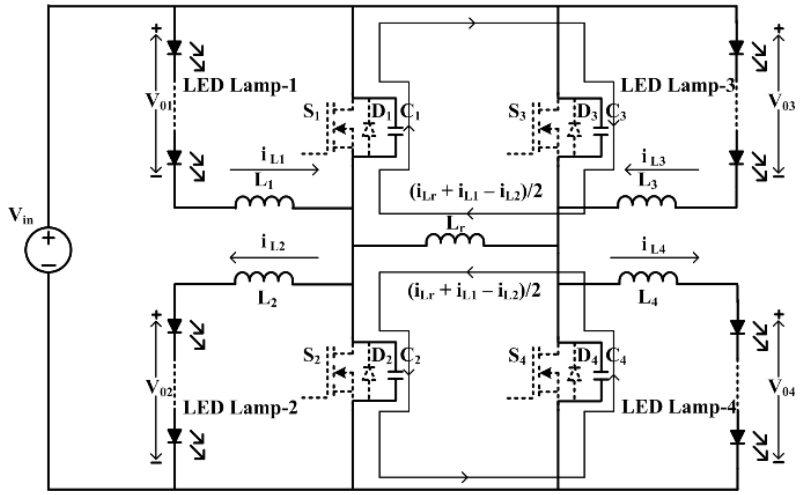

(c) Mode VI

Figure 3.5 Equivalent circuits of proposed LED driver when S2 and S3 are ON

3.3 Design Considerations

In the proposed work four LED lamps are used. Each LED lamp comprises of two strings of LEDs which are connected in parallel. In each string, 10 LEDs are connected in series. Each LED is operated at 3.3 V, 550 mA and 1.815 W. Each LED lamp is operated at 33 V, 1.1 A and 36.3 W.

From (3.17), input voltage V_{in} is given by

$$V_{in} = \frac{V_{0k}}{D} \tag{3.18}$$

With a duty ratio of 0.5, and V_{0k} of 33 V, the input voltage is calculated as $V_{in} = 66\text{V}$.

Rearranging (3.16),

$$L_k = \frac{V_{in} - V_{0k}}{\Delta i_{Lk}} DT \text{ , } k = 1, 2, 3, 4 \tag{3.19}$$

With V_{in} = 66 V, V_{0k} = 33 V, D = 0.5, T = 5 µs, peak to peak LED current Δi_{Lk} of 13%, the value of inductor L_k is calculated as $L_k \cong 577\mu\text{H}$.

To ensure ZVS during dead time, appropriate current magnitude is required to charge and discharge the output capacitors of the switches [65]. The inductor L_r is used to provide the required constant current during dead time. The peak current through L_r is assumed to be constant during dead time. At $t = t_2$, $i_{Lr}(t)$ reaches a maximum value. Hence from (3.6),

$$i_{Lr-pk} = \frac{V_{in}}{L_r}(t_2 - t_0) + i_{Lr}(t_0) = \frac{V_{in}}{L_r}(t_2 - t_0) - \frac{V_{in}}{L_r}(t_1 - t_0) \tag{3.20}$$

As $t_2 - t_0 = DT$ and $t_1 - t_0 = \frac{DT}{2}$, the (3.20) can be written as

$$i_{Lr-pk} = \frac{V_{in}}{L_r}(DT - \frac{DT}{2}) = \frac{V_{in}DT}{2L_r} \tag{3.21}$$

With a duty ratio of 0.5, the peak current through the L_r is given by

$$i_{Lr-pk} = \frac{V_{in}T}{4L_r} \tag{3.22}$$

The value of i_{Lr-pk} is inversely proportional to inductor L_r for a fixed value of V_{in} and T. For L_r = 120 µH, V_{in} = 66 V, T = 5 µs, i_{Lr-pk} is calculated as $i_{Lr-pk} = 0.6875\text{ A}$. For the calculation of the switch output capacitor value, the currents through L_k and current through L_r during dead

time are assumed to be constant. Assuming that dead time $t_{d1} = t_{d2} = t_d$, current flowing through output capacitors during t_{d1} or t_{d2} is given by

$$i_{Lr-pk} + \Delta i_{Lk} = \frac{2C_j V_{in}}{t_d},\ j = 1, 2, 3, 4 \tag{3.23}$$

From Eqn. (23), the value of switch output capacitor is obtained as

$$C_j = \frac{(i_{Lr-pk} + \Delta i_{Lk})(t_d)}{2V_{in}},\ j = 1, 2, 3, 4 \tag{3.24}$$

For i_{Lr-pk} = 0.6875 A, Δi_{Lk} = 13%, t_d = 100 ns, and V_{in} = 66 V, the value of C_j is calculated as $C_j = 629pF$. Hence in order to get the ZVS within 100 ns the switch output capacitor C_j must be less than 629 pF.

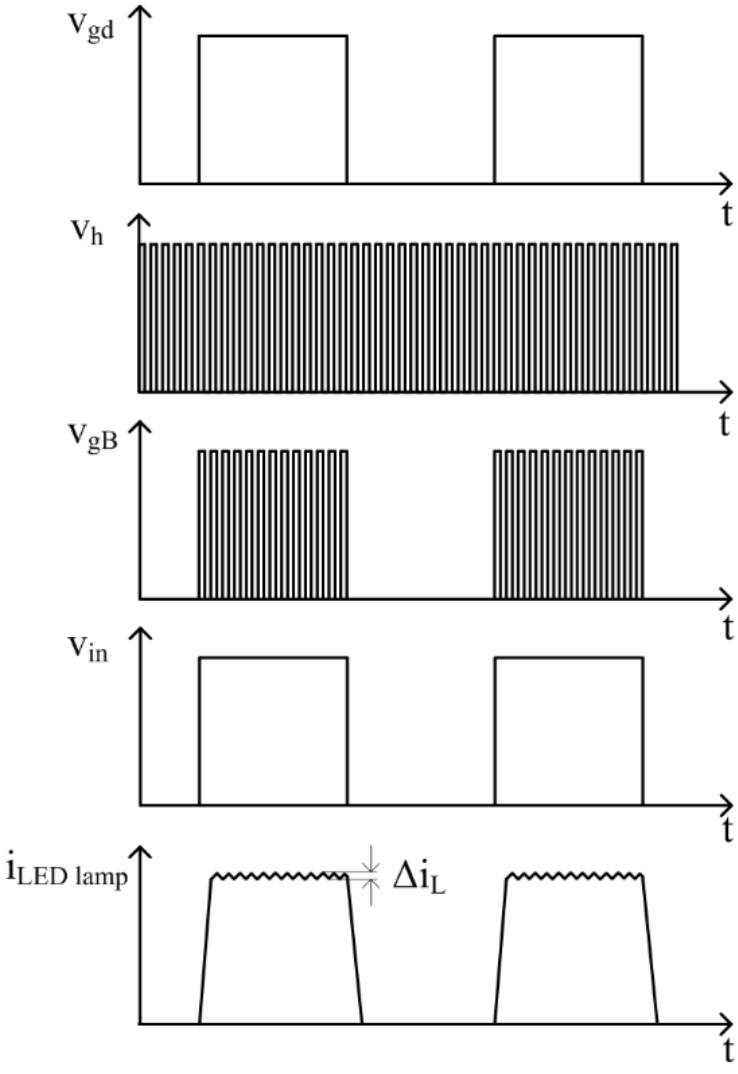

Figure 3.6 Gate signals of dimming and buck-boost switches, bridge circuit input voltage and LED lamp current under dimming control

3.4 Dimming Control and Current Regulation

Dimming can be achieved by amplitude modulation (AM) or pulse width modulation (PWM). In AM, dimming is attained by controlling the dc current through LED strings. As LED current is not constant, AM dimming causes chromaticity variations which is undesirable for sensitive lighting applications. Also, AM dimming does not provide wide dimming range due to nonlinear current-voltage characteristics of LED. To avoid aforementioned limitations, PWM dimming methods have been widely used. Here, the average current through LED is controlled by turning on and off the LED at a low frequency at nominal current. It offers high dimming range without chromaticity variations and provides smooth dimming. To incorporate dimming into the proposed LED driver, an ON-OFF control switch is connected in series with input dc source. This switch turns ON and OFF the whole converter by using a low frequency gate signal. Hence average current through each LED lamp is changed and brightness of each LED lamp is controlled. The dimming frequency is selected as 100 Hz, to overcome noticeable flickers.

A buck-boost converter is connected in series with input dc source as shown in Figure 3.1 (a) to regulate LED lamp currents against input voltage variations. This is an essential feature required in battery operated systems. The buck- boost converter is always in operation to provide control over variation in input voltage and its control signal must be synchronized with that of on-off switch. Gate signal (v_{gB}) for switch S_B of buck-boost converter is derived by ANDing a low frequency (100 Hz) control signal (v_{gd}) of dimming switch with a high frequency (100 kHz) signal (v_h) as shown in Figure 3.6. Bridge input voltage V_{in} and LED lamp current during dimming control are also shown in Figure 3.6.

3.5 Simulation and Experimental Results

In order to verify the feasibility of the proposed LED driver, a 145 W prototype has been developed. The proposed driver is first simulated using OrCAD PSpice software and then experimental prototype has been designed and tested. The parameters of the proposed driver are given in Table 3.1. For convenience, the dc voltages V_{DC1} and V_{DC2} are selected as 48 V and 12 V respectively. Low input voltage to buck-boost helps in operating it at high duty cycle. The remaining 6 V is supplied by capacitor *C*. The block diagram of control circuit of proposed circuit is shown in Figure 3.7. The picture of experimental prototype and setup are shown in Figure 3.8 (b) and (c) respectively. In order to verify the soft switching feature of the driver, experimental switch voltage and switch current waveforms are shown in Figure 3.9. The current

and voltage across L_r are indicated in Figure 3.10. Figure 3.11 shows the simulation waveforms of the proposed driver at full illumination level. Figure 3.12 shows the corresponding experimental waveforms. It is observed that experimental results are in good agreement with simulation results. It is also observed that switches are turned ON and OFF at zero voltage. With ZVS, switching losses are reduced. Also, switches are conducting only the difference in lamp currents and i_{Lr}. Thus conduction losses are also reduced. Hence the efficiency of the proposed driver is high and efficiency of the driver at full illumination level is found to be 93.88%.

Table 3. 1 Parameters of the proposed LED driver

Parameter Description	**Value / Model no.**
DC Input voltage, V_{in}	66 V
Number of LEDs used	80
LED operating current, $I_{operated}$	550 mA
Switching frequency, f_s	200 kHz
Duty ratio of switches in bridge configuration	0.5
L_1, L_2, L_3, and L_4	577 µH
L_r	120 µH
PWM dimming frequency	100 Hz
Duty ratio of dimming switch S_d	0 to 1
Frequency of buck-boost converter	100 kHz
Switching devices used	MOSFET IRF640N
Control ICs used	UC3875 and SG3525
Driver ICs used	IR2110, IR2117 and MIC4425

Figure 3.13 and 3.14 show the simulation and experimental results with 60% of dimming control respectively. The switching devices of the bridge configuration are operated at 200 kHz and at a duty cycle of 0.5. The dimming switch and buck-boost switch operations are synchronized to prevent input voltage fluctuations. The input voltage V_{in}, LED lamp currents, and voltages are at their operating values when the dimming switch is ON and they become zero when it is OFF. It is observed that the experimental results are in good agreement with simulation results and efficiency is found to be 94.96%.

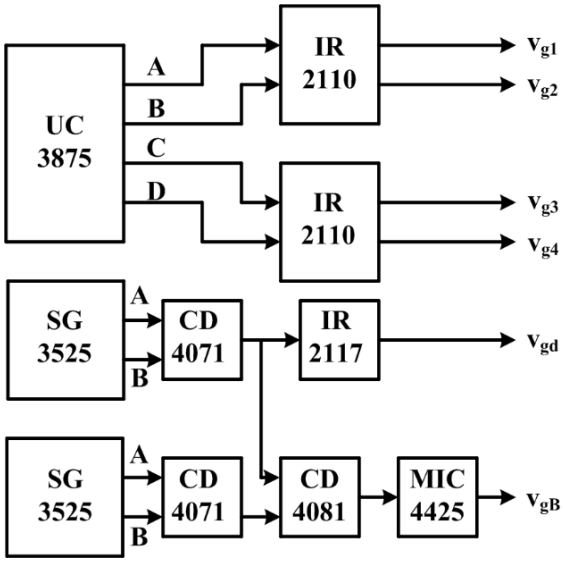

Figure 3.7 Block diagram of control circuit

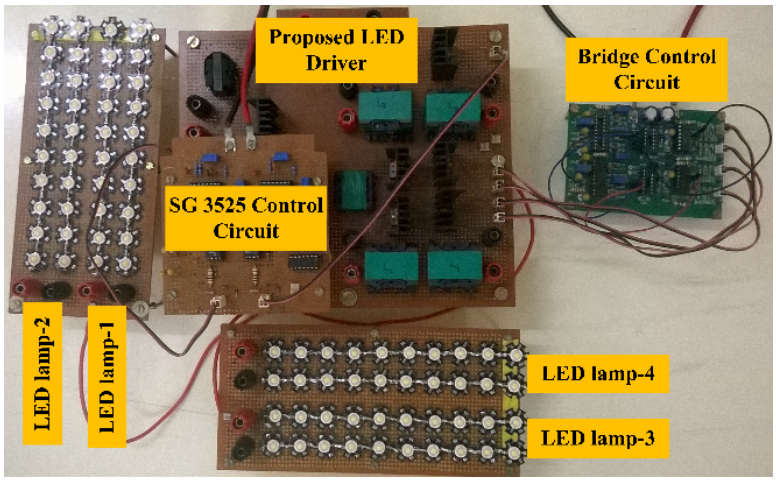

(a)

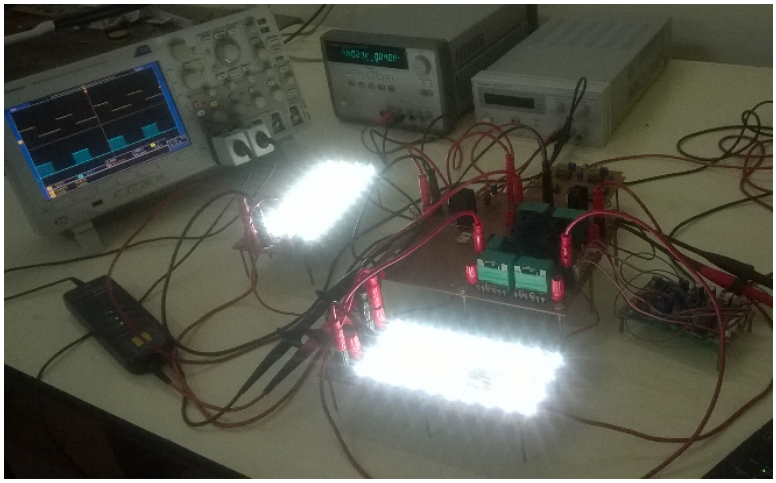

(b)

Figure 3.8 (a) Experimental prototype (b) Experimental setup

The proposed LED driver may be applicable to battery operated systems. Consider that dc voltages V_{dc1} and V_{dc2} are obtained through batteries. Figure 15 (a) shows capacitor voltage when V_{dc1} = 48 V and V_{dc2} = 12 V. Now input voltage to the bridge circuit is 66 V. If the battery voltages are reduced by 5%. i.e. V_{dc1} = 45.6 V and V_{dc2} = 11.4 V, the capacitor has to compensate the reduction in input voltage i.e. 9 V. The duty cycle of buck-boost converter is changed accordingly. Corresponding efficiency is found to be 92.46% and capacitor voltage waveform is shown in Figure 15 (b). Similarly, if the battery voltages are reduced by 10%, duty cycle is adjusted so that the capacitor can compensate 12 V. Corresponding efficiency is found to be 91.37% and capacitor voltage waveform is shown in Figure 15 (c). The efficiency curve of the proposed LED driver at various dimming levels is shown in Figure 15 (d). It is observed that a high efficiency is guaranteed at any dimming level. A relative comparison between H-bridge LED driver topologies and proposed topology is given in Table 3.2. It is observed that the number of diodes and capacitors are less in proposed configuration. And also it does not use high frequency transformer and rectifier stage. This feature considerably reduces the cost, weight, and volume. Besides, proposed driver circuit features soft switching, reduced current stress and high efficiency with dimming capability.

Table 3. 2 Comparison between H-bridge topologies and proposed topology

H-bridge topology	**Branas et al. [53]**	**Luo et al.[55]**	**Qu et al.[58]**	**Proposed topology**
Power switches	**4**	**4**	6	6
Diodes	2	8	4	**1**
Inductors	3	6	**2**	6
Capacitors	3	6	7	**1**
High frequency transformer	1	1	1	**0**
High frequency rectifier stage	1	2	4	**0**
LED lamps	1	2	**4**	**4**
Efficiency	>87%	>92%	>91%	**>93%**

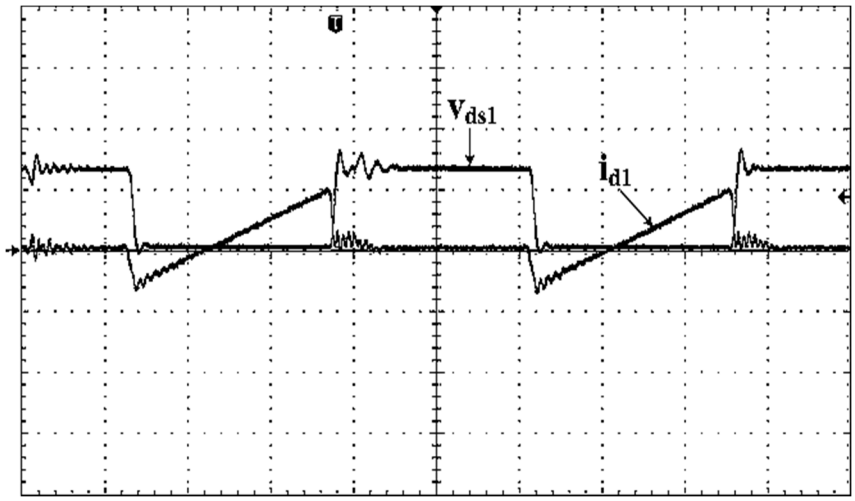

(a) Voltage and current in Switch S_1 (v_{ds1}: 50 V/div; i_{d1}: 1 A/div; time: 1 μs/div)

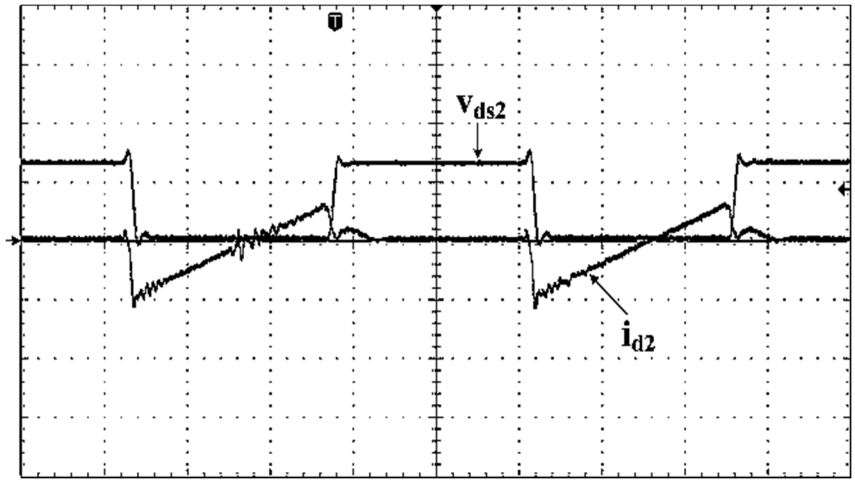

(b) Voltage and current in S_2 (v_{ds2}: 50 V/div; i_{d2}: 1 A/div; time: 1 μs/div)

Figure 3.9 Experimental switching waveforms

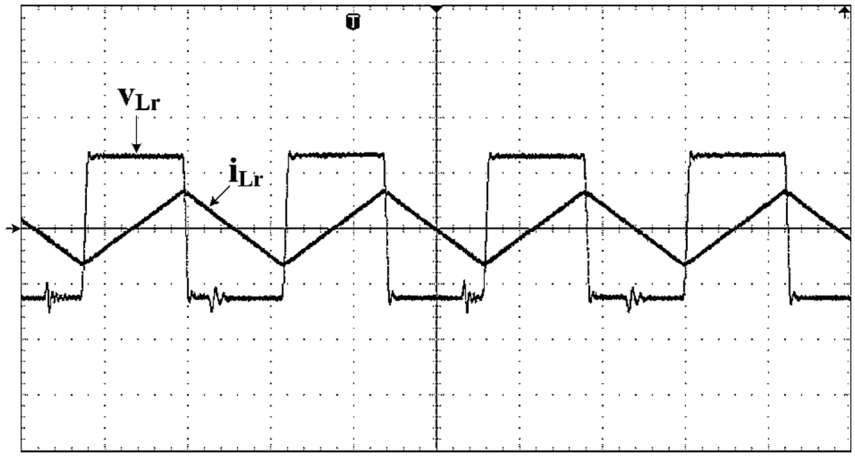

Figure 3.10 Voltage and current in L_r (v_{Lr}: 50 V/div; i_{Lr}: 1 A/div; time: 2 μs/div;)

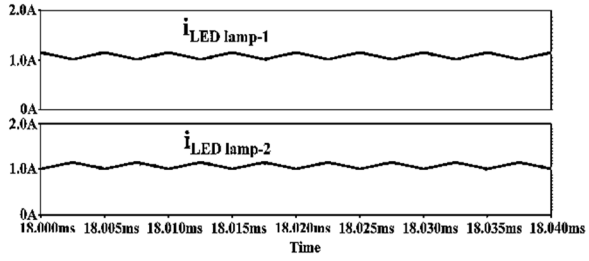

(a) Lamp-1 and lamp-2 currents

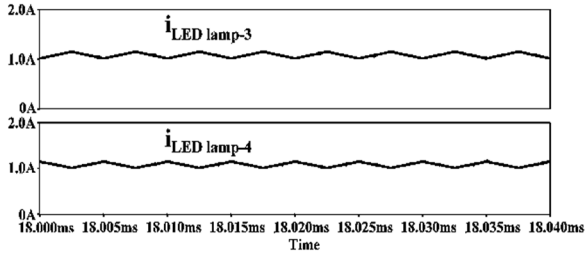

(b) Lamp-3 and lamp-4 currents

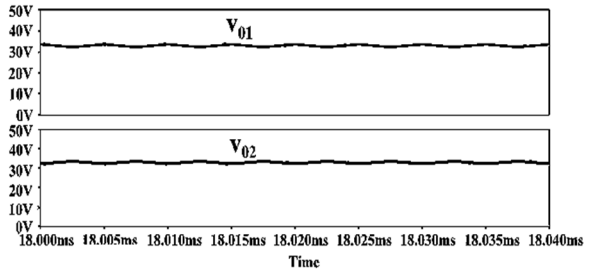

(c) Lamp-1 and lamp-2 voltages

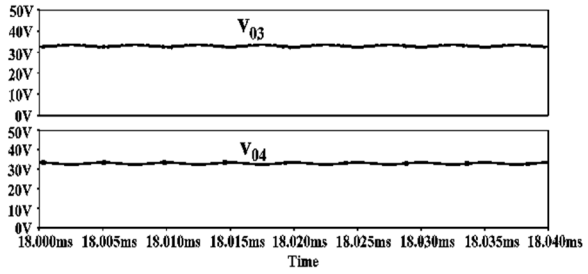

(d) Lamp-3 and lamp-4 voltages

Figure 3.11 Simulation waveforms at full illumination level

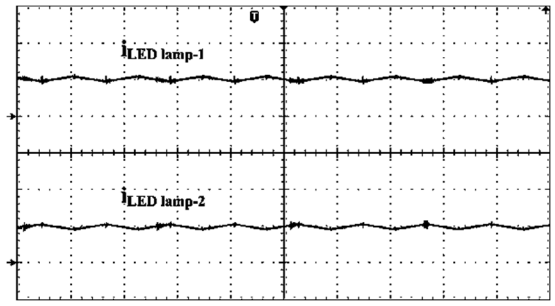

(a) Lamp-1 and lamp-2 currents

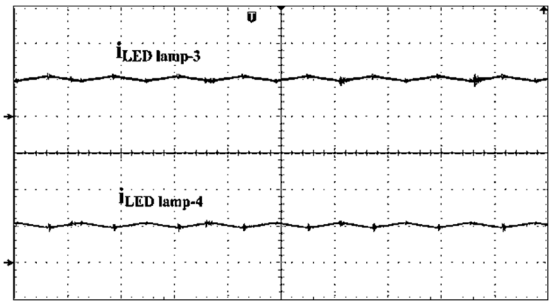

(b) Lamp-3 and lamp-4 currents

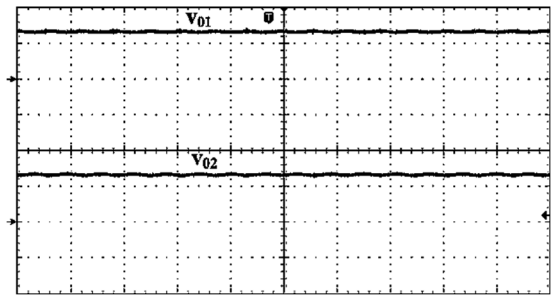

(c) Lamp-1 and lamp-2 voltages

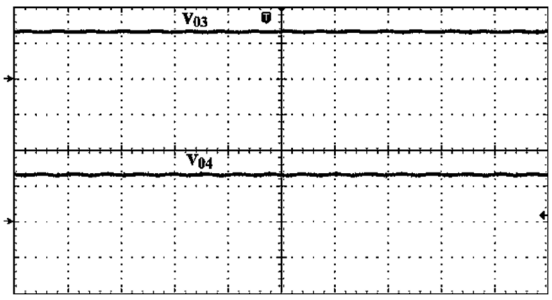

(d) Lamp-3 and lamp-4 voltages

Figure 3.12 Experimental waveforms at full illumination level (current: 1 A/div; voltage: 25 V/div; time: 8 μs/div)

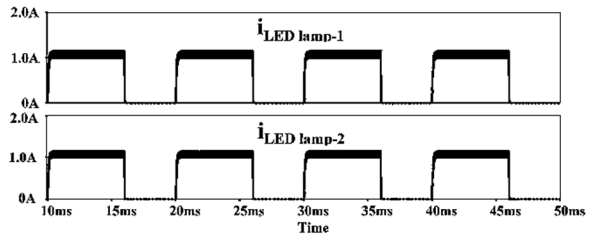

(a) Lamp-1 and lamp-2 currents

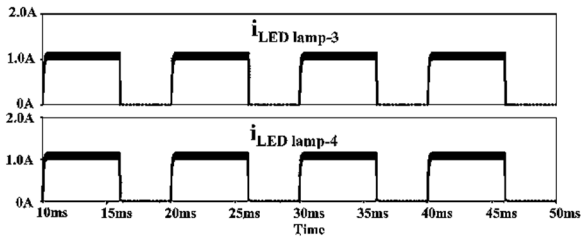

(b)) Lamp-3 and lamp-4 currents

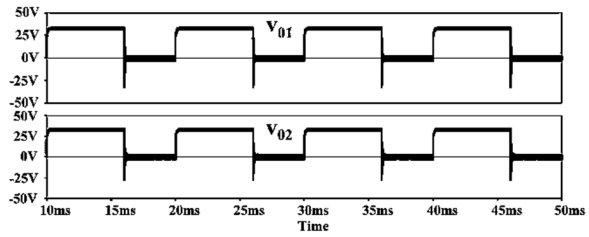

(c) Lamp-1 and lamp-2 voltages

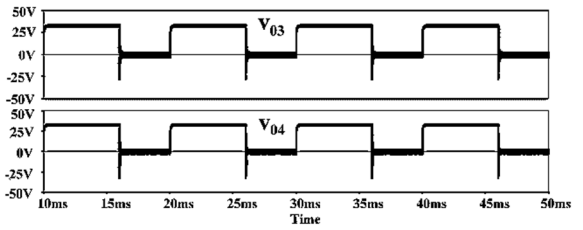

(d) Lamp-3 and lamp-4 voltages

Figure 3.13 Simulation waveforms with 60% dimming control

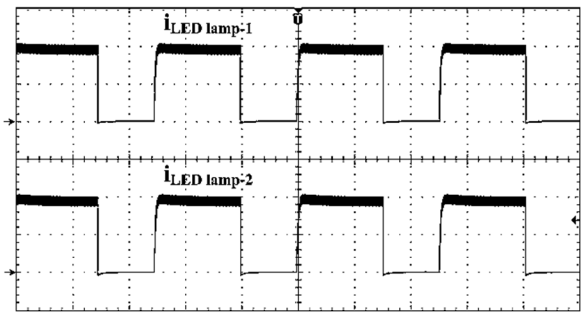

(a) Lamp-1 and lamp-2 currents

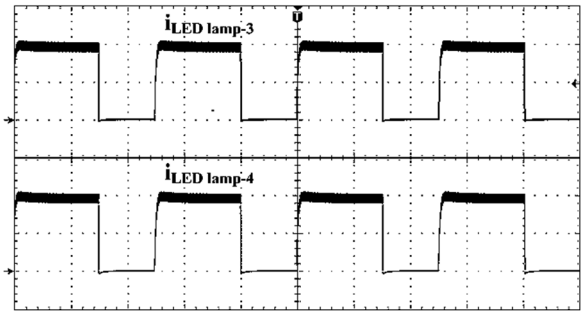

(b) Lamp-3 and lamp-4 currents

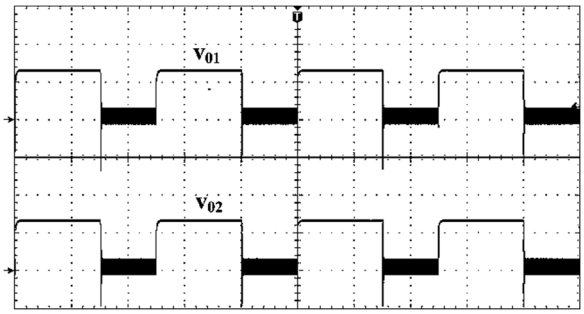

(c) Lamp-1 and lamp-2 voltages

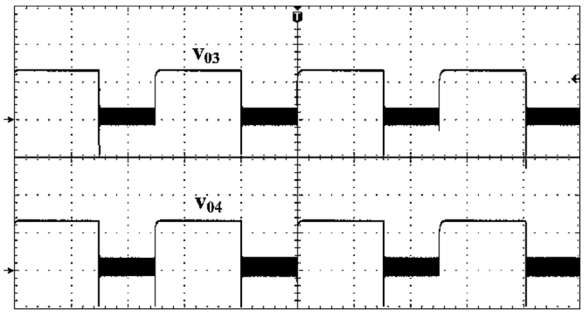

(d) Lamp-3 and lamp-4 voltages

Figure 3.14 Experimental waveforms with 60% dimming control (current: 0.5 A/div; voltage: 25 V/div; time: 4 ms/div)

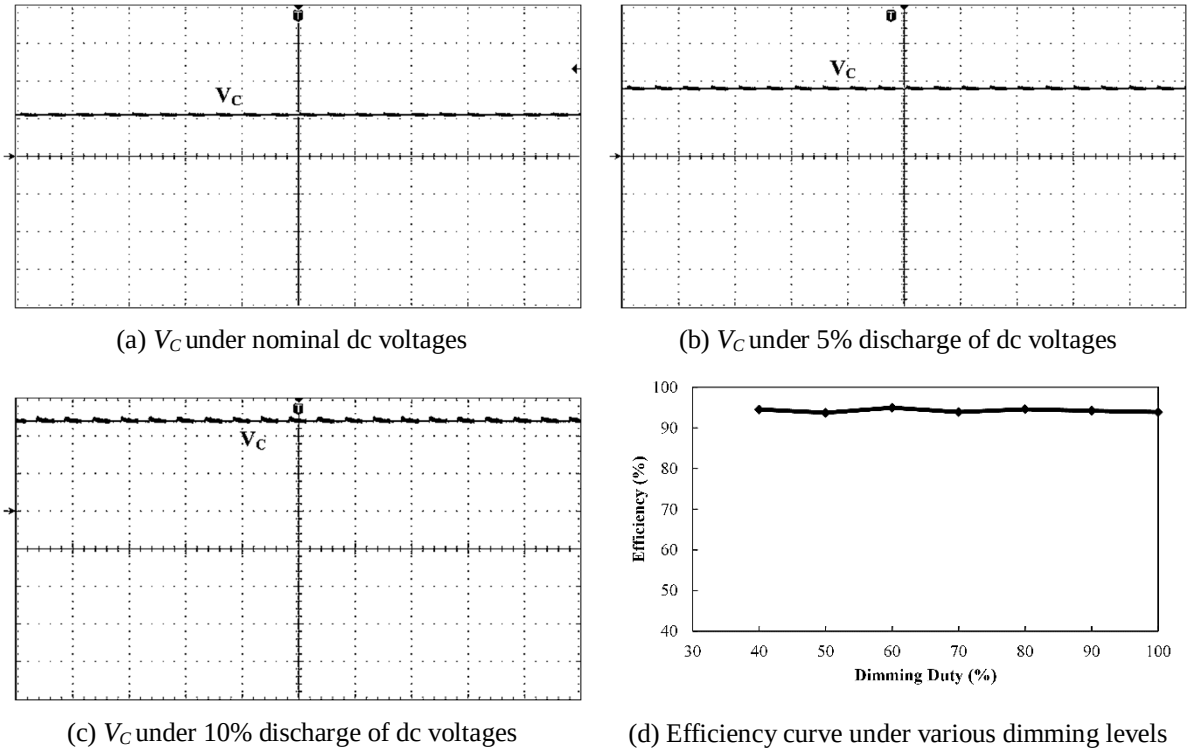

(a) V_C under nominal dc voltages

(b) V_C under 5% discharge of dc voltages

(c) V_C under 10% discharge of dc voltages

(d) Efficiency curve under various dimming levels

Figure 3.15 Capacitor voltage waveforms and efficiency curve (V_C: 5 V/div; time: 20 ms/div;)

3.6 Conclusions

In this chapter, a full-bridge converter for LED based street lighting application is presented. The switches in full-bridge are operated with constant duty ratio. The proposed configuration is studied in detail for its performance. Modes of operations and analysis are explained clearly. To validate experiment results with simulation results, a 146 W prototype is implemented. Experimental results are in good agreement with simulation results. This configuration is suitable for high power lighting applications.

The proposed configuration has the following advantages:

a) The current in bridge devices is almost independent lamp currents.
b) ZVS is obtained bridge devices.
c) Both switching and conduction losses are less.
d) Dimming operation is achieve for all lamps.
e) Input voltage is controlled for regulating LED lamp current.
f) High efficiency is obtained at both full and dimming levels.
g) Components count per lamp as well as the cost of the driver is less.

h) This configuration can be extended to multiple LED lamps by addition legs in bridge.

i) This configuration can be powered from battery operated systems.

The limitation of proposed converter is lack of independent dimming of LED lamps.

The next chapter proposes an efficient ripple free LED driver with zero-voltage switching for street lighting applications.

Chapter 4

An Efficient Ripple Free LED Driver with Zero-Voltage Switching for Street Lighting Applications

Chapter 4

An Efficient Ripple Free LED Driver with Zero-Voltage Switching for Street Lighting Applications

This chapter proposes an efficient ripple free light-emitting diode (LED) driver circuit. The proposed driver circuit utilizes a full-bridge configuration. The LED lamp current is the sum of two inductor currents which are out of phase. This makes the LED lamp current ripple free. Larger portion of lamp power is supplied by the dc voltage source connected in series with LED lamp. Small amount of power is processed by bridge circuit. An experimental prototype of 87 W has been developed and tested at full load and different dimming levels. Simulation results are verified by experimental results.

4.1 Proposed LED Driver Circuit Configuration

The proposed LED driver circuit is shown in Figure 4.1. It uses a full bridge configuration consisting of four power MOSFETs S_1, S_2, S_3, and S_4. $D_1 - D_4$ are the intrinsic body diodes of power MOSFETs and $C_1 - C_4$ indicate either the output capacitances of power MOSFETs or external capacitors. Two identical LED lamps are used in this circuit. Four inductors L_1, L_2, L_3 and L_4 of equal values are connected to LED lamps as shown in Figure 4.1. An inductor L_r is used in the circuit to provide ZVS operation in bridge devices. A dc voltage source (i.e. battery) of value which is slightly less than threshold voltage of each LED lamp is connected in series with each LED lamp. Majority of LED lamp power is supplied directly by corresponding voltage source. Small amount of power is processed through full bridge converter which acts as a current regulator. The concept of interleaving or multi-phasing has been utilized in full bridge converter. With this, each inductor L_1 and L_3 conduct half of the LED lamp-1 current. Similarly the inductors L_2, and L_4 conduct half of the LED lamp-2 current. This full- bridge configuration is powered by dc sources V_{DC1} and V_{DC2}. In order to regulate the input voltage (V_{in}) to the bridge circuit, a buck-boost converter is introduced with V_{DC2} as its input voltage. Now V_{in} is sum of V_{DC1}, V_{DC2} and V_C, where V_C is the output of buck-boost converter. In this proposed configuration, bridge converter processes only small portion of each LED lamp power. Hence the size of reactive components, and the voltage and current stress of bridge devices are reduced. To integrate dimming feature into the proposed configuration, a switch S_d has been connected in series with full bridge and is operated at low frequency.

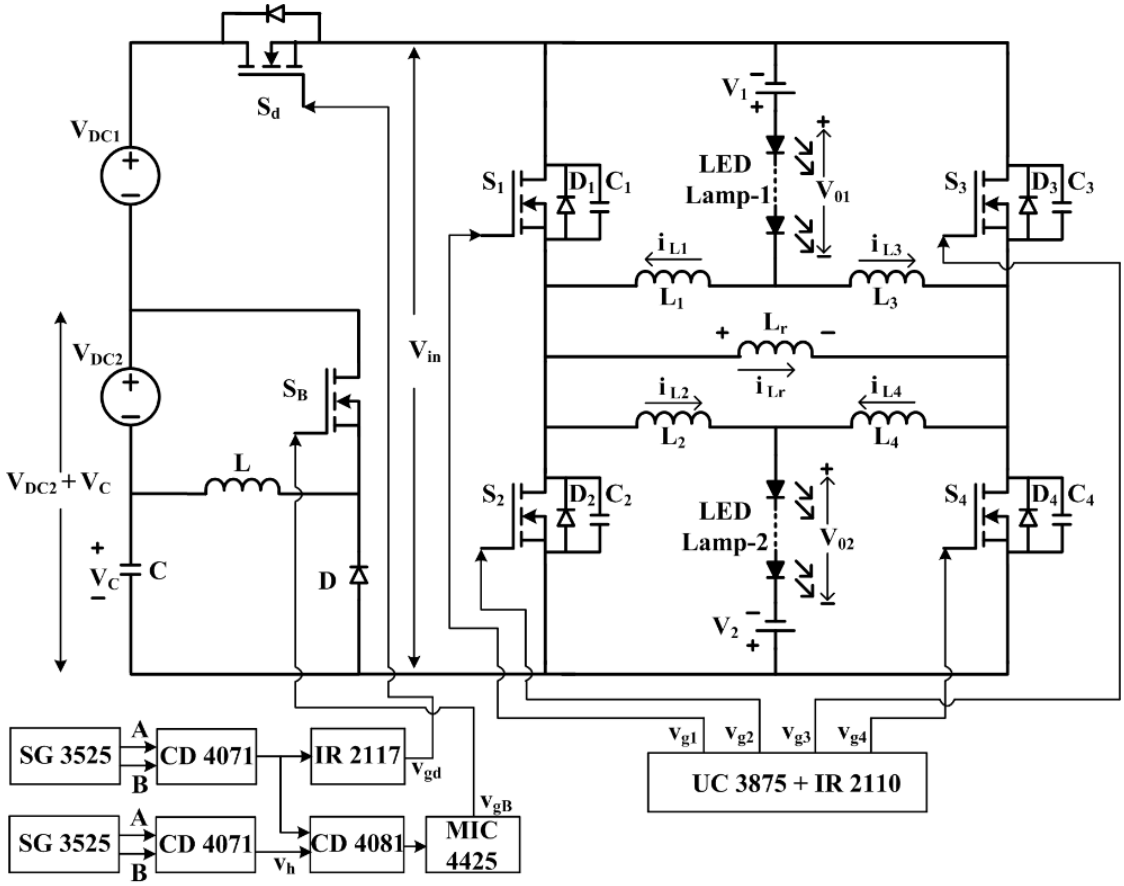

Figure 4.1 Schematic of proposed LED driver

4.2 Principle of Operation and Analysis of the Proposed LED Driver

The operating principle and circuit analysis of the proposed LED driver are discussed in the following sections.

4.2.1 Operation of the proposed driver

The switches in each leg of full bridge converter are alternately turned on and off with fixed duty cycle at fixed switching frequency. That means, in a switching cycle, S_1 and S_4 are on for 50% duty cycle and off for remaining period. Similarly S_2 and S_3 are on for 50% duty cycle and off for remaining period. A dead time is introduced between switching pulses of each leg to avoid short circuit across the dc power supply. As the dead times are very small, the LED lamp current and i_{Lr} are assumed to be constant during dead time. Figure 4.2 shows the operating waveforms of the proposed LED driver. The operation of proposed configuration can be divided into four modes. The equivalent circuit and conduction path for each mode where the input voltage V_{in} is represented by a voltage source are shown in Figure 4.3. Under all conditions of

V_{DC1} and V_{DC2}, V_{in} is kept constant. This is achieved by controlling V_C which is the output voltage of buck-boost converter by a gate driving signal v_h. Due to constant nature of V_{in}, duty cycle of switches S_1 to S_4 are also constant. This helps in achieving ZVS operation of S_1 to S_4. Also, this is helpful in reducing switching losses in switching devices. Devices in bridge circuit allow only ripple in load inductor and ZVS inductor. Hence conduction losses are also reduced. Reduction in ripple current in LED helps in reducing the size of inductors, reducing cost, space and weight of the system. Different modes of operations are explained below:

4.2.1.1 Mode I (t_0-t_1)

This mode begins when the switches S_1 and S_4 are switched on at zero voltage. The equivalent circuit of mode-I is shown in Figure 4.3 (a). In this mode, inductor L_2 and L_3 are energized linearly because of positive voltage across L_2 and L_3. At the same time, inductor L_1 and L_4 are free wheeled linearly because of negative voltage across L_1 and L_4. Thus the sum of currents through L_1 and L_3 which are 180^o out of phase flow through LED lamp-1 leading to ripple cancellation. Similarly the ripple free current through LED lamp-2 is obtained by the sum of current through L_2 and L_4 which are also 180^o out of phase. The current i_{Lr} rises up linearly through the switches S_1 and S_4 due to the application of positive voltage V_{in} across inductor L_r. The current stress on S_1 and S_4 is significantly reduced as only difference of i_{L2} and i_{L1} flows through S_1 along with i_{Lr} and difference of i_{L3} and i_{L4} flows through S_4 along with i_{Lr}. Therefore conduction losses mainly depend on i_{Lr}. This mode ends at t_1 where the current i_{Lr} reaches maximum.

4.2.1.2 Mode II (t_1-t_2)

This mode begins after removing gate signals for switches S_1 and S_4, which are carrying positive currents. The equivalent circuit of mode-II is shown in Figure 4.3 (b). The inductor L_r is used to achieve zero voltage switching of devices. At t_1 switches S_1 and S_4 are switched off at zero voltage as there is no voltage across capacitor C_1 and C_4. None of the switches conduct during t_1-t_2. Capacitor C_1 is charged by current $(i_{Lr} + i_{L2} - i_{L1})/2$ while the capacitor C_2 is discharged. Similarly, the current $(i_{Lr} + i_{L3} - i_{L4})/2$ charges the capacitor C_4 and discharges the capacitor C_3. The voltage across S_2 and S_3 decrease until D_2 and D_3 are forward biased. Now the switches S_2 and S_3 may be driven into on state by gate signal to ensure zero voltage switching. This mode ends when capacitors C_2 and C_3 are discharged from V_{in} to zero or C_1 and C_4 are charged from zero to V_{in}.

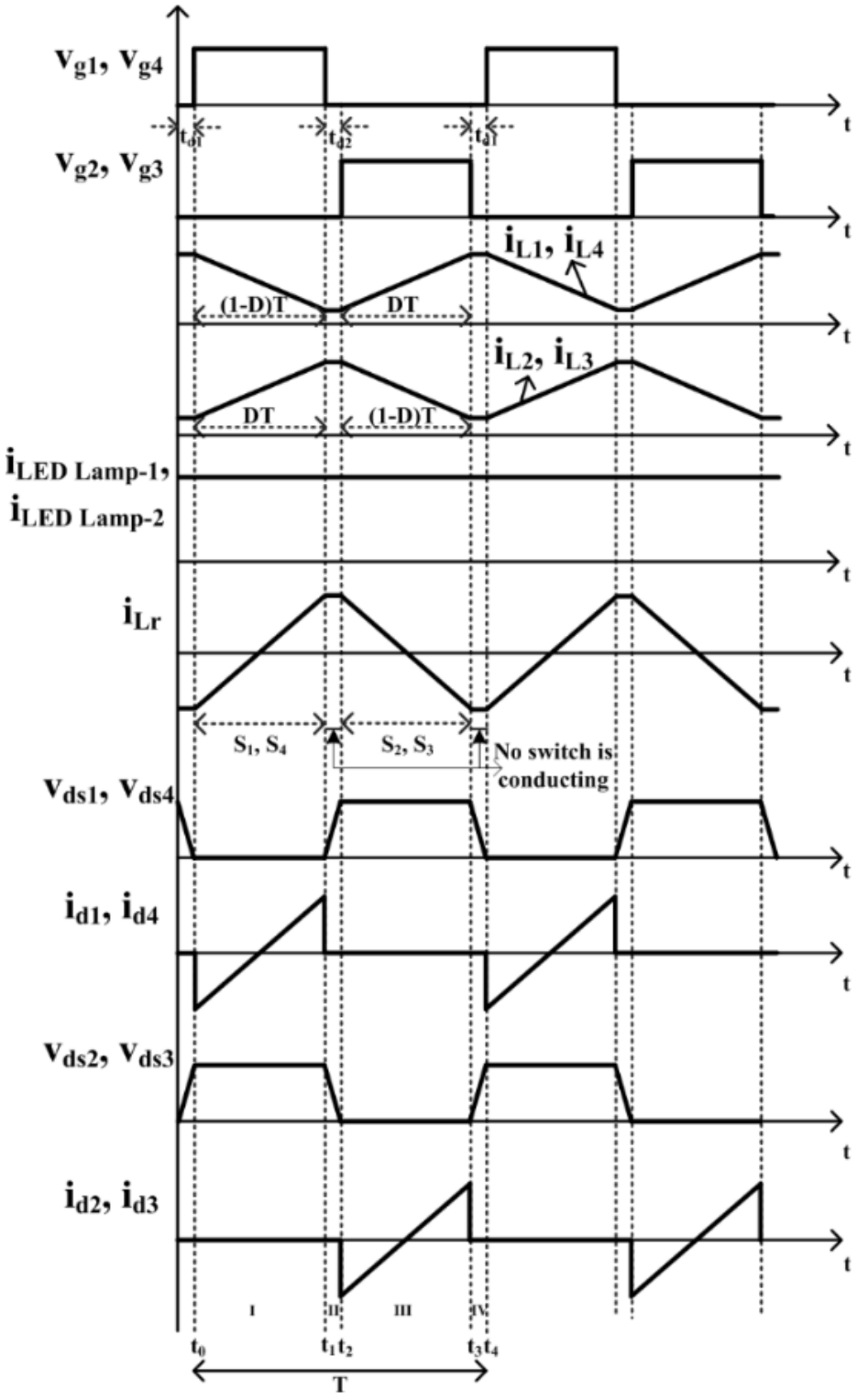

Figure 4.2 Operating waveforms

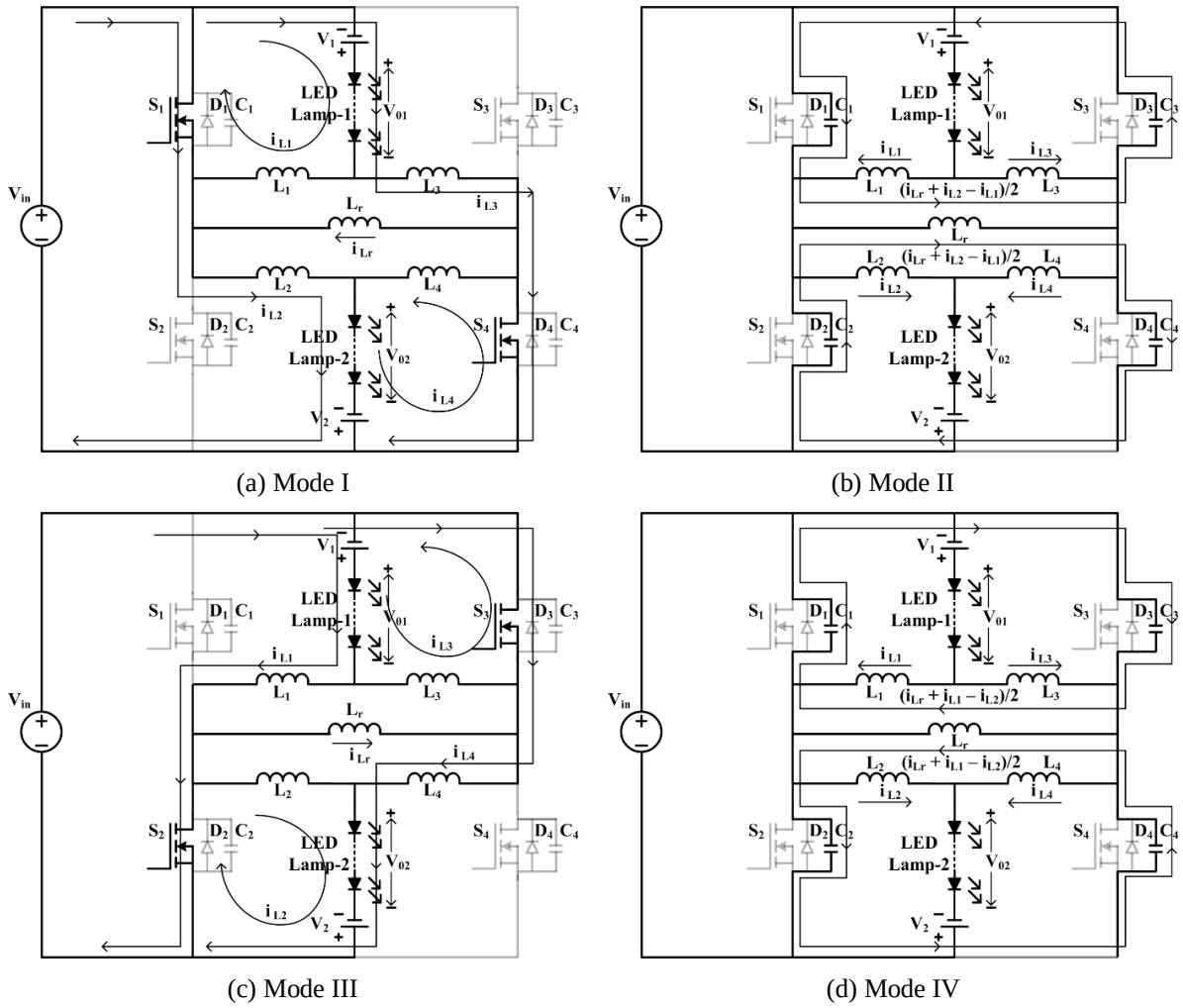

Figure 4.3 Equivalent circuits of proposed LED driver

4.2.1.3 Mode III (t_2-t_3)

Figure 4.3 (c) shows the equivalent circuit of mode-III. At t_2 gate pulses are given to switches S_2 and S_3 at zero voltage. In this mode, inductor L_1 and L_4 are charged linearly, while inductor L_2 and L_3 are discharged linearly. As it has been explained in Mode-I, a ripple free current flows in both lamps. The current i_{Lr} decreases linearly through the switches S_2 and S_3 due to the application of negative voltage V_{in} across the inductor L_r. In this mode also the current stress and conduction loss in S_2 and S_3 are significantly reduced. This mode ends at t_3 where the current i_{Lr} reaches minimum.

4.2.1.4 Mode IV (t_3-t_4)

At t_3 gate signals for switches S_2 and S_3 are withdrawn. The process of turning off of switches S_2, S_3 and turning on of switches S_1, S_4 with zero voltage is similar to that in mode III.

The equivalent circuit of this mode is shown in Figure 4.3 (d). This mode ends when capacitors C_1 and C_4 are discharged from V_{in} to zero or C_2 and C_3 are charged from zero to V_{in}.

4.2.2 Circuit analysis of the proposed LED driver

The following assumptions are considered to analyze the proposed circuit as LED driver:

i. The proposed converter is operating in steady state.
ii. The MOSFETs S_1, S_2, S_3, and S_4 are ideal.
iii. Current through inductors L_1, L_2, L_3, and L_4 are continuous.
iv. The two LED lamps are identical.
v. The voltage across each LED lamp is constant.

In this configuration, for control over LED lamp current, input voltage (V_{in}) is modulated. Input voltage (V_{in}) is derived as sum of two batteries V_{DC1}, V_{DC2} and V_C. A buck-boost converter with V_{DC2} as source produces a controllable voltage V_C for modulating V_{in}. The switches S_1 to S_4 are operated with constant duty cycle. This control makes on and off times equal for each switch. Since the two LED lamps and their operating currents are identical, the analysis is given for a single LED lamp, i.e LED lamp-1. At $t = t_0$, the switches S_1 and S_4 are switched-on. From the equivalent circuit shown in Figure 4.3 (a), voltage across inductor L_1 is expressed as

$$v_{L1} = -V_{01} + V_1 = L_1 \frac{di_{L1}}{dt} \qquad t_0 \le t < t_1 \tag{4.1}$$

The current through the inductor L_1 is obtained as

$$i_{L1}(t) = \frac{1}{L_1}\int_{t_0}^{t} v_{L1}(t)\,dt + i_{L1}(t_0) = \frac{-V_{01}+V_1}{L_1}(t-t_0) + i_{L1}(t_0) \quad t_0 \le t < t_1 \tag{4.2}$$

At the same time, the voltage across inductor L_3 is expressed as

$$v_{L3} = V_{in} + V_1 - V_{01} = L_3 \frac{di_{L3}}{dt} \qquad t_0 \le t < t_1 \tag{4.3}$$

The current through the inductor L_3 is obtained as

$$\begin{aligned} i_{L3}(t) &= \frac{1}{L_3}\int_{t_0}^{t} v_{L3}(t)\,dt + i_{L3}(t_0) \\ &= \frac{V_{in}+V_1-V_{01}}{L_3}(t-t_0) + i_{L3}(t_0) \end{aligned} \qquad t_0 \le t < t_1 \tag{4.4}$$

Where $i_{L1}(t_0)$, and $i_{L3}(t_0)$ are the initial currents in the inductor L_1 and L_3 respectively.

The current flowing through LED lamp-1 is given by

$$i_{\text{LED lamp -1}}(t) = i_{L1}(t) + i_{L3}(t) \tag{4.5}$$

From (4.2) and (4.4), the ripple current in inductor L_1 and L_3 are calculated as

$$\Delta i_{L1} = i_{L1}(t_1) - i_{L1}(t_0) = \frac{-V_{01} + V_1}{L_1}(t_1 - t_0) = \frac{-V_{01} + V_1}{L_1}(1 - D)T \tag{4.6}$$

$$\Delta i_{L3} = i_{L3}(t_1) - i_{L3}(t_0) = \frac{V_{in} + V_1 - V_{01}}{L_3}(t_1 - t_0) = \frac{V_{in} + V_1 - V_{01}}{L_3} DT \tag{4.7}$$

Where D is duty ratio of switches S_1 and S_4, and T is the switching period.

As the voltage across L_r is V_{in}, the current flowing through it increases linearly and is obtained as

$$i_{Lr}(t) = \frac{V_{in}}{L_r}(t - t_0) + i_{Lr}(t_0) \qquad t_0 \le t < t_1 \tag{4.8}$$

At $t = t_2$, switches S_2 and S_3 are switched-on. From the equivalent circuit shown in Figure 4.3 (c), voltage across inductor L_1 is expressed as

$$v_{L1} = V_{in} + V_1 - V_{01} = L_1 \frac{di_{L1}}{dt} \qquad t_2 \le t < t_3 \tag{4.9}$$

The current through the inductor L_1 is obtained as

$$\begin{aligned} i_{L1}(t) &= \frac{1}{L_1}\int_{t_2}^{t} v_{L1}(t)\, dt + i_{L1}(t_2) \\ &= \frac{V_{in} + V_1 - V_{01}}{L_1}(t - t_2) + i_{L1}(t_2) \end{aligned} \qquad t_2 \le t < t_3 \tag{4.10}$$

Similarly, the voltage across inductor L_3 is represented as

$$v_{L3} = -V_{01} + V_1 = L_3 \frac{di_{L3}}{dt} \qquad t_2 \le t < t_3 \tag{4.11}$$

The current through the inductor L_3 is obtained as

$$i_{L3}(t) = \frac{1}{L_3}\int_{t_2}^{t} v_{L3}(t)\, dt + i_{L3}(t_2) = \frac{-V_{01} + V_1}{L_3}(t - t_2) + i_{L3}(t_2) \quad t_2 \le t < t_3 \tag{4.12}$$

Where $i_{L1}(t_2)$, and $i_{L3}(t_2)$ are the initial currents in the inductor L_1 and L_3 respectively.

The current flowing through LED lamp-1 is given by

$$i_{\text{LED lamp -1}}(t) = i_{L1}(t) + i_{L3}(t) \tag{4.13}$$

From (4.10) and (4.12), the ripple current in inductor L_1 and L_3 are calculated as

$$\Delta i_{L1} = i_{L1}(t_3) - i_{L1}(t_2) = \frac{V_{in} + V_1 - V_{01}}{L_1}(t_3 - t_2) = \frac{V_{in} + V_1 - V_{01}}{L_1} DT \quad (4.14)$$

$$\Delta i_{L3} = i_{L3}(t_3) - i_{L3}(t_2) = \frac{-V_{01} + V_1}{L_3}(t_3 - t_2) = \frac{-V_{01} + V_1}{L_3}(1-D)T \quad (4.15)$$

Where D is duty ratio of switches S_1 and S_4 and T is the switching period.

Now the voltage across L_r is $-V_{in}$, the current flowing through it decreases linearly and is expressed as $i_{Lr}(t) = \frac{-V_{in}}{L_r}(t - t_2) + i_{Lr}(t_2) \qquad t_2 \le t < t_3$ (4.16)

By applying volt-sec balance either on L_1 or L_3 the voltage across LED lamp-1 is obtained as

$$[i_{L1}(t_1) - i_{L1}(t_0)] + [i_{L1}(t_3) - i_{L1}(t_2)] = 0 \text{ (or) } [i_{L3}(t_1) - i_{L3}(t_0)] + [i_{L3}(t_3) - i_{L3}(t_2)] = 0 \quad (4.17)$$

$$\begin{aligned} &\frac{-V_{01} + V_1}{L_1}(1-D)T + \frac{V_{in} + V_1 - V_{01}}{L_1} DT = 0 \text{ (or)} \\ &\frac{V_{in} + V_1 - V_{01}}{L_3} DT + \frac{-V_{01} + V_1}{L_3}(1-D)T = 0 \end{aligned} \quad (4.18)$$

$$V_{01} = DV_{in} + V_1 \quad (4.19)$$

Aforementioned analysis will also be applicable to LED lamp-2. Therefore ripple current through L_2, L_3, and voltage across LED lamp-2 are obtained as

$$\Delta i_{L2} = \frac{V_{in} + V_2 - V_{02}}{L_2} DT = \frac{-V_{02} + V_2}{L_2}(1-D)T \quad (4.20)$$

$$\Delta i_{L4} = \frac{-V_{02} + V_2}{L_4}(1-D)T = \frac{V_{in} + V_2 - V_{02}}{L_4} DT \quad (4.21)$$

$$V_{02} = DV_{in} + V_2 \quad (4.22)$$

Due to identical nature of both LED lamps, the voltage across each lamp and ripple current through L_1, L_2, L_3, and L_4 are expressed as

$$V_{0j} = DV_{in} + V_j, \text{ where j = 1, 2} \quad (4.23)$$

$$\Delta i_{Lk} = \frac{V_{in} + V_j - V_{0j}}{L_k} DT = \frac{-V_{0j} + V_j}{L_k}(1-D)T, \text{ where } k = 1, 2, 3, 4 \quad (4.24)$$

The values of L_1, L_2, L_3, and L_4 for selected current ripple can be calculated from (4.24) under continuous current.

4.3 Design Considerations

To select the values of components of proposed converter, the equivalent parameters of LED load must be considered. According to approximated model of an LED, it can be represented by a series connection of a cut-in or threshold voltage V_{th}, a dynamic resistance r_d and an ideal diode [67]. In the proposed LED driver, two parallel strings are used for each LED lamp. In each LED string, 12 LEDs are connected in series. The operating point for each LED is chosen at 3.3 V, 550 mA. And the cut-in voltage of each LED is 2.32 V. Therefore each LED lamp has a total cut-in voltage of 27.84 V, a total operating voltage of 39.6 V, and a current of 1.1 A. Consequently power supplied by each lamp is 43.56 W.

The input voltage V_{in} to the bridge can be expressed from (4.23) as

$$V_{in} = \frac{V_{0j} - V_j}{D} \tag{4.25}$$

The series dc voltage for each LED lamp V_j is selected as 24 V because LED lamp does not conduct below cut-in voltage. It has been explained that duty ratio of each switch in bridge configuration is equal. Therefore with a duty ratio of 0.5, and V_{0j} of 39.6 V, the input voltage is calculated as

$$V_{in} = \frac{39.6 - 24}{0.5} = 31.2 \text{ V}$$

To calculate inductor value L_k, switching frequency and allowed current ripple must be selected. The inductor L_k supplies one half of LED lamp current, i.e. 0.55 A. Under continuous conduction mode, the value of ripple current through L_k must be less than 1.1 A.

From (4.24), the value of inductor L_k is expressed as

$$L_k = \frac{V_{in} + V_j - V_{0j}}{\Delta i_{Lk}} DT \tag{4.26}$$

For a switching frequency of 200 kHz and a Δi_{Lk} value of 0.55 A, the value of L_k can be calculated from (4.26)

$$L_k = \frac{31.2 + 24 - 39.6}{0.55}(0.5)(5.10^{-6}) \cong 71\ \mu\text{H}$$

To achieve ZVS during dead time, an appropriate current source is required to charge and discharge the switch output capacitors [65]. An inductor L_r has been used to provide the required constant current during dead time. Since the nature of current through L_r is triangular,

peak current needs to be considered for ZVS. And it is assumed that peak current is constant during dead time and its value is calculated as follows:

From (4.8), at $t = t_1$, $i_{Lr}(t)$ reaches maximum value and the value is obtained as

$$i_{Lr-pk} = \frac{V_{in}}{L_r}(t_1 - t_0) + i_{Lr}(t_0) = \frac{V_{in}}{L_r}(t_1 - t_0) - \frac{V_{in}}{L_r}(\frac{t_1 - t_0}{2}) = \frac{V_{in}}{2L_r}(t_1 - t_0) \quad (4.27)$$

Since the duration $(t_1 - t_0) = DT$, (4.27) can be represented as

$$i_{Lr-pk} = \frac{V_{in}DT}{2L_r} \quad (4.28)$$

With a duty ratio of 0.5, the peak current through the L_r is obtained as

$$i_{Lr-pk} = \frac{V_{in}T}{4L_r} \quad (4.29)$$

It is observed that the value of i_{Lr-pk} is inversely proportional to inductor L_r for a fixed value of V_{in} and T. For L_r value of 130 μH, i_{Lr-pk} is obtained as

$$i_{Lr-pk} = \frac{(31.2)(5)(10^{-6})}{(4)(130)(10^{-6})} = 0.3A$$

Selection of proper values of switch output capacitor is also needed to ensure ZVS. To calculate, it is assumed that the currents through L_k and L_r during dead time are constant. Considering that dead time $t_{d1} = t_{d2} = t_d$, current flowing through output capacitors during t_{d1} or t_{d2} is obtained as

$$i_{Lr-pk} + \Delta i_{Lk} = \frac{2C_m V_{in}}{t_d} \quad (4.30)$$

From (4.30), the value of switch output capacitor is expressed as

$$C_m = \frac{(i_{Lr-pk} + \Delta i_{Lk})(t_d)}{2V_{in}}, \text{ where } m = 1, 2, 3, 4 \quad (4.31)$$

For a t_d value of 100 ns, C_m can be found as from (4.31) as

$$C_m = \frac{(0.3 + 0.55)(100)(10^{-9})}{(2)(31.2)} \cong 1362 \ p\text{F}$$

Therefore to get ZVS within 100 ns, the switch output capacitor C_m must be selected less than the calculated value.

4.4 Dimming Control and Regulation of Lamp Current

Dimming control is an important feature in LED lighting applications which improves power saving. Amplitude modulation (AM) and pulse width modulation (PWM) are the two available methods for dimming control of LEDs. In AM, dimming is accomplished simply by controlling the level of dc current through LED strings. Whereas, in PWM dimming, the average current through LED is controlled by turning on and off the LED at a low frequency at nominal current. To prevent the drawbacks due to AM like color shift, limited dimming range etc. PWM dimming methods have been widely implemented. In addition, they provide smooth dimming. In the proposed LED driver, dimming is realized by connecting a switch S_d in series with input, which totally turns ON and OFF the bridge converter by using a low frequency gate signal. Therefore the average current through each LED lamp can be controlled without changing the operating current. To avoid noticeable flickers, the dimming frequency is selected to be 100 Hz.

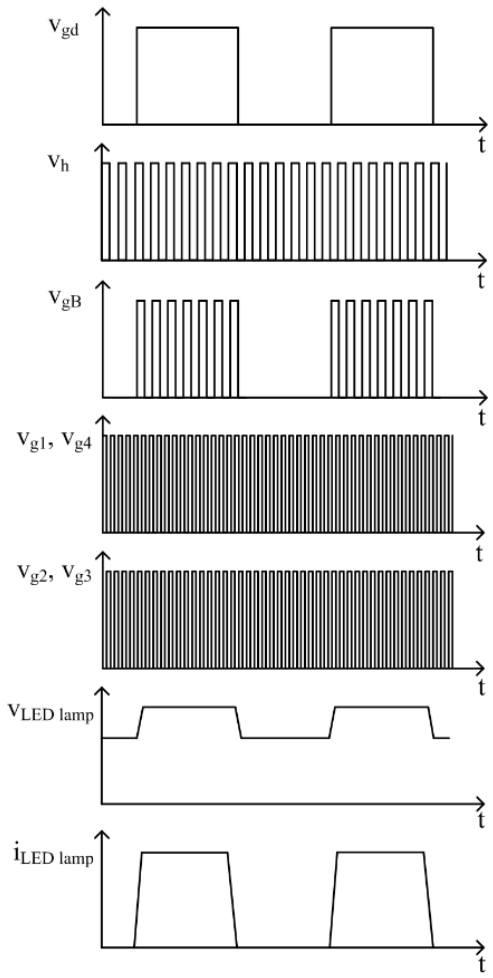

Figure 4.4 Gate signals of dimming, buck-boost switch and bridge devices, LED lamp voltage and current under dimming control

As it has been discussed that fixed duty cycle control is adopted for the switches in bridge configuration, LED lamps need to be regulated against variations in V_{in}, V_1, and V_2. Thus input voltage V_{in} is obtained by summing three dc voltages V_{DC1}, V_{DC2}, and V_C instead of supplying directly. With a buck-boost converter at the input side, the variations in V_{in}, V_1, and V_2 are compensated by controlling duty cycle of S_B. In order to reduce the power handled by buck-boost converter, the voltage V_C should be less than V_{DC2}. The switch S_B must be gated by a signal which is a combination of high frequency (100 kHz) signal (v_h) and low frequency (100 Hz) control signal (v_{gd}) of dimming switch to prevent overshoots in V_{in}. During dimming control, gate signals of dimming and buck-boost switches, voltage across and current through LED lamp are shown in Figure 4.4. The dc voltage sources V_1, V_2, V_{DC1}, and V_{DC2} can be obtained either from PV source or from rechargeable batteries like lead acid batteries.

Table 4. 1 Parameters of the proposed LED driver

Parameter Description	**Value / Model no.**
DC Input voltage, V_{in}	31.2 V
DC voltage source, V_1, V_2	24 V
Number of LEDs	48
LED operating current, $I_{operated}$	550 mA
Switching frequency, f_s	200 kHz
Duty ratio of switches in bridge configuration	0.5
L_1, L_2, L_3, and L_4	71 µH
L_r	130 µH
PWM dimming frequency	100 Hz
Duty ratio of dimming switch S_d	0 to 1
Capacitor, C	330 µF/25 V
Frequency of buck-boost converter	100 kHz
Switching devices used	MOSFET IRF640N
Control ICs used	UC 3875 and SG 3525
Driver ICs used	IR 2110, IR 2117 and MIC4425

4.5 Simulation and Experimental Results

In order to verify the feasibility of the proposed LED driver, an 87 W prototype has been simulated using OrCAD PSpice software and tested experimentally. The parameters used in the proposed driver are shown in Table 4.1. The experimental prototype and setup of the proposed LED driver are shown in Figure 4.5 (a) and (b) respectively. Voltage and current waveforms of

switch S_1 and S_2 are shown in Figure 4.6 (a) and (b) respectively to show the zero-voltage switching conditions. Figure 4.7 shows the simulated waveforms obtained from the proposed driver at full illumination level, considering V_{DC1} = 12 V, V_{DC2} = 12 V, V_C = 7.2 V. The corresponding experimental waveforms are shown in Figure 4.8. It is observed that experimental results are in good agreement with simulation results. It can be seen that there are no ripples in voltage and current waveforms of LED lamps. It can be observed that switches are switched ON and OFF at zero voltage, resulting in negligible switching losses. Switches conduct only ripple current in L_k and i_{Lr}. Thus conduction losses are also minimized. It results in high efficiency and it is found to be 94.26% at full illumination level.

Figure 4.9 shows the simulated and experimental waveforms with dimming at 70% of full illumination (at 70% of average current of each LED lamp). The dimming switch and buck-boost switch operations are synchronized to prevent overshoots in V_{in}. For the on-state of dimming switch, voltage and current waveforms of each lamp are maintained at their operating values. On the contrary, for off-state of the dimming switch, current waveform drops to zero and voltage waveform falls below cut-in voltage of each lamp. It is observed that experimental waveforms are in good agreement with simulated waveforms and efficiency is found to be 92.73% at 70% of full illumination.

The proposed ripple free current LED driver can be powered from PV/battery operated systems. The experimental prototype has been powered with 4% and 8% discharge in all batteries respectively. In both cases, the duty ratio of buck-boost converter has been increased to keep the current through each LED lamp constant. And under these two conditions efficiencies are found to be 91.93% and 90.03% respectively.

The measured efficiencies of the proposed LED driver at various dimming levels are shown in Figure 4.10. It is observed that a high efficiency is guaranteed at any dimming level. A relative comparison between proposed topology and other works in literature for LED lighting applications is given in Table 4.2. It is observed that proposed configuration does not use high frequency transformer and rectifier stage. It considerably reduces the cost, weight and volume. In addition, this configuration has lesser number of diodes and capacitor. This configuration powers both the lamps with low input voltage. Besides, proposed driver circuit features ripple free current, soft switching, reduced current stress and high efficiency with dimming capability.

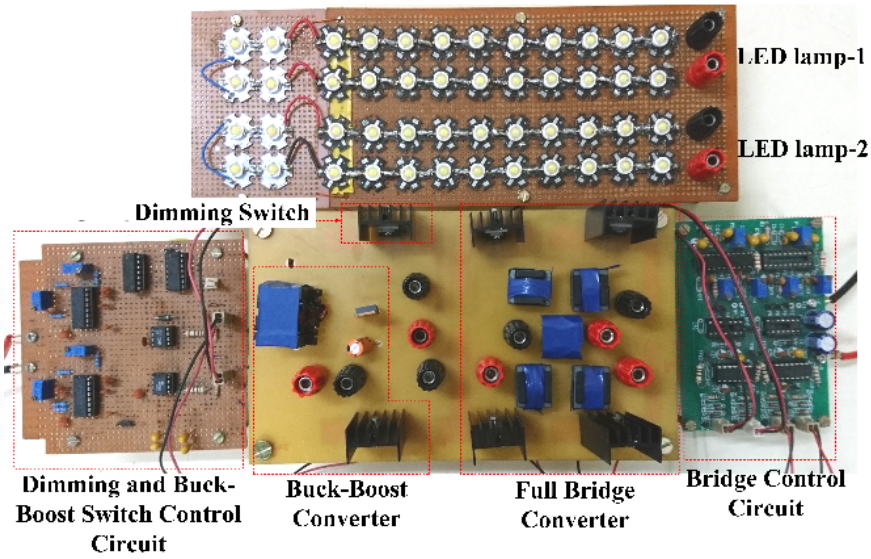

(a)

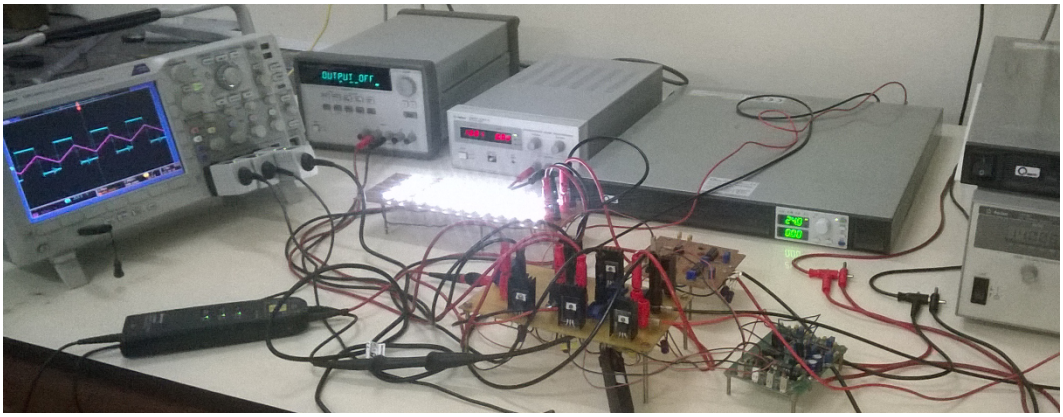

(b)

Figure 4.5 (a) Experimental prototype (b) Experimental setup

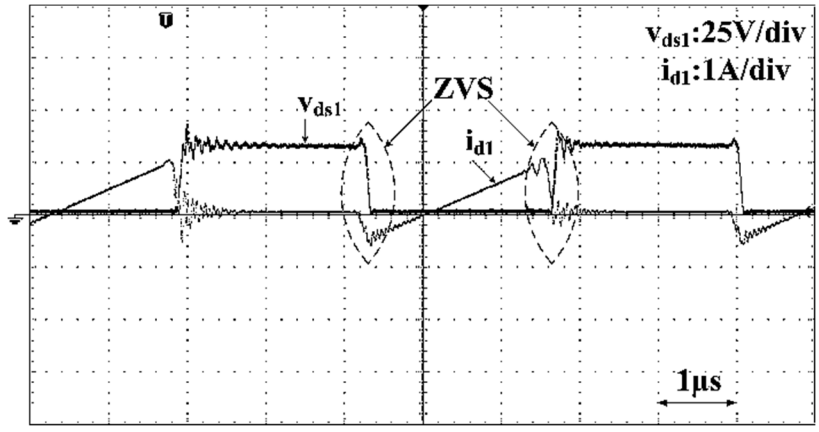

(a)

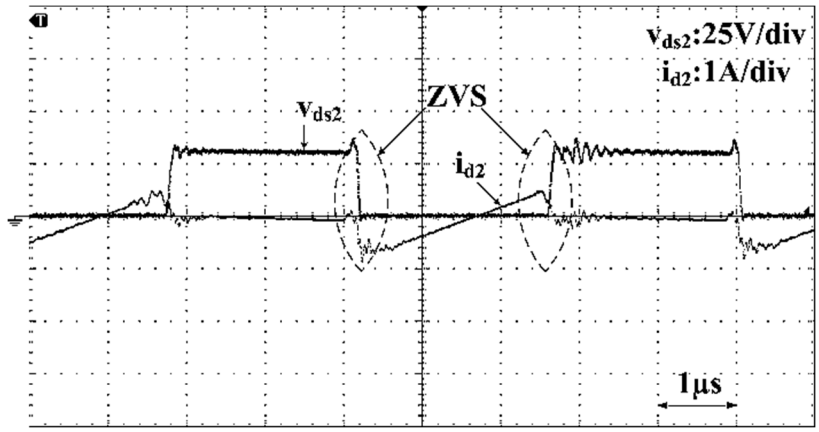

(c)

Figure 4.6 (a) Voltage and current in switch S_1 (b) Voltage and current in switch S_2

4.6 Extension of Proposed Driver Circuit to Multiple LED Lamps

The proposed driver configuration can be extended to multiple LED lamps. Two possible extensions for 4 LED lamps are shown in Figure 4.11 (a) and (b). In Figure 4.11 (a), an additional leg to the right of proposed configuration is added whose frequency and duty cycle are same as that of existing legs. In this configuration also, ripple free current flows through all the 4 identical lamps. DC voltage source V_1 supplies majority of lamp-1 and lamp-3 power directly. Similarly, DC voltage source V_2 processes majority of lamp-2 and lamp-4 power directly. Small amount of power for these four lamps is processed through bridge converter. In this, current stress on middle leg slightly increases compared to other legs. One more extension for 4 LED lamps is shown in Figure 4.11 (b). This is obtained by adding a full bridge to the right of proposed driver. Operating principle of this extension is similar to proposed configuration. Dimming and regulation of lamp currents for these two extensions can be achieved as that of proposed LED driver. Extension configuration with 4 legs has more

efficiency than with 3 legs. And also, it has uniform snubber capacitance though it has more switches. When the proposed configuration extended for more LED lamps, number of dc sources will remain same. Extensions are possible for more than 4 LED lamps also.

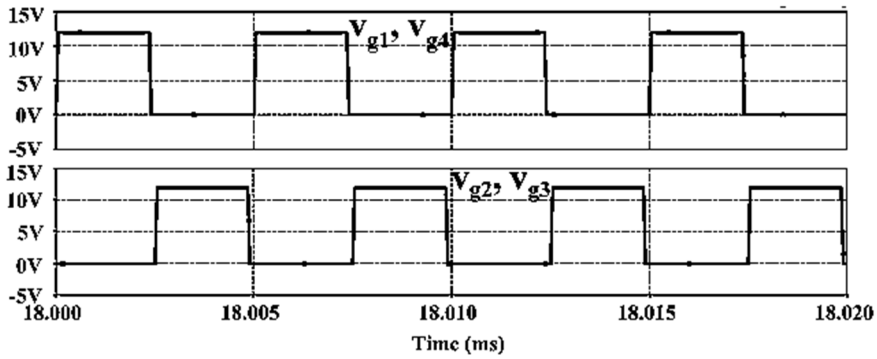

(a) Switching pulses of devices in bridge configuration

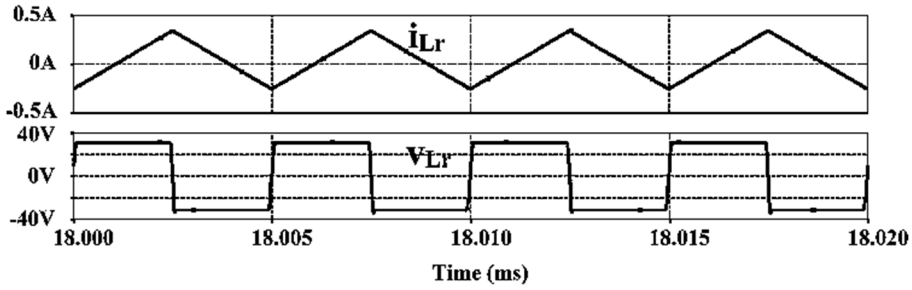

(b) Current and voltage waveform of L_r

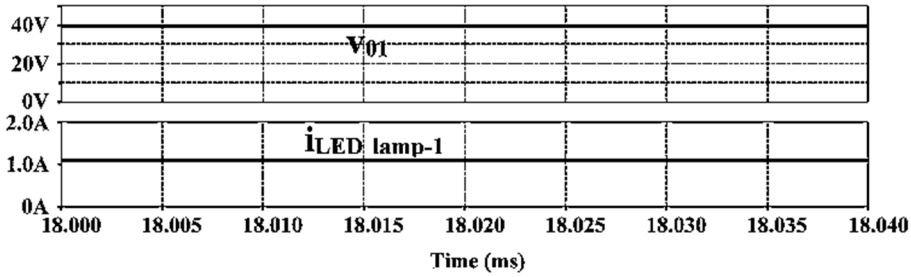

(c) Voltage and current of LED lamp-1

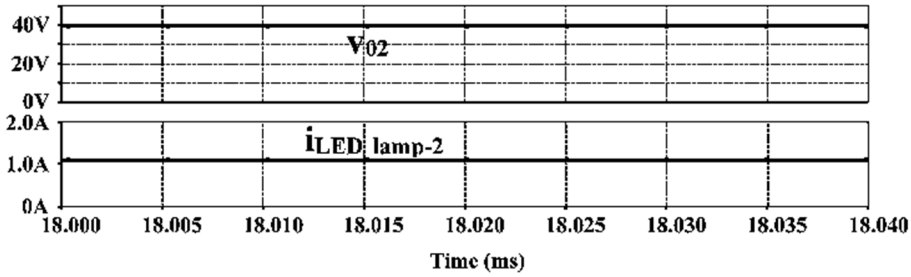

(d) Voltage and current of LED lamp-2

Figure 4.7 Simulation waveforms at full illumination level

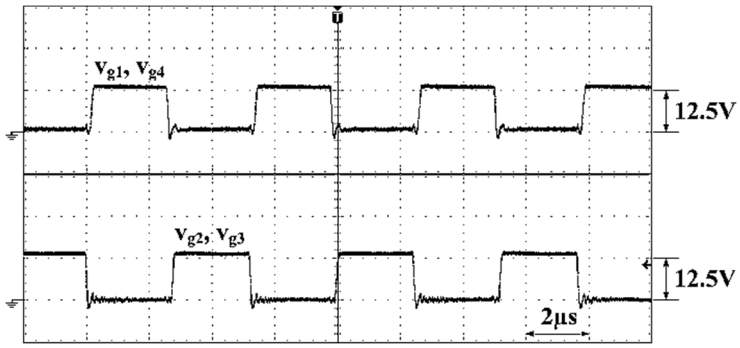

(a) Switching pulses of devices in bridge configuration

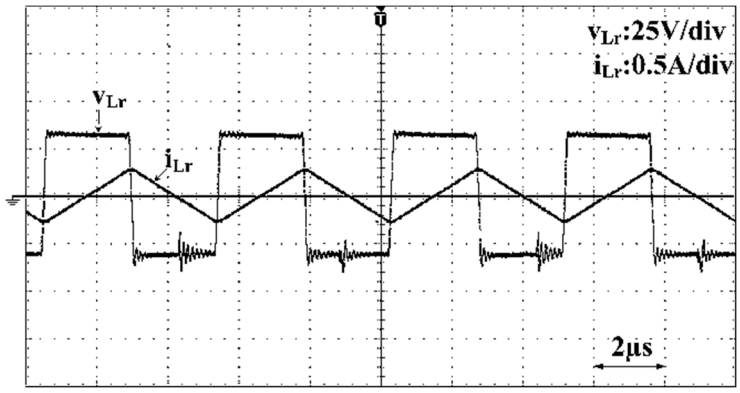

(b) Current and voltage waveform of L_r

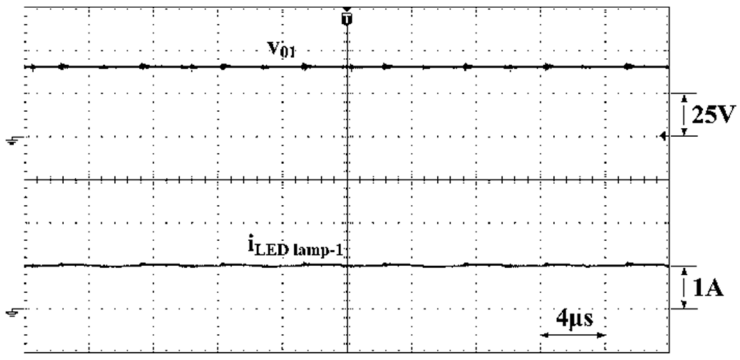

(c) Voltage and current of LED lamp-1

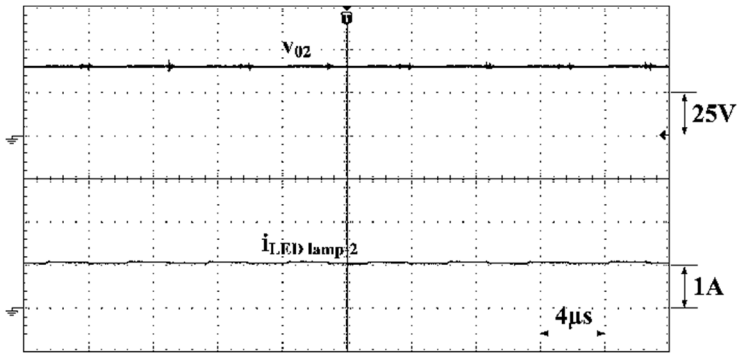

(d) Voltage and current of LED lamp-2

Figure 4.8 Simulation waveforms at full illumination level

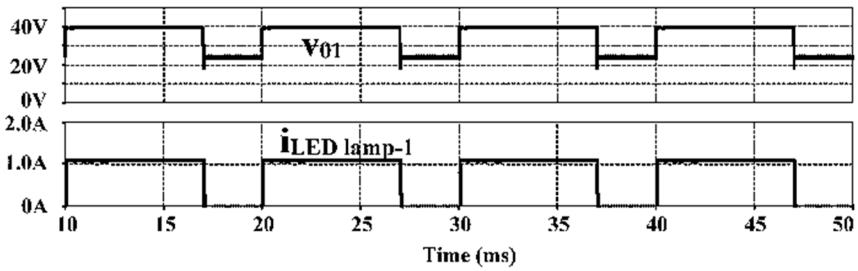

(a) Simulated voltage and current of LED lamp-1

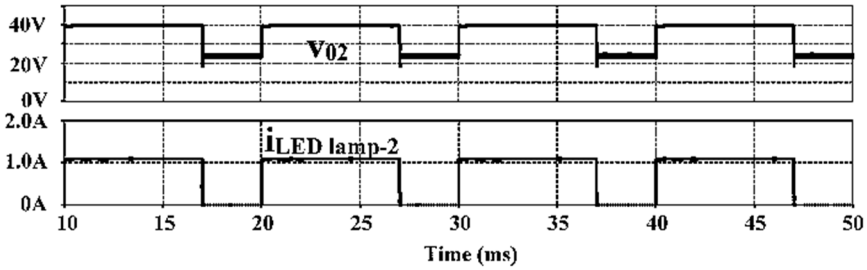

(b) Simulated voltage and current of LED lamp-2

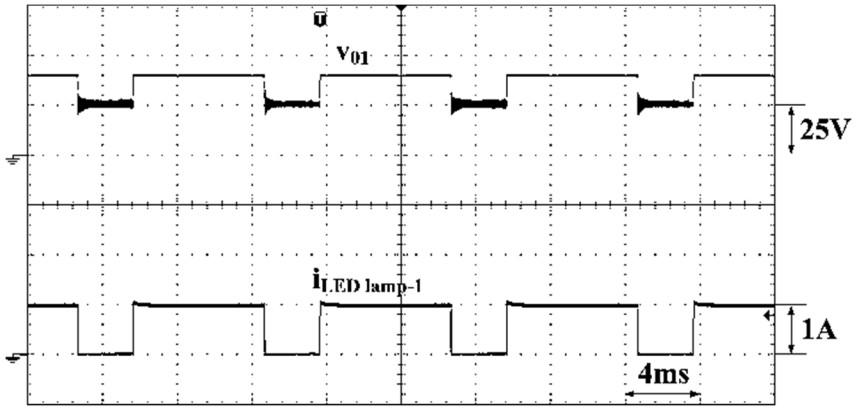

(c) Experimental voltage and current of LED lamp-1

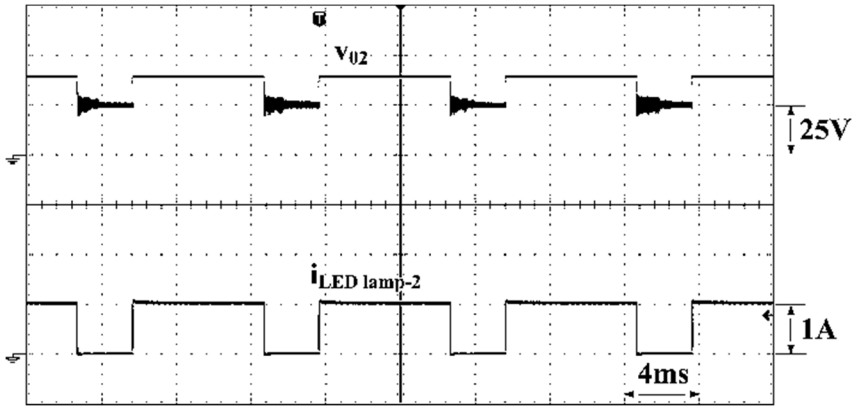

(d) Experimental voltage and current of LED lamp-2

Figure 4.9 Simulation and experimental waveforms with dimming at 70% of full illumination

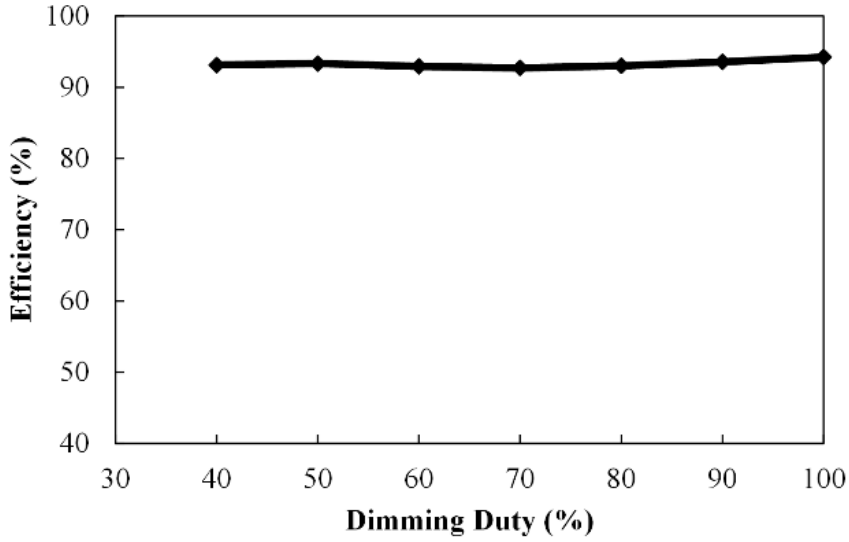

Figure 4.10 Efficiency curve of proposed driver circuit

Table 4. 2 Comparison between proposed topology and other works in literature

Topology	**[53]**	**[58]**	**[59]**	**[61]**	**[62]**	**[63]**	**[64]**	**Proposed**
Switches	4	6	3	4	3	**2**	6	6
Diodes	2	4	2	8	10	4	4	**1**
Inductors	3	2	**1**	2	3	2	3	6
Capacitors	3	7	3	10	17	3	7	**1**
Transformers	1	1	2	2	5	1	2	**0**
Rectifiers	1	4	1	2	5	1	2	**0**
Input voltage	400V	48V	380V	48V	380V	400V	380V	12-24V
Output power	120W	20W	50W	20W	270W	45W	200W	87W
LED lamps	1	4	1	4	10	2	4	2
Switching frequency	150kHz	90kHz	100kHz	70kHz	300kHz	113kHz	100kHz	200kHz
Efficiency	>87%	>91%	>84%	>93%	>94%	>95%	>96%	>94%

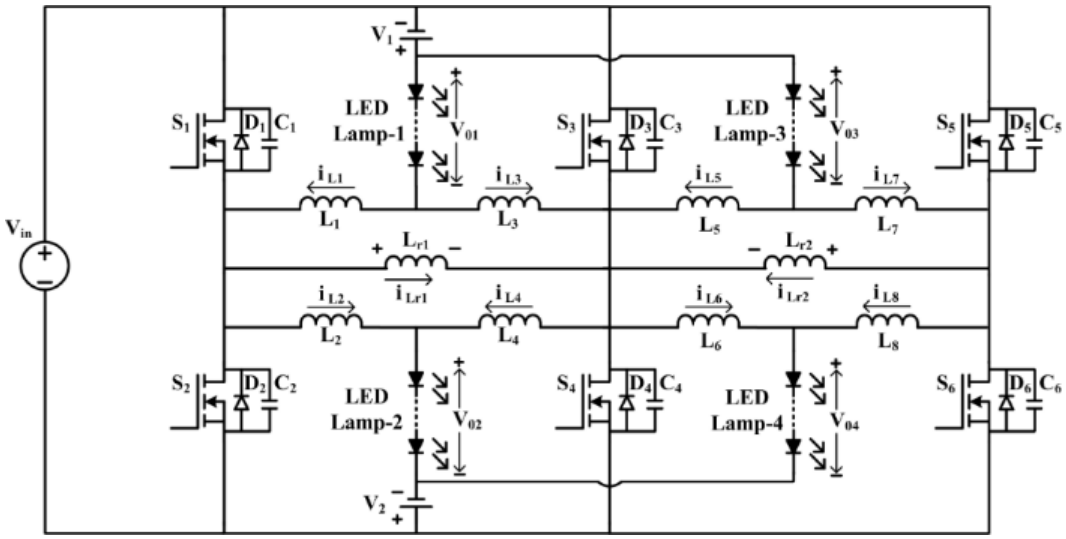

(a) Extension to 4-LED lamp configuration with 3 legs

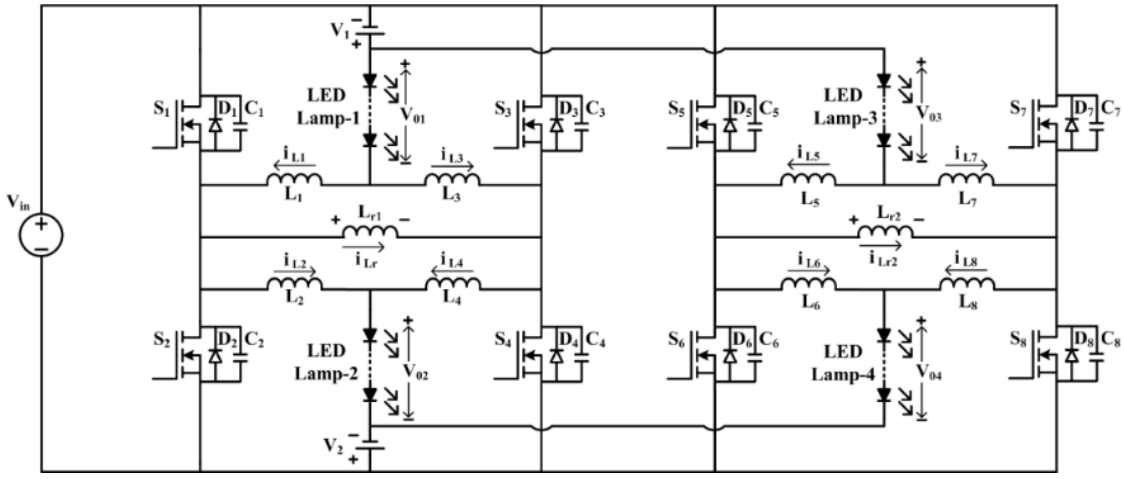

(b) Extension to 4-LED lamp configuration with 4 legs

Figure 4.11 Extension to multiple LED lamps of proposed driver circuit

4.7 Conclusions

In this chapter, an LED driver circuit with ripple free current for high power lighting applications has been proposed. It employs a power control scheme in which only a small portion of LED lamp power is processed through bridge circuit and majority of LED lamp power is provided directly from a dc source. Hence losses in bridge circuit are reduced. The proposed configuration operating principle, analysis and design procedure are given in detail for its validation. Switches in bridge conduct sum of ripple current in load inductor and current in ZVS inductor. In this configuration, voltage stress and current stress in bridge devices are reduced greatly. Buck-boost configuration in input stage, regulates LED lamp currents against input voltage variation. Experimental results obtained from the prototype prove high efficiency at any dimming level.

The proposed configuration has the following advantages

a) Switches in bridge are operated with constant duty cycle.
b) Ripple free current flows through both LED lamps.
c) Conversion power is small.
d) Conduction losses are reduced.
e) ZVS operation of switching devices,
f) Overall conversion efficiency is high (>94%).
g) Reduction in size of reactive components.
h) Dimming feature.
i) Regulation of LED lamp current.
j) This configuration can be extended to drive multiple LED lamps.

The limitation of this configuration is lack of independent dimming operation of LED lamps.

The next chapter proposes a three-leg resonant converter for two output LED lighting application with independent control.

Chapter 5

A Three-leg Resonant Converter for Two Output LED Lighting Application with Independent Control

Chapter 5

A Three-leg Resonant Converter for Two Output LED Lighting Application with Independent Control

This chapter proposes a three-leg resonant converter to drive two Light Emitting Diode (LED) lamps of different power ratings. This may be required when both main and local lighting are essential. The proposed converter is operated simultaneously at two different frequencies. Two series resonant circuits are used to generate the two different frequency currents. Each lamp is powered through a series resonant circuit. Phase modulation control and asymmetrical duty ratio control are used for lamp current regulation. A 126 W prototype has been developed experimentally to confirm its working principle, performance and validity.

5.1 Proposed Configuration

The proposed three leg resonant converter for LED applications is shown in Figure 5.1. Leg-1 and leg-2 form one full bridge inverter operating at high frequency (HF). Similarly leg-1 and leg-3 form another full bridge inverter. Leg-3 is switched at low frequency (LF). Series combination of L_{r1}, C_{r1} and a full bridge rectifier formed by D_1-D_4 is connected between leg-1 and leg-2. Similarly, series connection of L_{r2}, C_{r2} and a full bridge rectifier formed by D_5-D_8 is connected between leg-1 and leg-3. Inductor L_{r1} and capacitor C_{r1} are selected to respond to fundamental component in the voltage between leg-1 and leg-2 to output stage. And, Inductor L_{r2} and capacitor C_{r2} respond to only LF fundamental component in the voltage between leg-1 and leg-3 to output stage. Capacitor C_{01} and C_{02} are filter capacitors which make LED lamp-1 and lamp-2 voltages constant respectively. An auxiliary inductor L_{aux} is connected between leg-1 and leg-2 to improve ZVS conditions in switches S_1 and S_2.

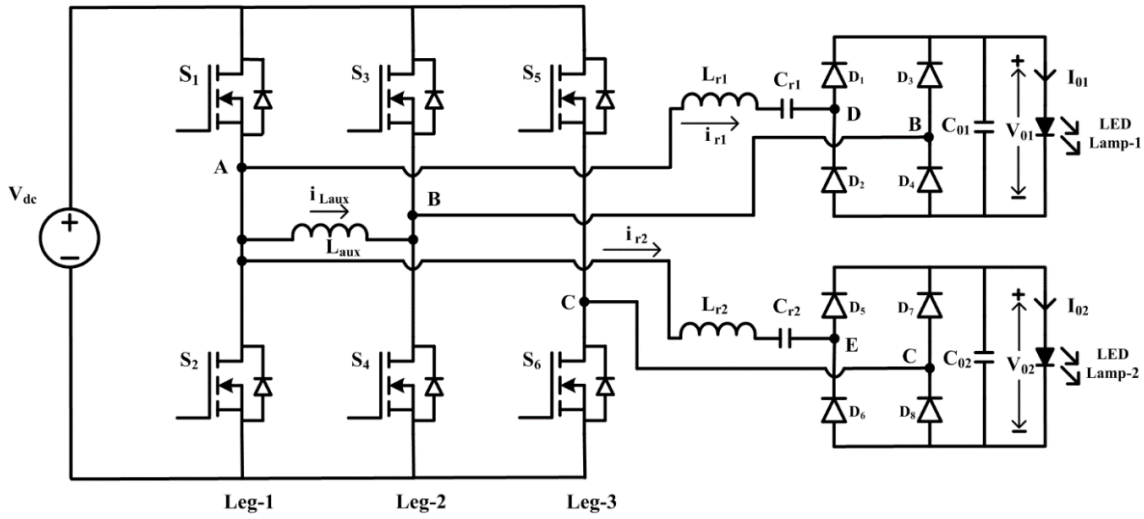

Figure 5.1 Schematic of proposed LED driver

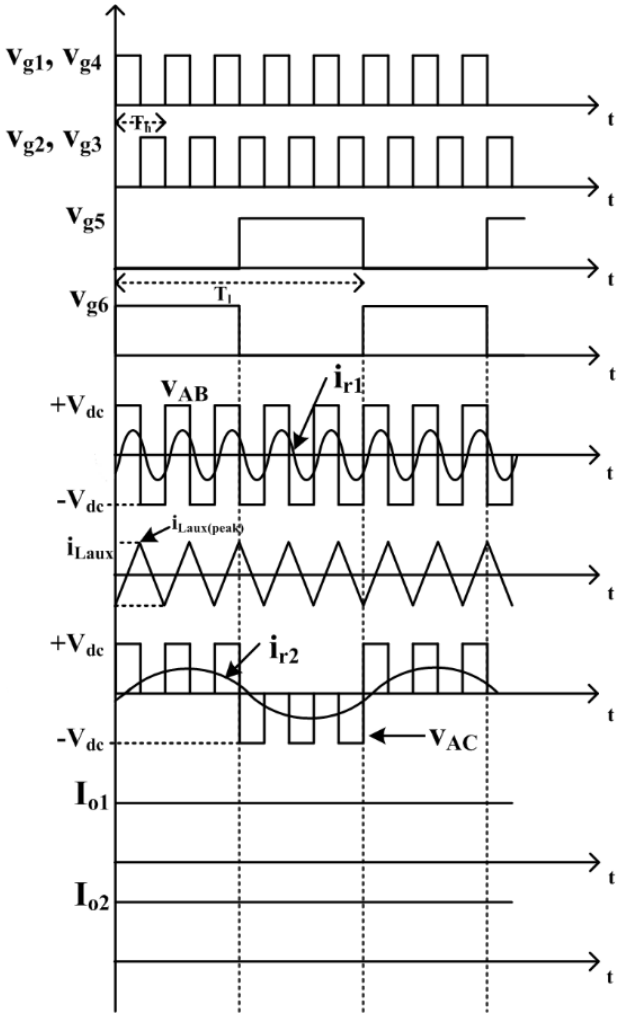

Figure 5.2 Operating waveforms of proposed LED driver

5.2 Operation and Analysis of Proposed LED driver

The principle of operation and circuit analysis of the proposed LED driver are discussed in the following sections.

5.2.1 Operation of the proposed driver

The switches in full bridge formed by leg-1 and leg-2 are alternately switched on for 50% duty cycle and off for 50% duty cycle at fixed HF. Switches in leg-3 are alternately switched on for 50% duty cycle and off for 50% duty cycle at fixed LF. To prevent short circuit across the dc power supply, sufficient dead time must be inserted between the gate voltages of each leg. However it is not shown in the operating waveforms of the proposed LED driver shown in Figure 5.2. The switches in leg-1 and leg-2 produce a square wave voltage v_{AB}. Similarly switches in leg-1 and leg-3 produce voltage v_{AC} which contains both HF and LF voltage waveforms. The concept of series resonance is used for powering both LED lamps. The HF resonant circuit is formed by series connection of L_{r1} and C_{r1}, diode bridge rectifier by D_1-D_4 and LED lamp-1. The LF resonant circuit is formed by series connection of L_{r2} and C_{r2}, diode bridge rectifier by D_5-D_8 and LED lamp-2. HF resonant circuit offers low impedance to fundamental component of v_{AB}. Thus HF alternating current i_{r1} is generated. And it is rectified and filtered to feed LED lamp-1. Similarly LF resonant circuit offers low impedance to only LF fundamental component of v_{AC}. Thus LF alternating current i_{r2} is produced and is rectified and filtered to power LED lamp-2.

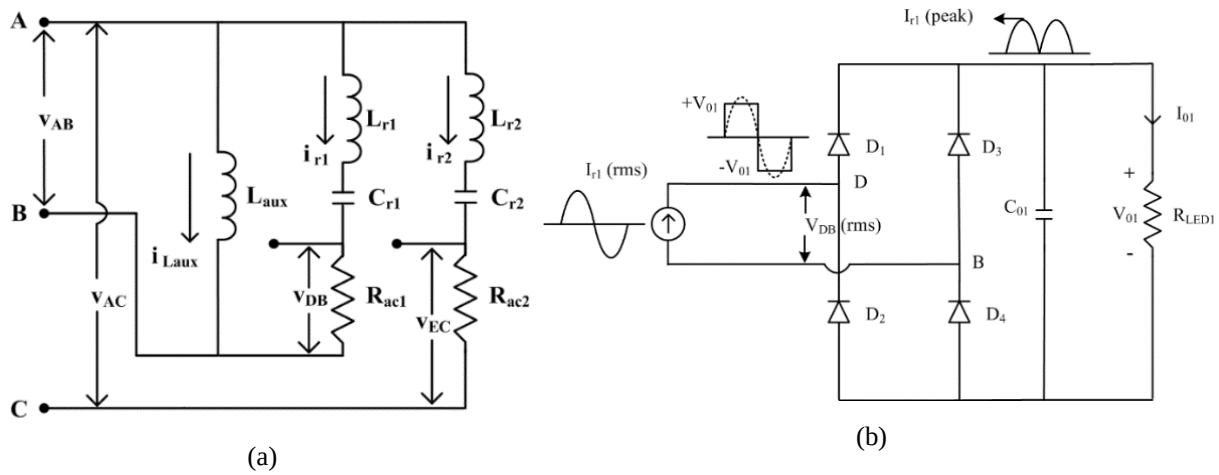

Figure 5.3 (a) AC equivalent circuit (b) Equivalent circuit for R_{ac1}

5.2.2 Analysis of Proposed LED Driver

The following assumptions are considered to analyze the proposed LED driver:

i. The converter is operating in steady state.
ii. The power MOSFETs and power diodes are ideal.
iii. The voltage across each LED lamp is constant.
iv. The exponential decay in fundamental current during transient is neglected.

In the proposed converter, v_{AB} of magnitude V_{dc} is applied to HF resonant circuit. Similarly v_{AC}, which is a sum of HF and LF square waves of magnitude $V_{dc}/2$ is applied to LF resonant circuit. These resonant circuits allow only fundamental components. Therefore conventional ac analysis can be used to calculate the static gain of the proposed converter. The ac equivalent circuit of proposed LED driver circuit is shown in Figure 5.3 (a). The analysis is given for only LED lamp-1. Similar analysis is applicable to LED lamp-2.

The HF resonant circuit filters all the harmonic voltage components except fundamental component present in the voltage v_{AB}. The ac resistance R_{ac1}, which is used in ac equivalent circuit, accounts for the non-linearity present in rectifier. The reactance offered by L_{r1} and C_{r1} are denoted as X_{Lr1} and X_{Cr1} respectively. From the equivalent circuit shown in Figure 5.3 (a), static gain of the proposed driver is represented by using simple voltage division principle:

$$\frac{V_{DB}}{V_{AB}} = \frac{R_{ac1}}{R_{ac1} + j(X_{Lr1} - X_{Cr1})} = \frac{1}{\left[1 + j\left(\frac{X_{Lr1} - X_{Cr1}}{R_{ac1}}\right)\right]} \tag{5.1}$$

Note that V_{AB} is the fundamental component of the square wave voltage applied to HF resonant circuit and V_{DB} is the fundamental component of square wave voltage of magnitude V_{01} across R_{ac1}.The ac resistance R_{ac1} is calculated by using the circuit shown in Figure 5.3 (b) in which the resistance offered by LED lamp-1 is represented as R_{LED1}. The R_{ac1} is given by

$$R_{ac1} = \frac{V_{DB}(rms)}{I_{r1}(rms)} = \frac{4V_{01}}{\sqrt{2}\pi} \Big/ \frac{\pi I_{01}}{2\sqrt{2}} = \frac{8}{\pi^2}\frac{V_{01}}{I_{01}} = \frac{8}{\pi^2} R_{LED1} \tag{5.2}$$

and

$$X_{Lr1} = 2\pi f_h L_{r1} \tag{5.3}$$

$$X_{Cr1} = \frac{1}{2\pi f_h C_{r1}} \tag{5.4}$$

The sharpness in the HF resonant current is measured by quality factor (Q_1), and it is defined by

$$Q_1 = \frac{\omega_{0,1} L_{r1}}{R_{LED1}} = \frac{1}{\omega_{0,1} C_{r1} R_{LED1}} \tag{5.5}$$

where $\omega_{0,1}$ is high resonant frequency in radians per seconds and it is given by

$$\omega_{0,1} = 2\pi(f_{0,1}) = \frac{1}{\sqrt{L_{r1} C_{r1}}} \tag{5.6}$$

Therefore high resonant frequency in hertz is represented as

$$f_{0,1} = \frac{1}{2\pi\sqrt{L_{r1} C_{r1}}} \tag{5.7}$$

By substituting (5.2), (5.3), (5.4) and (5.5) in Eqn. (5.11), the gain is finally expressed as

$$\frac{V_{DB}}{V_{AB}} = \frac{4V_{01}/\pi}{4V_{dc}/\pi} = \frac{V_{01}}{V_{dc}} = \frac{1}{\left[1 + j\frac{\pi^2}{8} Q_1 \left(\frac{f_h}{f_{0,1}} - \frac{f_{0,1}}{f_h}\right)\right]} \tag{5.8}$$

The steady state analysis for LED lamp-2 is similar to aforementioned analysis under 50% duty cycle of leg-3 switches. Hence the static gain of the proposed converter with respect to LED lamp-2 is given as

$$\frac{V_{BC}}{V_{AC}} = \frac{4V_{02}/\pi}{2V_{dc}/\pi} = \frac{V_{02}}{V_{dc}} = \frac{1}{2\left[1 + j\frac{\pi^2}{8} Q_2 \left(\frac{f_l}{f_{0,2}} - \frac{f_{0,2}}{f_l}\right)\right]} \tag{5.9}$$

where, V_{AC} is the fundamental component of the square wave voltage applied to LF resonant circuit, V_{EC} is the fundamental component of square wave voltage of magnitude V_{02} across R_{ac2}. Q_2 is the quality factor of LF resonant circuit and is defined as

$$Q_2 = \frac{\omega_{0,2} L_{r2}}{R_{LED2}} = \frac{1}{\omega_{0,2} C_{r2} R_{LED2}} \tag{5.10}$$

and $f_{0,2}$ is low resonant frequency in hertz is represented as

$$f_{0,2} = \frac{1}{2\pi\sqrt{L_{r2} C_{r2}}} \tag{5.11}$$

5.3 Regulation of LED Lamp Current and Dimming Control

In the proposed configuration, if input voltage V_{dc} is changed, the operating voltage and current of both the LED lamps are changed. Consequently, the illumination from the both LED lamps changes. Therefore, LED lamp currents need to be regulated against variation in input dc voltage V_{dc}. To regulate LED lamp-1 current against variation in V_{dc}, phase-modulation control is used. In this control, input voltage to the HF resonant circuit v_{AB} is controlled by introducing a phase angle (α_h) between the gate voltages of switches in leg-1 and leg-2 as shown in Figure 5.4 (a). Similarly to regulate LED lamp-2 current against variation in V_{dc}, asymmetrical duty ratio control is applied for switches in leg-3. In this control, input voltage to the LF resonant circuit v_{AC} is controlled by introducing a phase angle (α_l) between the gate voltages of switches in leg-3 as shown in Figure 5.4 (a). Since only fundamental voltage components are allowed by both HF and LF resonant circuit, their magnitudes [66] are given as

$$V_{AB} = \frac{4V_{dc}}{\pi}\cos\left(\frac{\alpha_h}{2}\right) \tag{5.12}$$

$$V_{AC} = \frac{2V_{dc}}{\pi}\cos\left(\frac{\alpha_l}{2}\right) \tag{5.13}$$

By substituting (5.2), (5.3), (5.4), (5.5) and (5.12) in (5.1), static gain of the proposed LED driver with respect to LED lamp-1 is modified as

$$\frac{V_{01}}{V_{dc}} = \frac{\cos\left(\frac{\alpha_h}{2}\right)}{\left[1 + j\frac{\pi^2}{8}Q_1\left(\frac{f_h}{f_{0,1}} - \frac{f_{0,1}}{f_h}\right)\right]} \tag{5.14}$$

By substituting (5.2), (5.3), (5.4), (5.5) and (5.13) in (1), static gain of the proposed LED driver with respect to LED lamp-2 is modified as

$$\frac{V_{02}}{V_{dc}} = \frac{\cos\left(\frac{\alpha_l}{2}\right)}{2\left[1 + j\frac{\pi^2}{8}Q_2\left(\frac{f_l}{f_{0,2}} - \frac{f_{0,2}}{f_l}\right)\right]} \tag{5.15}$$

The magnitude of input voltage V_{dc} can be found by using either (5.14) or (5.15) after selecting the LED lamps, both high switching and resonant frequency and low switching and resonant frequency. And the variation in V_{dc} is compensated by adjusting phase angle (α_h) in HF resonant circuit and phase angle (α_l) in LF resonant circuit.

Adjustable illumination in LED lamp is called dimming. It is an important requirement for LED applications which improves power saving. In the proposed study, PWM dimming is incorporated independently for both LED lamps. To realize PWM dimming in LED lamp-1, the input voltage to the HF resonant circuit v_{AB} is made zero by dimming signal S_{dim1}. And to implement PWM dimming in LED lamp-2, the input voltage to the LF resonant circuit v_{AC} is made zero by dimming signal S_{dim2}. Thus average currents through both LED lamps are controlled independently without changing the operating voltage and current. The two dimming signals, voltages v_{AB} and v_{AC} and LED lamp currents are shown in Figure 5.4 (b).

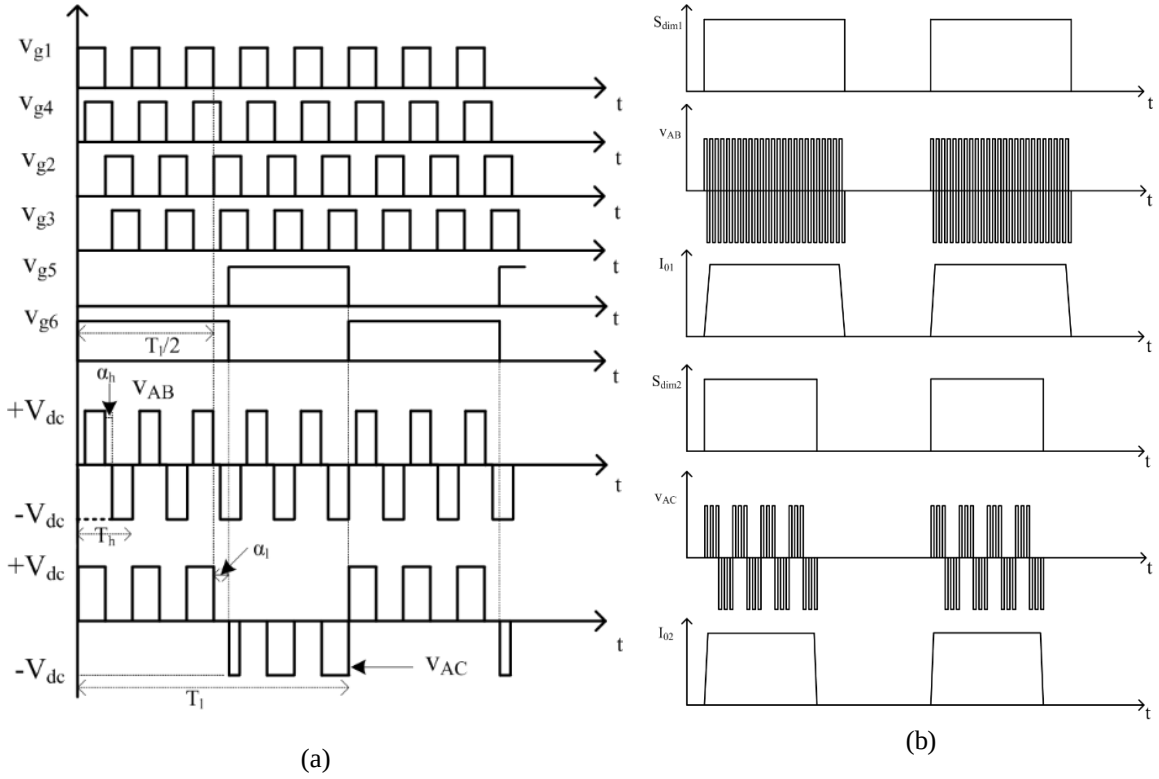

Figure 5.4 (a) Switching sequence and input voltages to HF and LF resonant circuits under LED lamp regulation (b) Dimming signals and input voltages to HF and LF resonant circuits and both LED lamp currents

5.4 Design Considerations

The approximated model [67] of an LED is considered to select the component values of proposed driver circuit. In the proposed LED driver, two LED lamps are used. In LED lamp-1, four parallel strings are used. In each LED string, 13 LEDs are connected in series. In LED lamp-2, four LED strings are connected in parallel. In each string, 6 LEDs are connected in series. The operating point for each LED is selected at 3.25 V, 510 mA. And the cut-in voltage of each LED is 2.32 V. Therefore operating voltage and current of LED lamp-1 are 42.25 V and

2.04 A. And operating voltage and current of LED lamp-2 are 19.5 V and 2.04 A. Consequently power consumed by LED lamp-1 and lamp-2 are 86 W and 40 W respectively.

5.4.1 Selection of switching frequencies

The criteria for selecting f_h and f_l should not affect the operation of HF and LF resonant circuits. HF component of v_{AB} should power only HF resonant circuit. LF component of v_{AC} should power only LF resonant circuit. To achieve this, f_h should be far greater than f_l. f_h can be taken either as integer multiples or as non-integer multiples of f_l. If f_h is non-integer multiples of f_l, effect of harmonic component of f_l on HF resonant circuit can be avoided. Therefore f_h is selected at 168 kHz and f_l is selected at 30 kHz. For ZVS, $f_{0,1}$ and $f_{0,2}$ are taken 5-10% less than f_h and f_l. Therefore $f_{0,1}$ is selected at 153 kHz and $f_{0,2}$ is selected at 28.67 kHz.

5.4.2 Calculation of HF resonant circuit parameters

The product of L_{r1} and C_{r1} is obtained from (5.7) and it is expressed as

$$L_{r1}C_{r1} = \left[\frac{1}{2\pi f_{0,1}}\right]^2 \tag{5.16}$$

After selecting $f_{0,1}$ as 153 kHz, (5.16) is expressed as

$$L_{r1}C_{r1} = 1.082\times10^{-12} \tag{5.17}$$

From (5.5), quality factor Q_1 is expressed as

$$Q_1 = \frac{1}{R_{LED1}}\sqrt{\frac{L_{r1}}{C_{r1}}} \tag{5.18}$$

With Q_1 = 1.52 and R_{LED1} = 20.83Ω, from (5.17) and (5.18), the inductor L_{r1} and capacitor C_{r1} are calculated as 33µH and 33nF respectively. To allow ripple current less than 10% of I_{01} in LED lamp-1, C_{01} of 1.22 µF is selected.

5.4.3 Calculation of LF resonant circuit parameters

From (5.11) the product of L_{r2} and C_{r2} is expressed as

$$L_{r2}C_{r2} = \left[\frac{1}{2\pi f_{0,2}}\right]^2 \tag{5.19}$$

After selecting $f_{0,2}$ as 28.67 kHz, (5.19) is expressed as

$$L_{r2}C_{r2} = 3.082\times10^{-11} \tag{5.20}$$

From (5.10), quality factor Q_2 is expressed as

$$Q_2 = \frac{1}{R_{LED\,2}}\sqrt{\frac{L_{r2}}{C_{r2}}} \tag{5.21}$$

With Q_1 = 2.64 and R_{LED2} = 9.558 Ω, from (5.20) and (5.21), the inductor L_{r2} and capacitor C_{r2} are calculated as 140 µH and 0.22 µF respectively. To allow ripple current less than 10% of I_{02} in LED lamp-2, C_{02} of 14.7 µF is selected.

5.4.4 Calculation of input dc voltage V_{dc}

In this configuration, ±5% variation in V_{dc} is considered. The criteria to calculate V_{dc} is that at minimum value of V_{dc} i.e. (V_{dc} – 5%) the switches in all the 3-legs are at 50% duty ratio. In other words voltage v_{AB} and v_{AC} are full square wave voltages. Thus (5.8) or (5.9) can be used to calculate V_{dc}. With V_{01} of 42.25V, Q_1 of 1.52, f_h of 168 kHz and $f_{0,1}$ of 153 kHz, the input voltage V_{dc} is calculated from (5.8) as,

$$\frac{42.25}{(1-0.05)V_{dc}} = \frac{1}{\left[1+j\frac{\pi^2}{8}1.52(0.187)\right]}$$

$$\Rightarrow V_{dc} \cong 48V$$

After selecting V_{dc}, the phase angle α_h and α_l can be calculated from (5.14) and (5.15) respectively by substituting V_{dc} = 48V.

5.4.5 Calculation of auxiliary inductor's value L_{aux}

In the proposed configuration, leg-1 is common for both HF resonant circuit and LF resonant circuit. Therefore switches in leg-1 conduct sum of HF resonant current (i_{r1}) and LF resonant current (i_{r2}). Hence certain ZVS conditions are affected for leg-1. To reduce this effect, an auxiliary inductor L_{aux} is connected between leg-1 and leg-2. This inductor L_{aux} increases turn-on and off current for switches in leg-1. The voltage across L_{aux} is $\pm V_{dc}$. Hence current through L_{aux} is triangular. And peak current through L_{aux} appears during dead time between gate voltages of leg-1 switches. The peak current through L_{aux} at V_{dc} – 5% is expressed as

$$i_{Laux(peak)} = \frac{0.95V_{dc}T_h}{4L_{aux}} \tag{5.22}$$

The value of $i_{Laux(peak)}$ is inversely proportional to the value of L_{aux} for a fixed V_{dc} and T_h. For $i_{Laux(peak)}$ of 2.26 A, V_{dc} of 48 V, T_h of 5.952 µs, L_{aux} is calculated as 30 µH.

5.5 Simulation and Experimental Results

To verify the feasibility of proposed configuration for LED applications, a total of 126 W prototype has been implemented. It is first simulated using OrCAD PSpice software and then experimental prototype has been developed and verified. Table 5.1 shows the parameters used in the proposed LED driver. Figure 5.5 (a) shows the schematic of control circuit of proposed configuration and experimental prototype is shown in Figure 5.5 (b). Both LED lamps are powered with input voltage V_{dc} = 48 V. Figure 5.6 and 5.7 show the simulated and experimental waveforms of proposed LED driver for HF resonant circuit at full illumination respectively. It is observed that experimental waveforms of HF resonant circuit are in good agreement with simulated waveforms. And Fast Fourier Transform (FFT) of i_{r1} shows that it has only fundamental current component and has negligible LF resonant current component. Figure 5.8 and 5.9 show the simulated and experimental waveforms of proposed LED driver for LF resonant circuit at full illumination respectively. It is observed that experimental waveforms of LF resonant circuit are in good agreement with simulated waveforms. And FFT of LF resonant current i_{r2} shows that it has only fundamental current component and has negligible HF resonant current component. To show zero voltage switching feature in this LED driver, experimental switch voltage, current of S_1 and S_3 are shown in Figure 5.10. It is observed that switches in leg-1 and leg-2 are turned on and off at zero voltage. Thus switching losses are reduced. Hence the efficiency of the proposed converter is high and efficiency of the proposed LED driver at full illumination level of both HF and LF resonant circuits is found to be 92.45%. The proposed LED driver is also powered with ±5% variation in V_{dc} at full illumination of both LED lamp-1 and lamp-2. Under −5% variation in V_{dc}, efficiency of the driver is found to be 91.3%. And under +5% variation in V_{dc}, efficiency of the driver is found to be 90.87%.

In the proposed LED driver, LED lamps can be dimmed independently. Figure 5.11 (a) shows LED lamp-1 voltage and current at 70% of full illumination and Figure 5.11 (b) shows LED lamp-2 voltage and current at 50% of full illumination with V_{dc} = 48V. It is observed that LED lamp voltage and currents are at their operating values when their dimming signal is ON. When their dimming signal is OFF, LED lamp currents become zero and LED lamp voltages drop below their cut-in voltages. The efficiency curves of both LED lamps under various dimming levels are shown in Figure 5.12. Figure 5.12(a) shows the efficiency curve of LED lamp-1 under various dimming levels by keeping LED lamp-2 at full illumination. Similarly, Figure 5.12 (b) shows the efficiency curve of LED lamp-2 under various dimming levels by

keeping LED lamp-1 at full illumination. It is observed that high efficiency is guaranteed at any dimming level of both LED lamps.

Table 5. 1 Parameters of the proposed LED driver

Parameter Description	**Value / Model no.**
DC Input voltage, V_{dc}	48±5% V
High switching frequency, f_h	168 kHz
High resonant frequency, f_{r1}	153 kHz
Resonant inductor L_{r1}	33 µH
Resonant capacitor C_{r1}	0.033 µF
Output capacitor C_{01}	1.22 µF
V_{01}	42.25 V
I_{01}	2.04 A
P_{01}	86 W
Low switching frequency, f_l	30 kHz
Low resonant frequency, f_{r2}	28.67 kHz
Resonant inductor L_{r2}	140 µH
Resonant capacitor C_{r2}	0.22 µF
Output capacitor C_{02}	14.7 µF
V_{02}	19.5 V
I_{02}	2.04 A
P_{02}	40 W
PWM dimming frequency	100 Hz
Switching devices used	IRF 540N
Power diodes used	MUR 860
Control ICs used	UC 3875, SG 3525
Driver ICs used	IR 2110

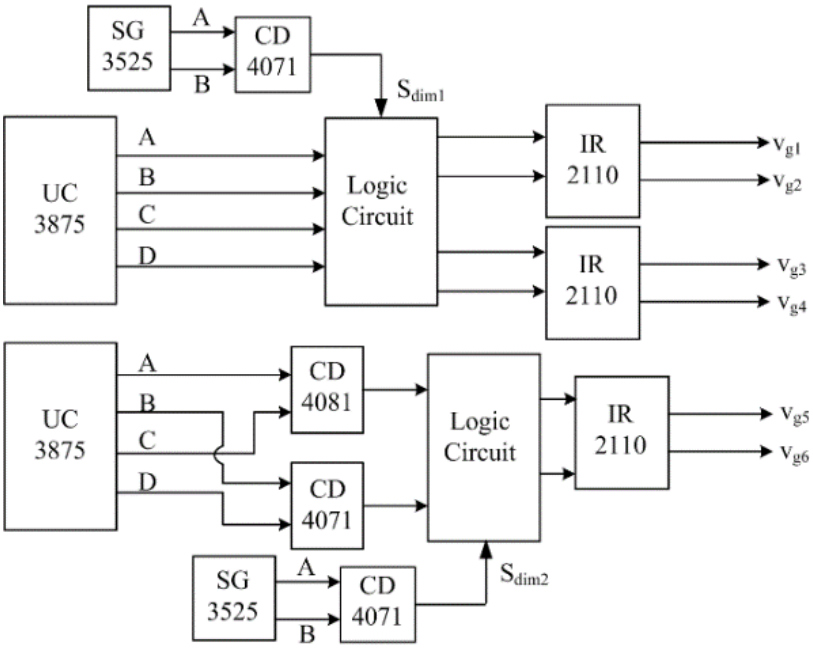

(a)

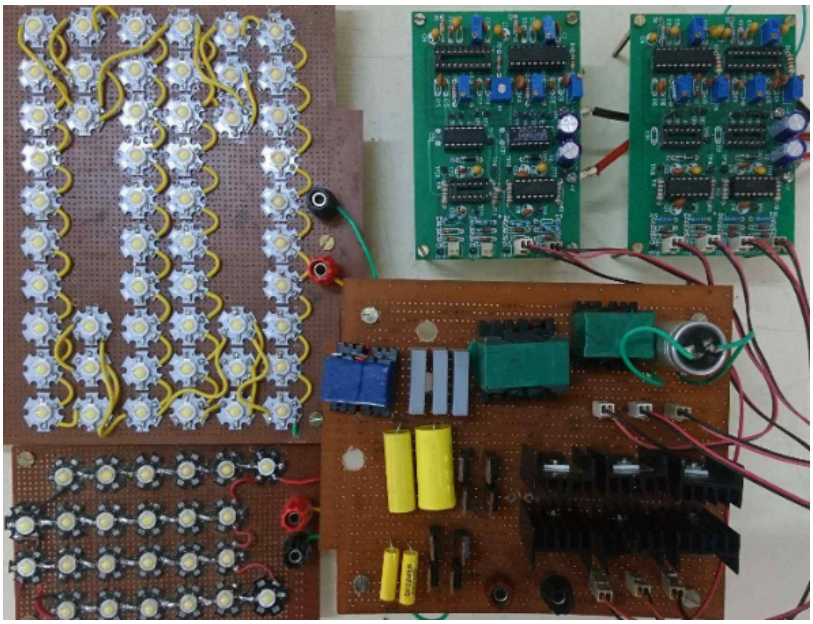

(b)

Figure 5.5 (a) Schematic of control circuit of proposed LED driver (b) Experimental prototype

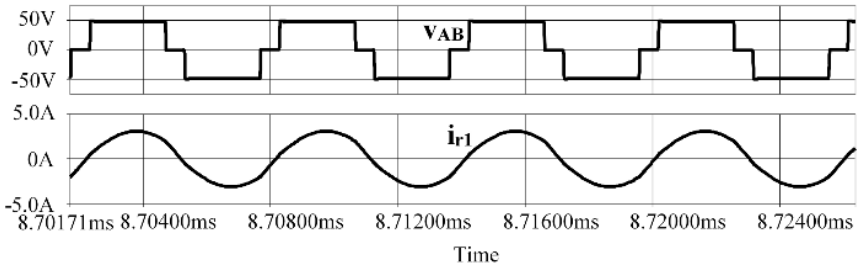

(a) Input voltage to the HF resonant circuit and HF resonant current

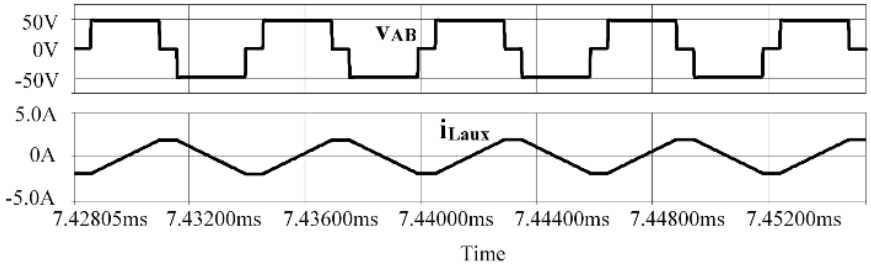

(b) Input voltage to the HF resonant circuit and current in L_{aux}

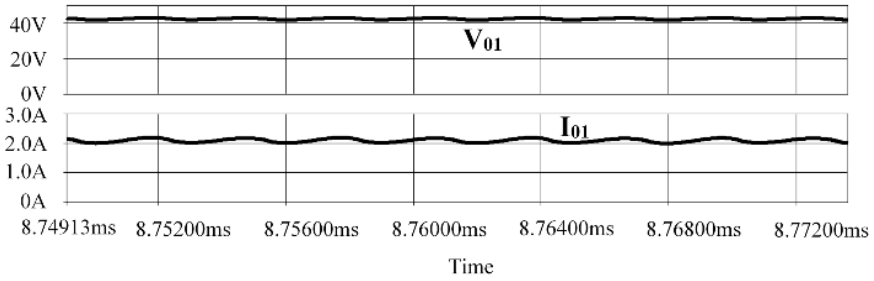

(c) Voltage and current of LED lamp-1

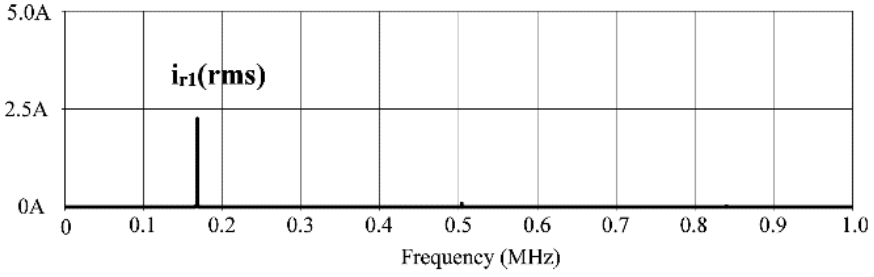

(d) FFT of HF resonant current

Figure 5.6 Simulated waveforms of HF resonant circuit at full illumination

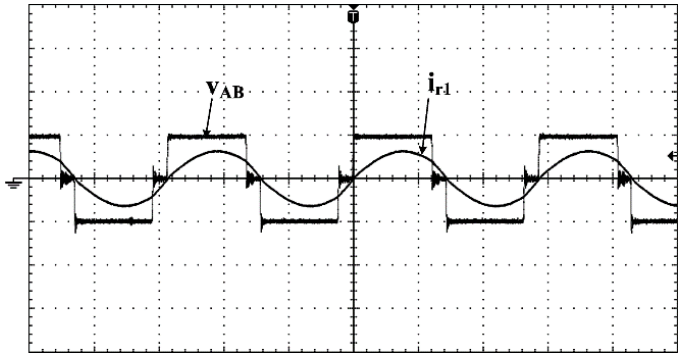

(a) Input voltage to the HF resonant circuit and HF resonant current (v_{AB}: 50 V/div; i_{r1}: 5 A/div; time: 2 µs/div)

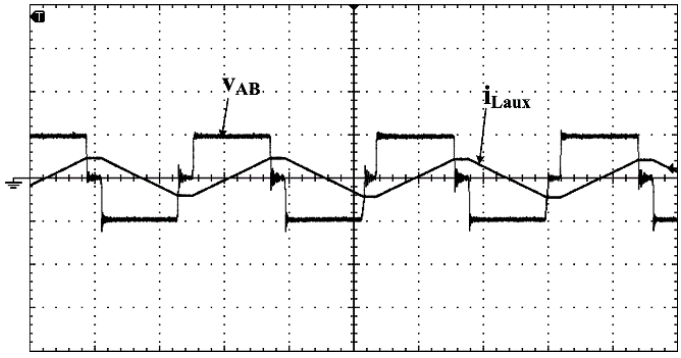

(b) Input voltage to the HF resonant circuit and current in L_{aux} (v_{AB}: 50 V/div; i_{Laux}: 5 A/div; time: 2 µs/div)

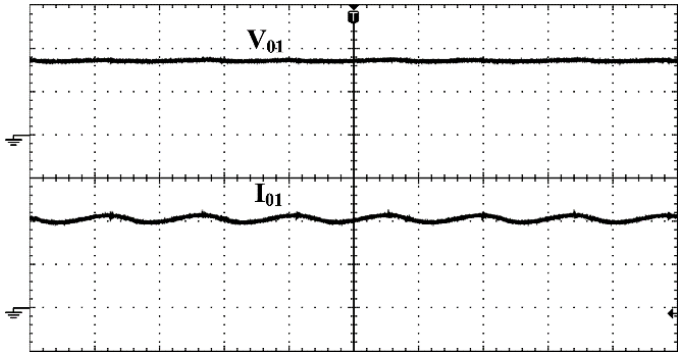

(c) Voltage and current of LED lamp-1 (V_{01}: 25 V/div; I_{01}: 1 A/div; time: 2 µs/div)

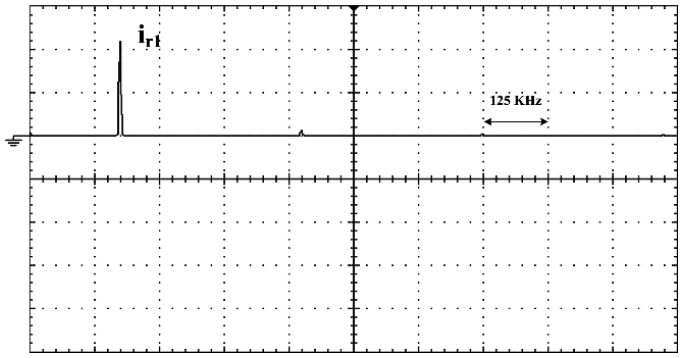

(d)) FFT of HF resonant current (i_{r1}: 1 A/div)

Figure 5.7 Experimental waveforms of HF resonant circuit at full illumination

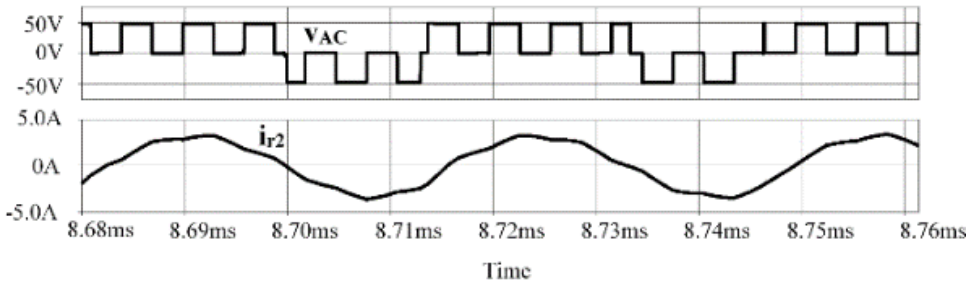

(a) Input voltage to the LF resonant circuit and LF resonant current

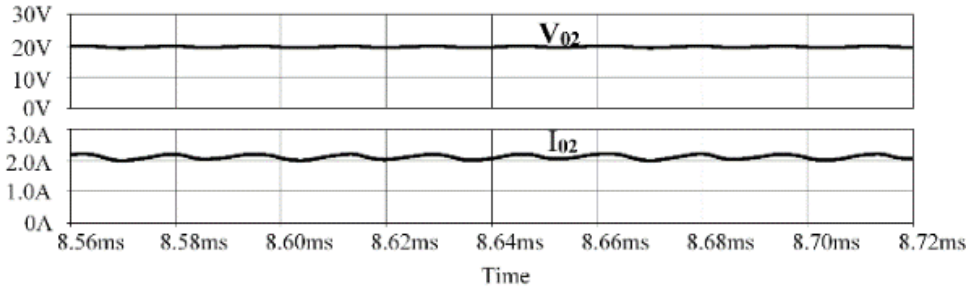

(b) Voltage and current of LED lamp-2

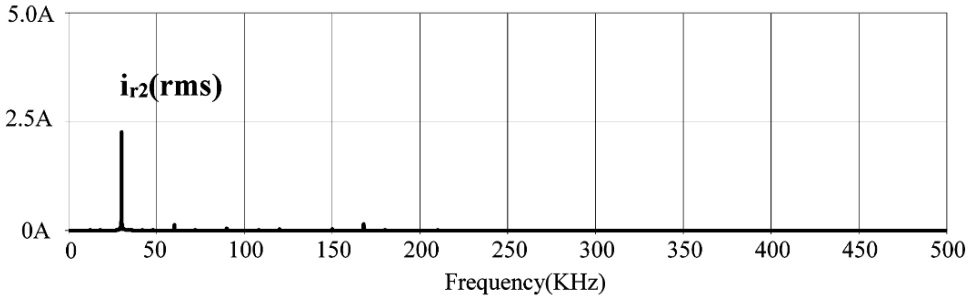

(c) FFT of LF resonant current

Figure 5.8 Simulated waveforms of LF resonant circuit at full illumination

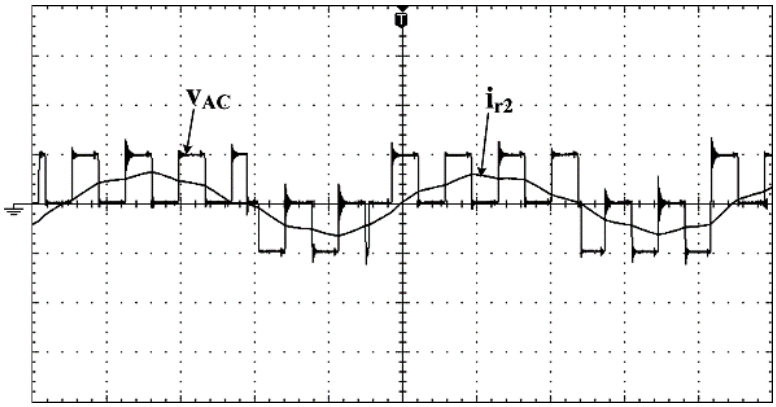

(a) Input voltage to the LF resonant circuit and LF resonant current (v_{AC}: 50 V/div; i_{r2}: 5 A/div; time: 8 μs/div)

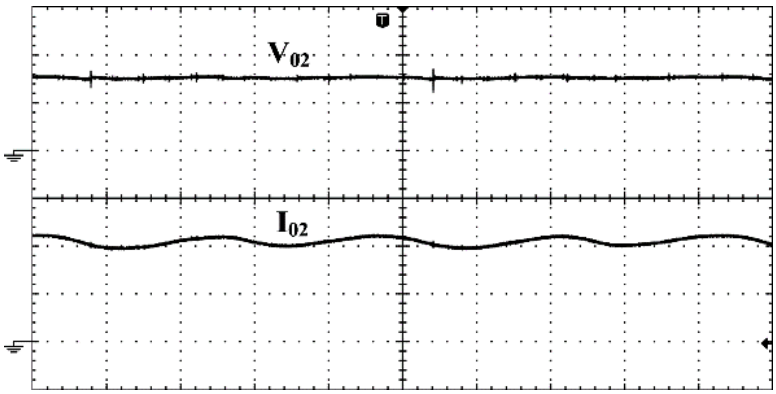

(b) Voltage and current of LED lamp-2 (V_{02}: 12.5 V/div; I_{02}: 1 A/div; time: 8 μs/div)

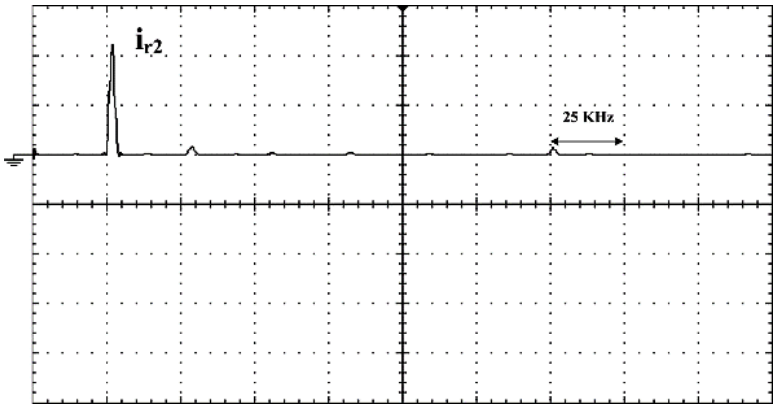

(c) FFT of LF resonant current (i_{r2}: 1 A/div)

Figure 5.9 Experimental waveforms of LF resonant circuit at full illumination

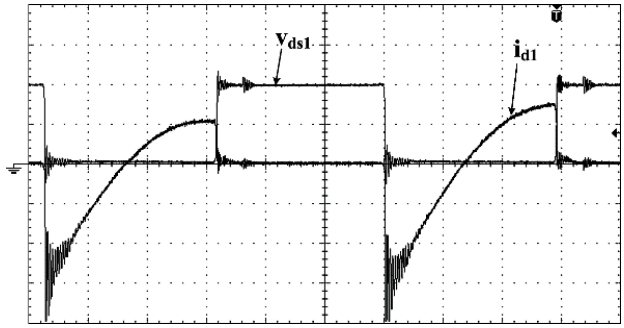

(a) Voltage and current in switch S_1 (v_{ds1}: 25 V/div; i_{d1}: 2 A/div; time: 1 µs/div)

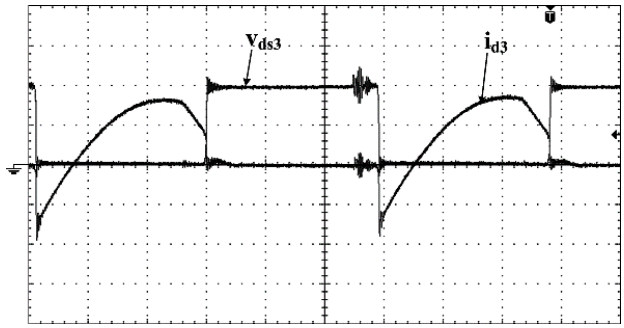

(b) Voltage and current in switch S_3 (v_{ds3}: 25 V/div; i_{d3}: 2 A/div; time: 1 µs/div)

Figure 5.10 Switching waveforms

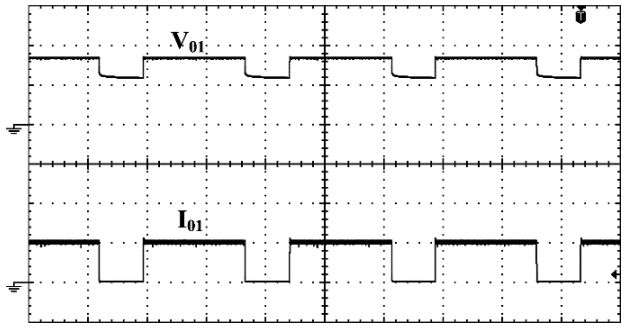

(a) Voltage and current of LED lamp-1 at 70% dimming (V_{01}: 25 V/div; I_{01}: 2 A/div; time: 4 ms/div)

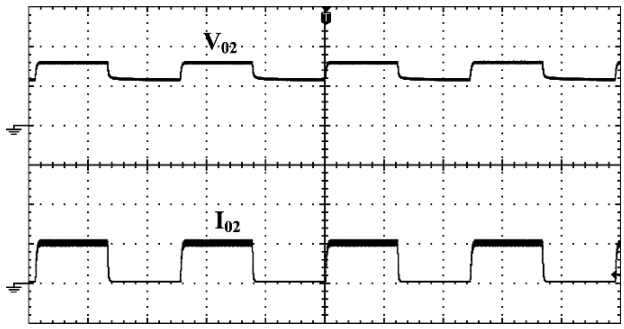

(b) Voltage and current of LED lamp-2 at 50% dimming (V_{02}: 12.5 V/div; I_{02}: 2 A/div; time: 4 ms/div)

Figure 5.11 Voltage and current waveforms of both lamps under dimming control

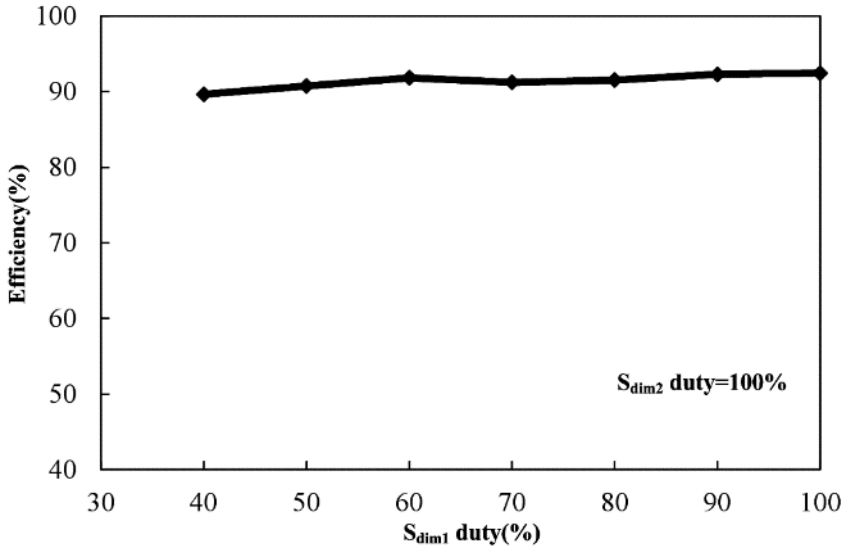

(a) Efficiency curve of LED lamp-1 under various dimming levels

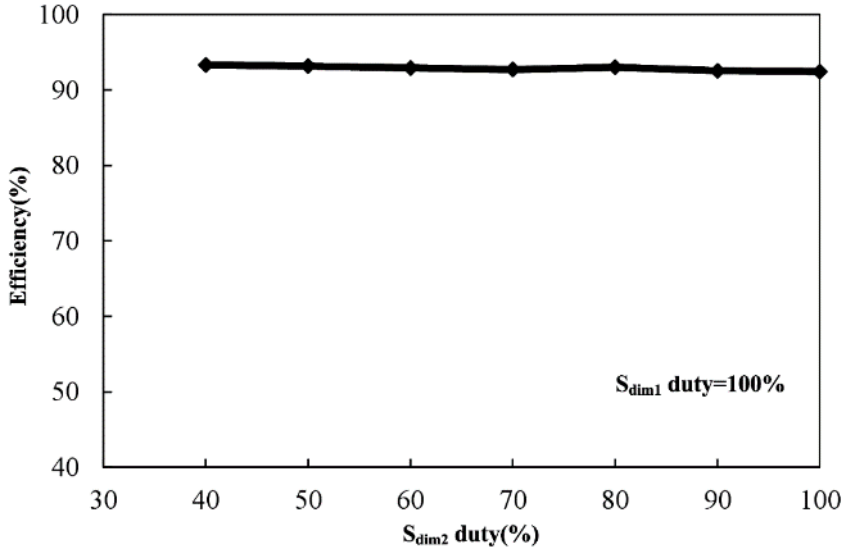

(b) Efficiency curve of LED lamp-2 under various dimming levels

Figure 5.12 Efficiency curves

5.6 Conclusions

In this chapter, a three leg converter has been developed to power two LED lamps with different power ratings. Leg-1 and leg-2 devices are switched at HF. Leg-3 devices are switched at LF. Two series resonant circuits which have two different frequency components are used for powering LED lamps. Principle of operation, analysis, design procedure and current regulation feature are explained in detail. Experimental results obtained from a 126 W prototype are in good agreement with simulation results. The FFT of two HF and LF resonant current is evident of independent operation.

This configuration has the following advantages;

1) Drives two LED lamps of different power rating with same input voltage.
2) Both HF and LF operations are independent.
3) Provide ZVS.
4) Both LED lamps can be regulated at the required operating voltage and current.
5) And both LED lamps can be dimmed independently.
6) High efficiency is obtained at any dimming level of both LED lamps.
7) The proposed topology can be suitable for smart lighting applications.
8) It can be powered from low voltage dc grid or battery operated systems.

The limitations of this configurations are partial ZVS in devices in leg-1, high current stress and lack of extension to multiple LED lamps.

The next chapter proposes a full-bridge resonant converter for LED lighting application with simple current control.

Chapter 6

An Efficient Full-Bridge Resonant Converter for LED Lighting Application with Simple Current Control

Chapter 6

An Efficient Full-Bridge Resonant Converter for LED Lighting Application with Simple Current Control

A new power control is introduced in full bridge dc-dc converter to drive LED lamp in this chapter. LEDs are semiconductor devices which behave like a constant voltage load with low equivalent series resistance (ESR). Hence they require precise control for current regulation. The simplified circuit of proposed configuration is shown in Figure 6.1, in which LED lamp is driven by two voltage sources V_1 and V_2. V_1 is a constant dc source which supplies majority of lamp power and V_2 is a controlled pulsed dc source which processes small power to LED lamp. Both voltages are generated through full bridge dc-dc resonant converter. Working principle, performance and prototype validation are given in this chapter.

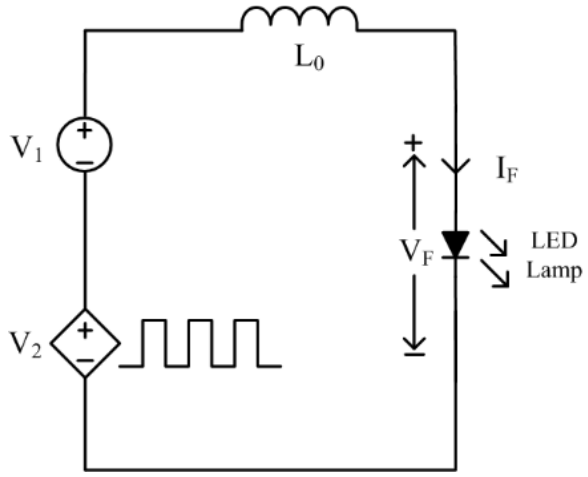

Figure 6.1 Simplified circuit of proposed configuration

6.1 Proposed Configuration

The description, principle of operation and analysis of proposed LED driver are explained in the following sections.

6.1.1 Description of proposed LED driver

Figure 6.2 shows the proposed full bridge resonant converter for LED applications. It consists of a full-bridge inverter, a diode bridge rectifier and a centre tapped rectifier. Four power MOSFETs S_1, S_2, S_3 and S_4 form full-bridge inverter. Diode bridge rectifier consists of power diodes $D_1 - D_4$. The centre tapped rectifier uses diodes D_5 and D_6. These rectifiers are

connected in parallel. A series resonant branch with L_r and C_r is connected between terminals A and B as shown in Figure 6.2. V_{01} is the output voltage of bridge rectifier and V_{02} is output voltage of centre tapped rectifier. Inductor L_r and capacitor C_r are selected to allow fundamental component of the inverter output. The current i_r is rectified to power the LED lamp. C_{01} and C_{02} are the filter capacitors. LED lamp is driven by sum of voltages V_{01} and V_{02}. V_{01} supplies majority of lamp power. For any variation in input voltage V_{dc}, centre tapped rectifier output voltage V_{02} is controlled through switch S_R. This switch is operating at high frequency. Hence small filter inductor L_0 is sufficient to reduce the ripple in LED lamp current.

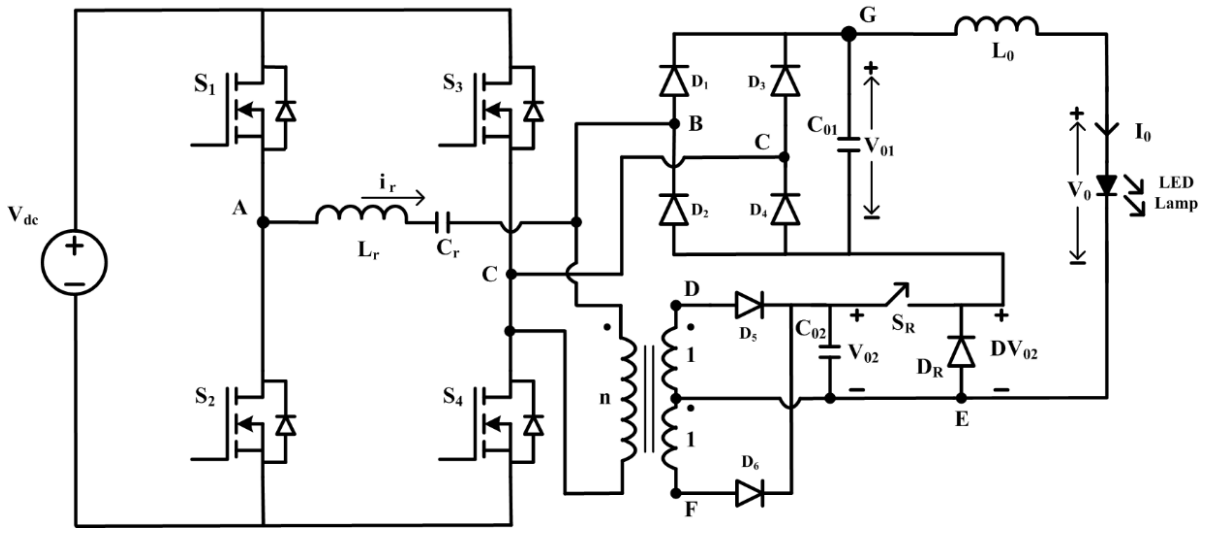

Figure 6.2 Schematic of proposed LED driver

6.1.2 Principle of Operation

The full bridge switches are operated at constant frequency with duty cycle of 50%. Suitable dead time must be introduced between the gate voltages of each leg to avoid high currents in switches. However it is not shown in the operating waveforms of the proposed LED driver shown in Figure 6.3. The switches in full bridge produce a square wave voltage v_{AC}. The concept of series resonance is utilized for powering LED lamp. Series resonant circuit is formed with L_r and C_r. It offers low impedance to fundamental component of v_{AC}. Thus an alternating current i_r is generated. And it is rectified through both bridge and centre tapped rectifier and filtered to produce voltage V_{01} and V_{02} respectively. V_{02} is controlled through switch S_R and a pulsed voltage of magnitude V_{02} is produced across diode D_R as shown in Figure 6.2. Hence sum of this pulsed voltage and V_{01} is applied to LED lamp. Inductor L_0 is used to provide continuous current through LED lamp.

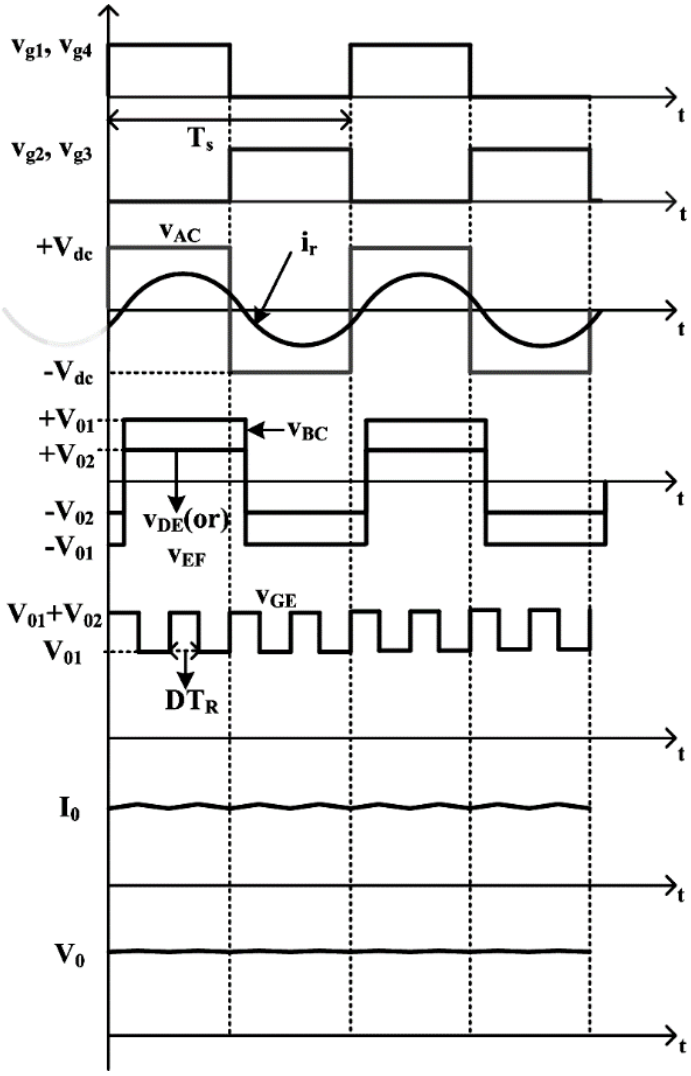

Figure 6.3 Operating waveforms of proposed LED driver

6.1.3 Analysis of Proposed LED driver

The following assumptions are made to analyze the proposed LED driver:

a) The converter is operating in steady state.
b) All power MOSFETs and diodes are ideal.
c) The voltage across LED lamp is constant.
d) The parasitic components in all passive elements are neglected.

In the proposed configuration, a square wave voltage of magnitude V_{dc} is generated through switching action. And it is applied to $L_r - C_r$ network that produces sinusoidal current component. Therefore conventional ac analysis can be used to calculate the static gain of the converter. Figure 6.4 (a) shows the ac equivalent circuit which can be used to analyse the behaviour of proposed LED driver. The series resonant circuit filters all the harmonic voltage

components except fundamental component present in the voltage v_{AC}. The ac resistance R_{ac}, which is used in ac equivalent circuit, accounts for the non-linearity present in both bridge and centre tapped rectifier. The reactance offered by L_r and C_r are denoted as X_{Lr} and X_{Cr} respectively. From the equivalent circuit shown in Figure 6.4 (a), static gain of the proposed driver is represented by using simple voltage division principle:

$$\frac{V_{BC}}{V_{AC}} = \frac{R_{ac}}{R_{ac} + j(X_{Lr} - X_{Cr})} = \frac{1}{\left[1 + j\left(\frac{X_{Lr} - X_{Cr}}{R_{ac}}\right)\right]} \tag{6.1}$$

Note that V_{AC} is the fundamental component of the square wave voltage applied to series resonant circuit and V_{BC} is the fundamental component of square wave voltage of magnitude V_{01} across R_{ac}. The ac resistance R_{ac} is calculated by using the circuit shown in Figure 6.4 (b) in which the resistance offered by LED lamp-1 is represented as R_{LED}. The R_{ac} is given by

$$R_{ac} = \frac{V_{BC}(rms)}{I_r(rms)} = \frac{4V_{01}}{\sqrt{2}\pi} \Big/ \frac{\pi I_0}{2\sqrt{2}} = \frac{8}{\pi^2}\frac{V_0}{I_0} = \frac{8}{\pi^2}R_{LED} \tag{6.2}$$

And,

$$X_{Lr} = 2\pi f_s L_r \tag{6.3}$$

$$X_{Cr} = \frac{1}{2\pi f_s C_r} \tag{6.4}$$

The sharpness in the series resonant current is measured by quality factor (Q), and it is defined by

$$Q = \frac{\omega_0 L_r}{R_{LED}} = \frac{1}{\omega_0 C_r R_{LED}} \tag{6.5}$$

where ω_0 is resonant frequency in radians per seconds and it is given by

$$\omega_0 = 2\pi f_0 = \frac{1}{\sqrt{L_r C_r}} \tag{6.6}$$

Therefore resonant frequency in hertz is represented as

$$f_0 = \frac{1}{\left[2\pi\sqrt{L_r C_r}\right]} \tag{6.7}$$

By substituting (6.2), (6.3), (6.4) and (6.5) in (6.1), the gain is finally expressed as

$$\frac{V_{BC}}{V_{AC}} = \frac{4V_{01}/\pi}{4V_{dc}/\pi} = \frac{V_{01}}{V_{dc}} = \frac{1}{\left[1 + j\frac{\pi^2}{8}Q\left(\frac{f_s}{f_0} - \frac{f_0}{f_s}\right)\right]} \tag{6.8}$$

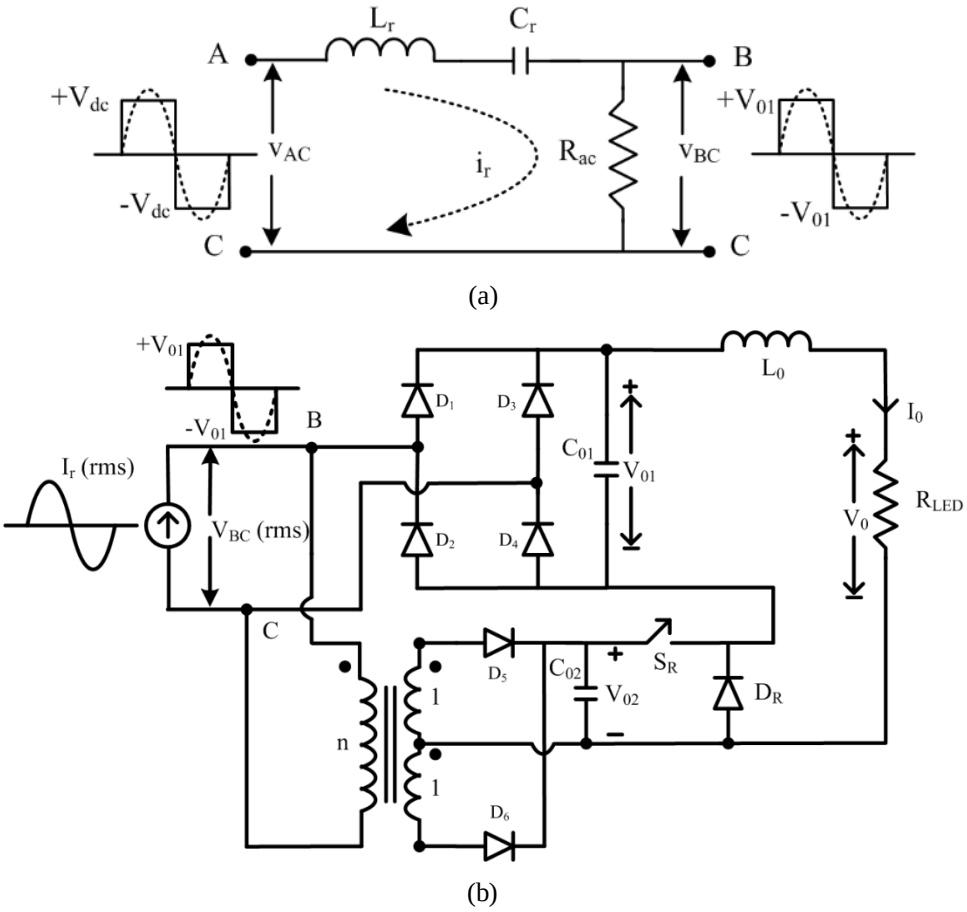

Figure 6.4 (a) AC equivalent circuit (b) Equivalent circuit for *Rac*

6.2 Regulation of LED Lamp Current and Dimming Control

To achieve constant illumination from LED lamp, its operating current and voltage must not be changed. In the proposed configuration, the variation in input voltage V_{dc} changes the operating voltage and current of the LED lamp. Consequently, lumen output from the LED lamp changes. Therefore lamp current needs to be regulated against variation in input dc voltage V_{dc}. In this converter, to regulate lamp current against input voltage variations, a stepped dc voltage of magnitude V_{02} is generated through a center tapped rectifier. And its magnitude is controlled by duty ratio (D) of switch S_R as shown in Figure 6.2. This controlled voltage is connected in series with V_{01} to supply required operating voltage and current of LED lamp.

Dimming is an important feature for present LED applications. It saves good amount of power. In the proposed study, PWM dimming is implemented for LED lamp. To realize PWM dimming in LED lamp, the input voltage to the series resonant circuit v_{AC} is made zero by dimming signal S_{dim}. Thus average illumination from LEDs is controlled without changing the

operating voltage and current. The dimming signal, voltage v_{AC}, LED lamp voltage and current are shown in Figure 6.5.

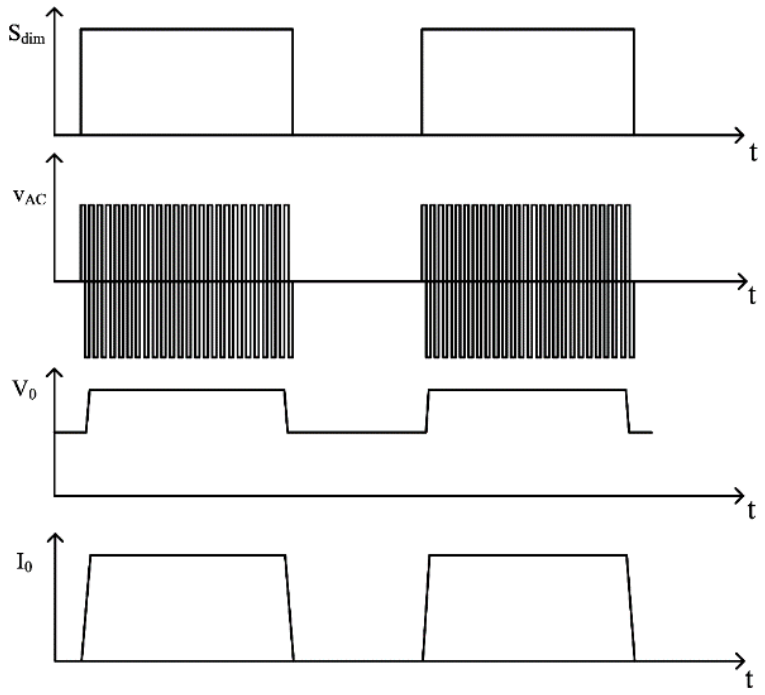

Figure 6.5 Dimming signal, input voltage to series resonant circuit and LED lamp voltage and current

6.3 Design Aspects

LED approximated model is considered to select the component values of proposed driver circuit. In LED lamp, four parallel strings are used. In each LED string, 15 LEDs are connected in series. The operating point for each LED is selected at 3.3 V, 560 mA. And the cut-in voltage of each LED is 2.32 V. Therefore operating voltage and current of LED lamp are 49.5 V and 2.24 A. Therefore power consumed by LED lamp is 110 W.

6.3.1 Calculation of series resonant circuit parameters

The product of L_r and C_r is obtained from (6.7) and it is expressed as

$$L_r C_r = \left[\frac{1}{2\pi f_0}\right]^2 \tag{6.9}$$

For zero voltage switching (ZVS), f_0 is taken 5-12% less than f_s. With switching frequency f_s of 175 kHz, f_0 is selected at 153 kHz. .After selecting f_0 as 153 kHz, (6.9) is expressed as

$$L_r C_r = 1.082 \times 10^{-12} \tag{6.10}$$

From (6.5), quality factor Q is expressed as

$$Q = \frac{1}{R_{LED}}\sqrt{\frac{L_r}{C_r}} \tag{6.11}$$

With Q = 1.43 and R_{LED} = 22.09 Ω, from (6.10) and (6.11), the inductor L_r and capacitor C_r are calculated as 33 µH and 33 nF respectively. To allow less than 1% ripple in V_{01} and V_{02}, a value of 1.36 µF is selected as C_{01} and C_{02}. And to allow ripple current less than 10% of I_0 in LED lamp, L_0 of 50 µH is selected.

6.3.2 Calculation of output voltage V_{01} and V_{02}

From (6.8), V_{01} is expressed as

$$V_{01} = \frac{V_{dc}}{\left[1 + j\frac{\pi^2}{8}Q\left(\frac{f_s}{f_0} - \frac{f_0}{f_s}\right)\right]} \tag{6.12}$$

With V_{dc} of 48V, Q of 1.43, f_s of 175 kHz and f_0 of 153 kHz, V_{01} is calculated from (6.12) as,

$$V_{01} = \frac{48}{\left[1 + j\frac{\pi^2}{8}1.43(0.269)\right]} \cong 43.5V$$

However, the selected operating voltage of LED lamp is 49.5V. Remaining 6V is supplied through centre tapped rectifier. To supply this voltage, V_{02} of 14V is generated through centre tapped transformer with turns ratio of n=3.

Table 6. 1 Parameters of the proposed LED driver

Parameter Description	Value / Model no.
DC Input voltage, V_{dc}	48±5% V
Switching frequency, f_s	175 kHz
Resonant frequency, f_0	153 kHz
Resonant inductor, L_r	33 µH
Resonant capacitor, C_r	0.033 µF
Filter capacitor C_{01} and C_{02}	1.36 µF
Filter inductor L_0	50 µH
V_0	49.5 V
I_0	2.24 A
P_0	110 W
Center tapped transformer	n=3; PQ 26/25 core
Frequency of switch S_R	400 kHz
PWM dimming frequency	100 Hz
Switching devices used	IRF 540N
Power diodes used	MUR 860
Control ICs used	UC 3875 and SG 3525
Driver ICs used	IR 2110 and MIC 4425

6.4 Simulation and Experimental Results

To validate the proposed configuration for LED applications, 110 W prototype has been implemented. The experimental prototype has been verified through the obtained results from OrCAD PSpice software. The parameters used in the proposed LED driver are shown in Table 6.1. The schematic of switch control and experimental prototype of proposed LED driver are shown in Figure 6.6 (a) and (b) respectively. LED lamp is powered with input voltage V_{dc} = 48V at full illumination. Both simulated and experimental waveforms of full bridge inverter voltage, resonant current, center-tapped transformer input and output voltages, and LED lamp voltage and current at full illumination are shown in Figure 6.7 and 6.8 respectively. It is observed that both experimental waveforms and simulated waveforms are in good agreement.

To show soft switching feature in this LED driver, experimental voltage and current for switches in one leg of full bridge are shown in Figure 6.9. They show that both turn-on and turn-off transition of switches are completed at zero voltage. Thus switching losses are

minimized. Hence high efficiency is obtained and it is found to be 93.2% at full illumination level.

In this driver, operating voltage and current of LED lamp are maintained constant against the variations in input voltage V_{dc}. And ±5% variation in V_{dc} is considered. Under +5% variation in V_{dc}, the duty ratio of switch S_R is reduced to maintain lamp current at selected value. Similarly, under -5% variation in V_{dc}, the duty ratio of switch S_R is increased to maintain lamp current constant. Simulated and experimental wave forms of voltage across series combination of inductor L_0 and LED lamp, and LED lamp current at three voltage levels at full illumination are shown in Figure 6.10 and 6.11 respectively. It is observed that LED lamp is operated at selected values at all three input voltage levels. And these variations do effect the ZVS conditions of switches in full bridge. Hence of efficiency of 92.4% and 91.8% are obtained under +5% and -5% variation in V_{dc} respectively.

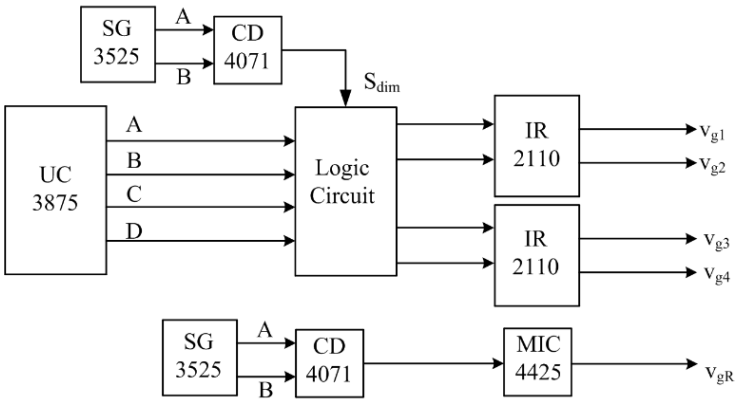

(a)

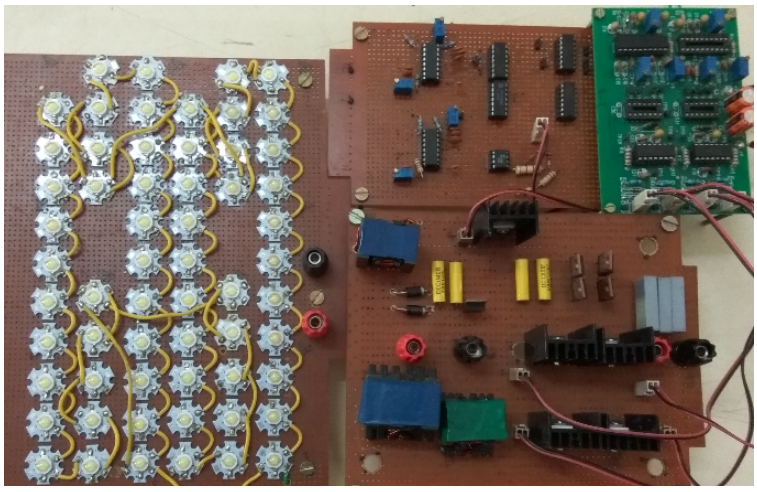

(b)

Figure 6.6 (a) Schematic of switch control (b) Experimental prototype

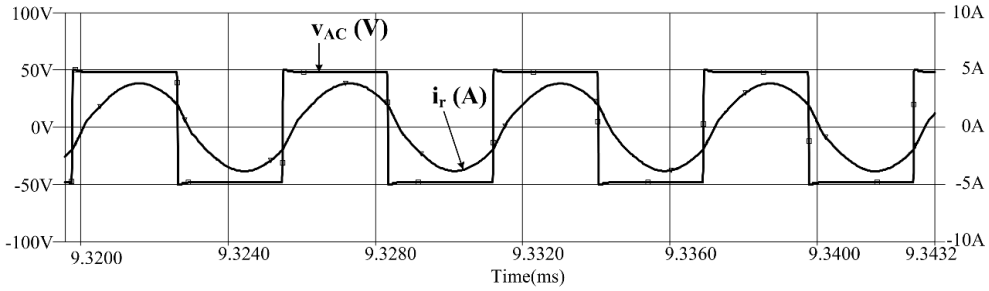

(a) Full bridge inverter voltage v_{AC} and resonant current i_r

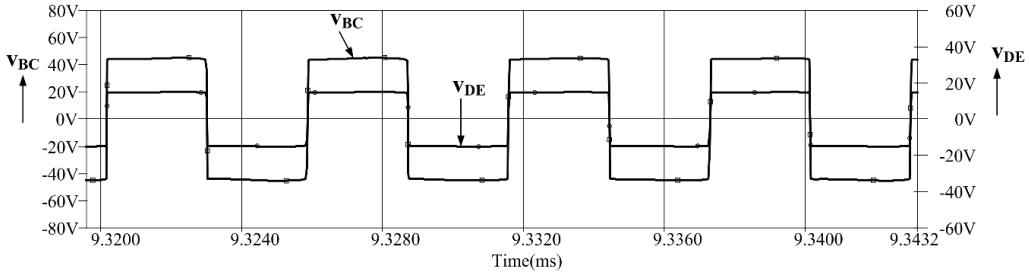

(b) Transformer primary and secondary voltages

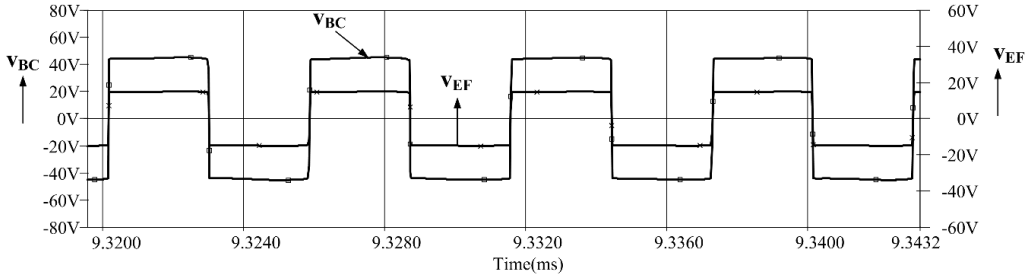

(c) Transformer primary and tertiary voltages

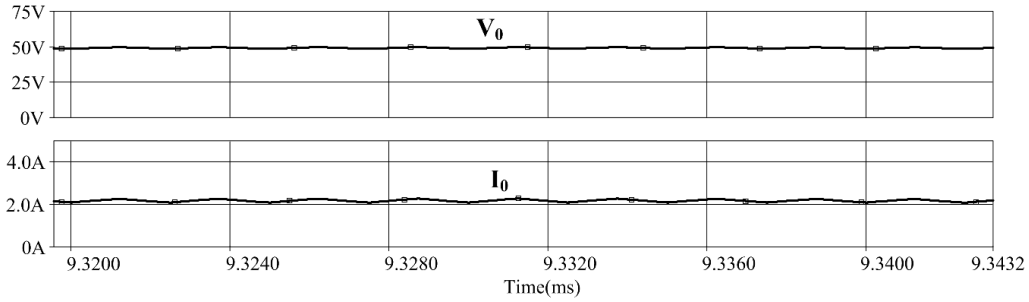

(d) LED lamp voltage and current

Figure 6.7 Simulated waveforms at full illumination

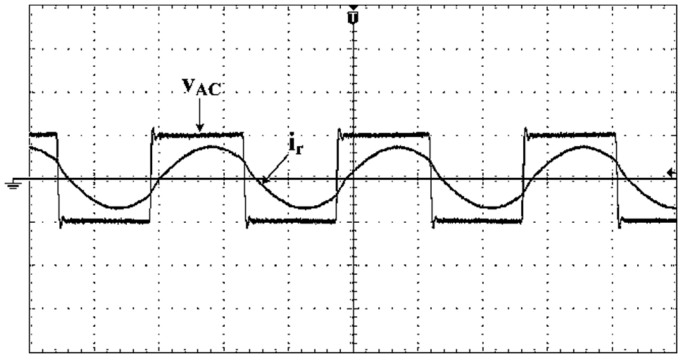

(a) Full bridge inverter voltage v_{AC} and resonant current i_r (v_{AC}: 50 V/div; i_r: 5 A/div; time: 2 μs/div)

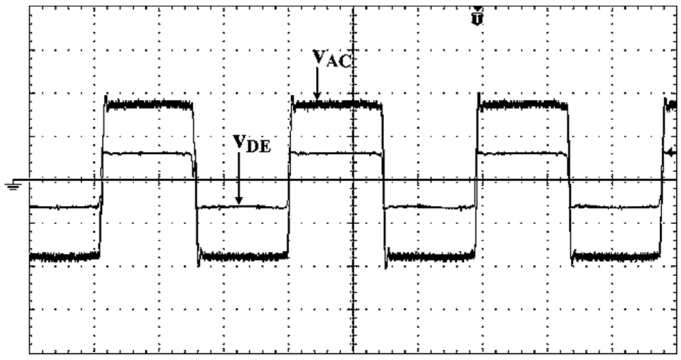

(b) Transformer primary and secondary voltages (v_{BC}: 25 V/div; v_{DE}: 25 V/div; time: 2 μs/div)

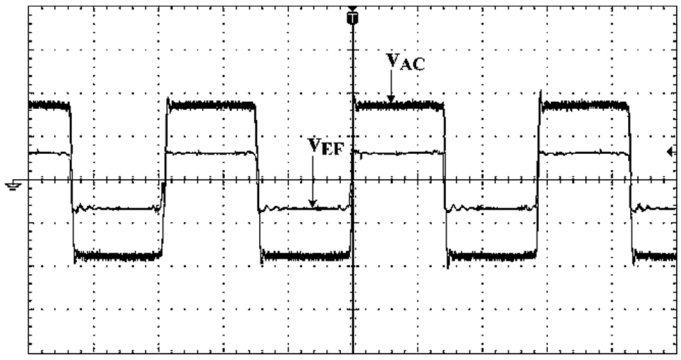

(c) Transformer primary and tertiary voltages (v_{BC}: 25 V/div; v_{EF}: 25 V/div; time: 2 μs/div)

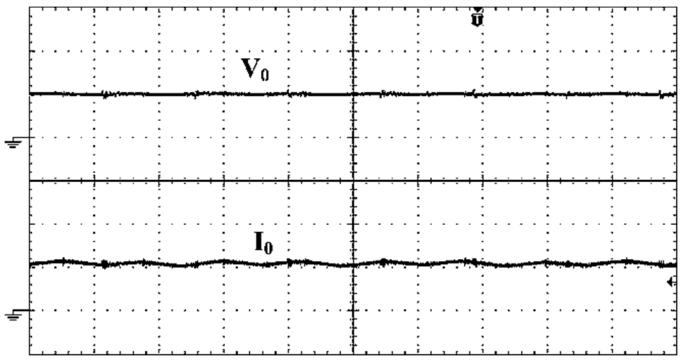

(d) LED lamp voltage and current (V_0: 50 V/div; I_0: 2 A/div; time: 2 μs/div)

Figure 6.8 Experimental waveforms at full illumination

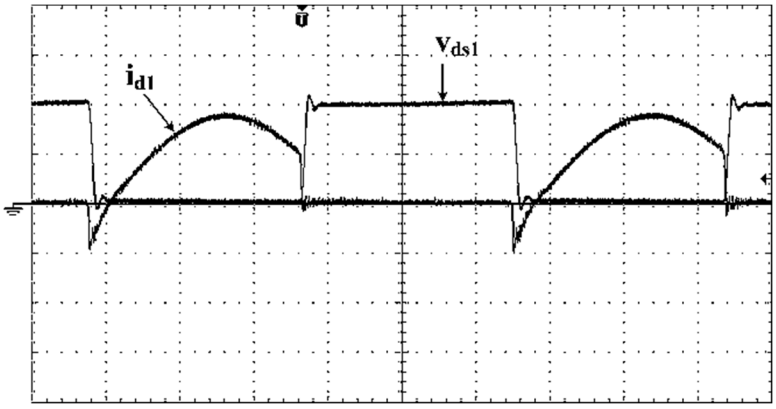

(a) Voltage and current in S_1 (v_{ds1}: 25 V/div; i_{d1}: 2 A/div; time: 1 μs/div)

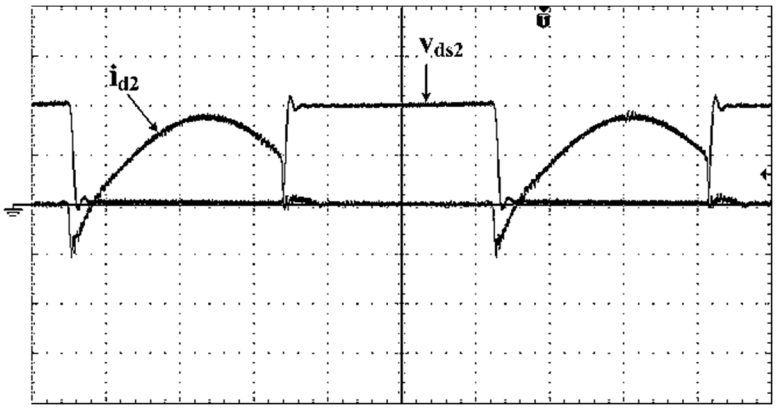

(b) Voltage and current in S_2 (v_{ds2}: 25 V/div; i_{d2}: 2 A/div; time: 1 μs/div)

Figure 6.9 Experimental waveforms of switch voltage and currents

Figure 6.12 shows the experimental dimming waveforms of proposed LED driver at various dimming levels. It is observed from Figure 6.12 (b) that series resonant circuit input voltage and current are at their rated values when dimming signal is ON and are zero when dimming signal is OFF. Similarly, LED lamp voltage and currents are at their operating values when dimming signal is ON and LED lamp current becomes zero and LED lamp voltage drops below their cut-in voltage when dimming signal is OFF. The measured efficiency curve of LED lamp under various dimming levels is shown in Figure 6.13. It is observed that high efficiency is guaranteed at any dimming level.

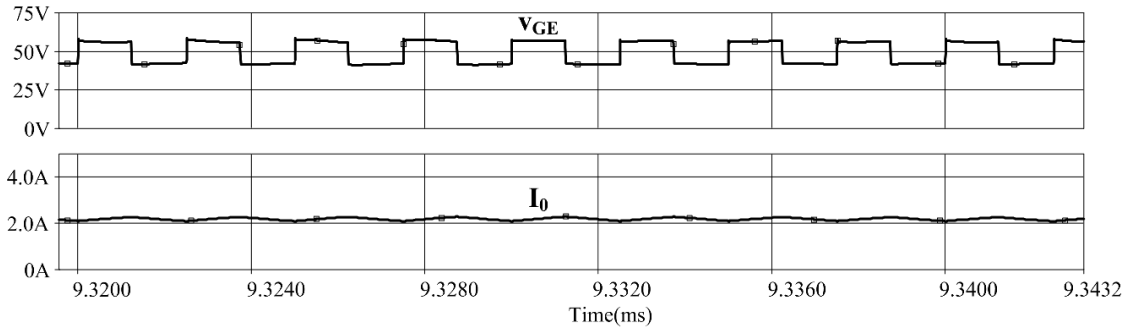

(a) At V_{dc} = 48 V

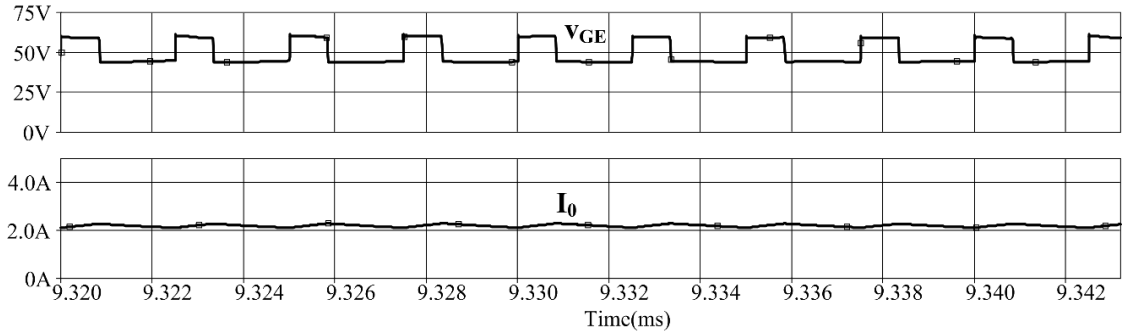

(b) At V_{dc} = (48 + 5%) V

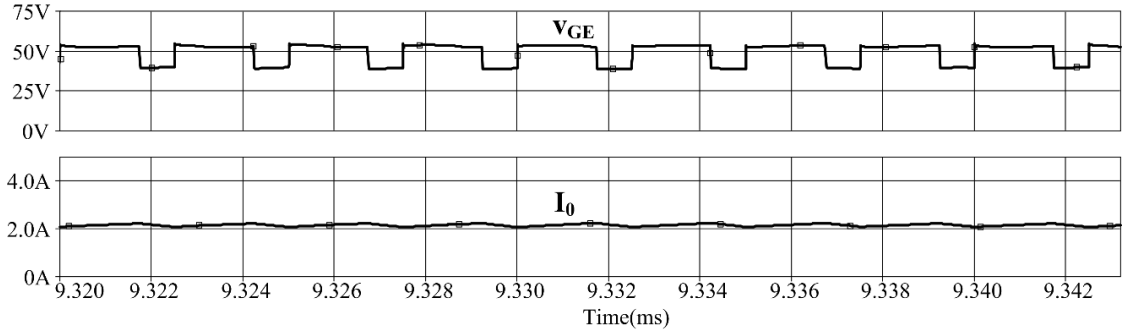

(c) At V_{dc} = (48 - 5%) V

Figure 6.10 Simulated waveforms of voltage across series connection of L_0 and LED lamp current

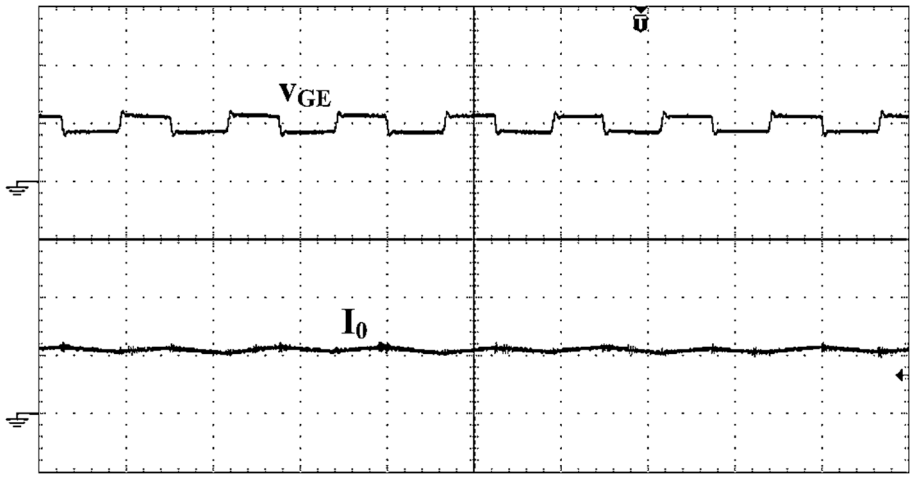

(a) At V_{dc} = 48 V (v_{GE}: 50 V/div; I_0: 2 A/div; time: 2 μs/div)

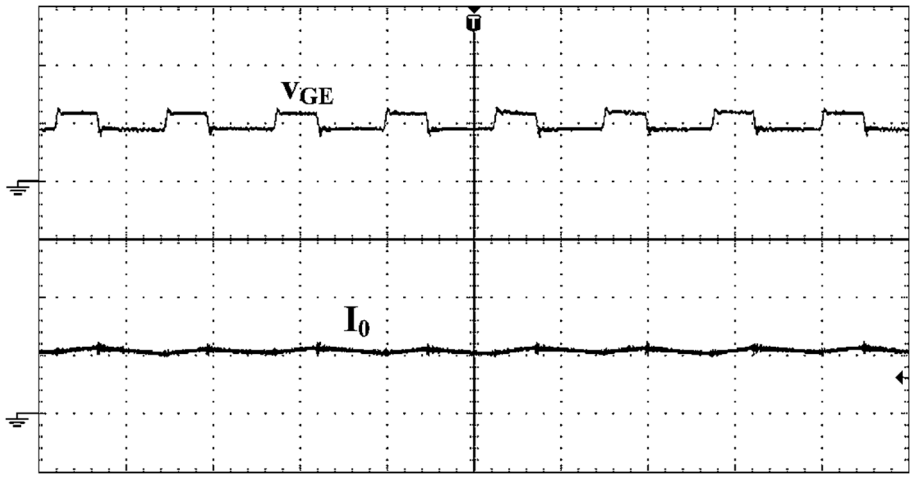

(b) At V_{dc} = (48 + 5%) V (v_{GE}: 50 V/div; I_0: 2 A/div; time: 2 μs/div)

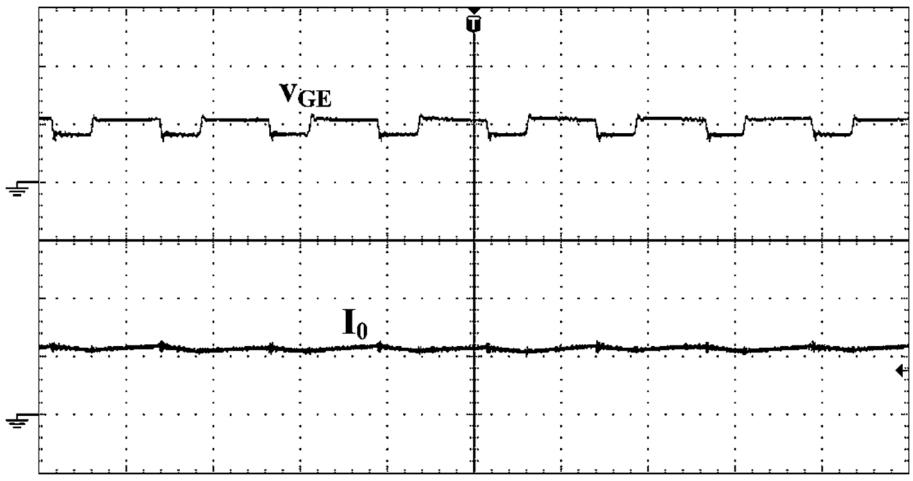

(c) At V_{dc} = (48 - 5%) V (v_{GE}: 50 V/div; I_0: 2 A/div; time: 2 μs/div)

Figure 6.11 Experimental waveforms of voltage across series connection of L_0 and LED lamp current

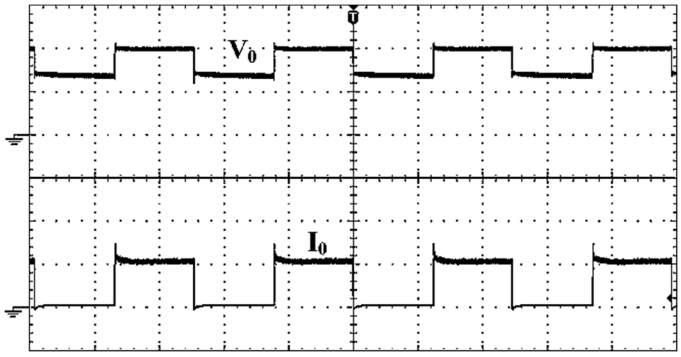

(a) Lamp voltage and current at 50% of full illumination (V_0: 25 V/div; I_0: 2 A/div; time: 4 ms/div)

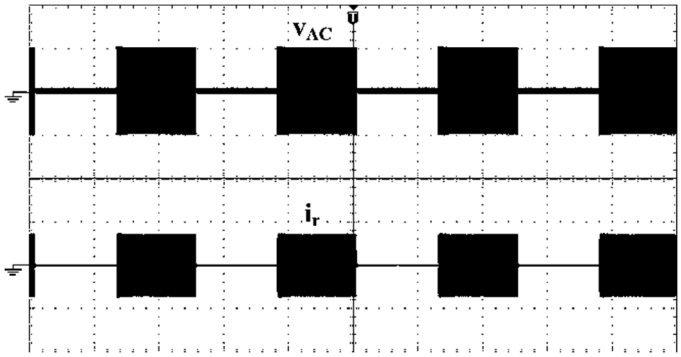

(b) Serie resonant circuit input voltage and current at 50% of full illumination (v_{AC}: 50 V/div; i_r: 5 A/div; time: 4 ms/div).

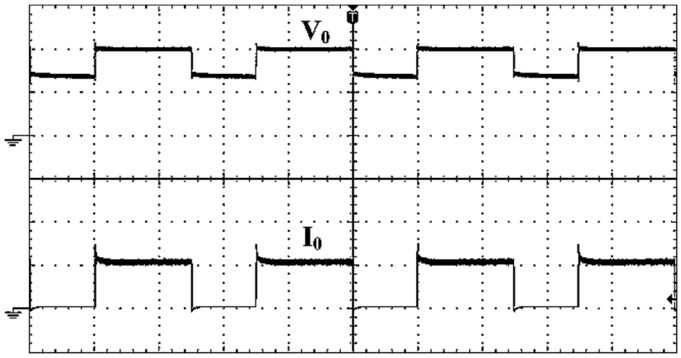

(c) Lamp voltage and current at 60% of full illumination (V_0: 25 V/div; I_0: 2 A/div; time: 4 ms/div)

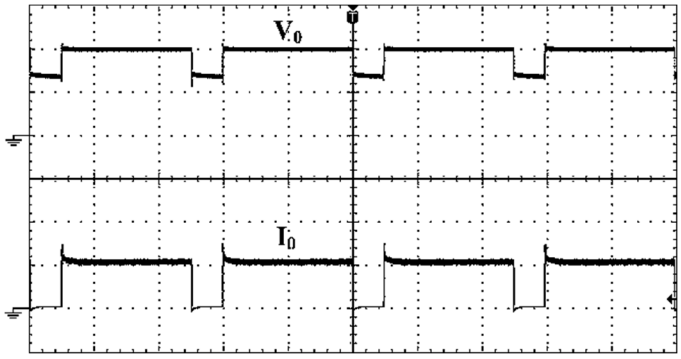

(d) Lamp voltage and current at 80% of full illumination (V_0: 25 V/div; I_0: 2 A/div; time: 4 ms/div)

Figure 6.12 Experimental dimming waveforms

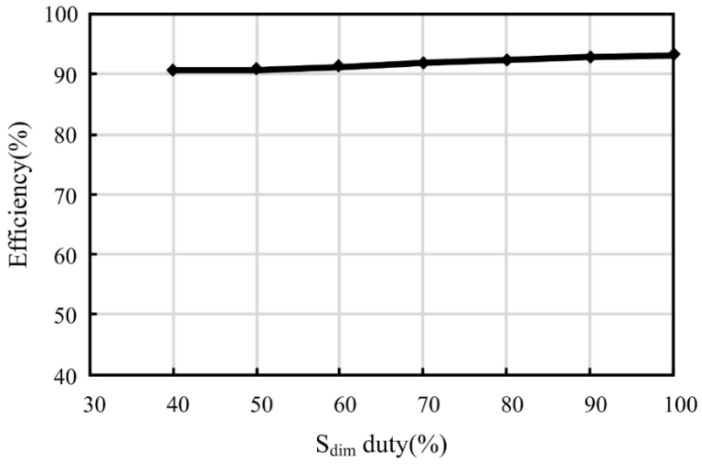

Figure 6.13 Efficiency curve of LED lamp under various dimming levels

6.5 Conclusions

In this chapter, a full bridge resonant converter with a simple current regulation has been proposed for LED applications. Series connection of two dc voltages supplies required operating voltage and current of LED lamp. And these voltages are generated by using series resonance. The proposed configuration is studied in detail for its performance. Principle of operation, analysis and design aspects are explained clearly. The dimming operation and current regulation feature are also presented. A 110 W prototype is implemented to validate the simulation results. High efficiency is achieved at both rated and different dimming conditions.

The advantages of proposed resonant converter are:

1) Constant switching frequency operation of switches in full bridge reduces electro-magnetic interference (EMI).
2) Constant duty cycle operation helps in ZVS of switches S_1 to S_4.
3) Ability to regulate the illumination level of LED lamp.
4) Dimming is implemented with simple pulse width modulation (PWM) technique.
5) Since series resonance is used for powering LED lamp, it can be designed for high power LED applications.
6) High power conversion efficiency and high frequency operation reduce the size of LED driver system.
7) This topology is suitable for applications where lamp voltages are smaller than supply voltages like dc micro grid applications.

Chapter 7

Conclusions and Scope for Future work

Chapter 7

Conclusions and Scope for Future work

7.1 Conclusions

In present lighting industry, Light Emitting Diode (LED) becomes a prominent light source for wide range of residential, industrial and commercial lighting applications. LED based lighting systems have gained remarkable attention over conventional lighting systems due to their several advantages such as energy efficient, high operating life, high brightness, environment friendly nature, and compactness. LEDs are current controlled or current driven devices. Hence LED based lighting systems require efficient constant current regulators. The essential requirements of LED driver circuits are: high efficiency, LED load current regulation, dimming control, compact size, high reliability etc.

Keeping in view the requirements of LED driver circuits, FOUR driver circuit configurations for LED based lighting applications have been proposed in this thesis. All configurations provide zero-voltage switching (ZVS), dimming control and current regulation.

In first proposed configuration, a full-bridge converter for LED based street lighting application is presented. Proposed converter operates with constant duty ratio at 200 kHz. It powers four LED lamps. This converter uses only an inductor to obtain ZVS. Moreover, the device current stress in this configuration is very low. Hence conductions losses are reduced. Regulation of LED lamp current is achieved by controlling the input voltage to the converter. A buck- boost converter at the input side compensates the variations in the input voltage. The overall power conversion efficiency is high in this configuration. Dimming for all LED lamps is attained through on-off technique at high efficiency. This configuration is suitable for high power lighting applications. It also reduces components count per lamp as well as the cost of the driver. The number of LED lamps can be increased by adding legs in the bridge. The proposed converter can be powered from battery or PV operated systems.

The second proposed configuration presents an LED driver circuit with ripple free current for high power street lighting applications. This configuration also operates with constant duty ratio at a frequency of 200 kHz. It drives two LED lamps. Majority of lamp power is supplied directly. Only small power is processed through converter. In this configuration, ripple free current flows through both LED lamps due to interleaving concept. Moreover, device current stress is low. Also, ZVS is achieved in bridge devices. Hence the proposed LED driver

features an efficiency of 94.26% at full illumination level. In this configuration also, input voltage is controlled through buck-boost converter for regulating LED lamp currents. PWM dimming is achieved for two lamps. In this converter, reduction in ripple current in LED helps in reducing the size of inductors, reducing cost, space and weight of the system. In addition, it can be extended to drive multiple LED lamps.

In third proposed configuration, a three leg resonant converter to power two LED lamps with different power ratings is presented. Proposed converter operates at two different frequencies simultaneously. Two series resonant circuits are used to generate two different frequency currents simultaneously for powering two different lamps. Both lamps are controlled against input voltage variations. Also, both LED lamps can be dimmed independently. In addition, it offers ZVS. High efficiency is achieved at any dimming level of both LED lamps. It can be powered from low voltage dc grid or battery operated systems.

The fourth proposed configuration presents a full bridge resonant converter with a simple current regulation for LED applications. In the proposed converter, LED lamp is driven by two voltage sources with different power capabilities. Both voltages are generated through full bridge dc-dc resonant converter. The advantage of this topology is that it always operates with constant duty ratio at fixed frequency which can simplify many design aspects. Moreover, LED lamp current can be regulated against the input voltage variations. This driver provides dimming control also which helps in energy savings. High efficiency is achieved at both rated and different dimming conditions. This topology is suitable for applications where lamp voltages are smaller than supply voltages like dc micro grid applications.

A relative comparison among proposed four configurations is shown table 7.1. It is observed that all the four proposed configurations offer high efficiency (>92%), less ripple in LED lamp current, soft switching operation, dimming control and good current regulation. All are suitable for high power lighting applications. In addition to the above mentioned advantages, each configuration is having its unique advantages and is suitable for particular applications.

The additional advantages of configuration-1 are low device current stress and low circuit component count per lamp. The proposed configuration-2 offers additional advantage of ripple free LED current. Both first and second configuration are suitable for street lighting as well as domestic lighting. The additional advantage of third configuration is that it can control lamps of different wattages. Hence it is much suitable for domestic and industry lighting applications. The fourth configuration is suitable for applications where lamp voltages are

smaller than the supply voltage. For instance, in dc micro grid lighting applications where the grid voltage level is 380 V. It will offer high efficiency, as majority of the output power is uncontrolled and only small controlled power is used for regulating the lamp current. All four proposed configurations can be extended to drive multiple LED lamps.

Table 7. 1 Comparison among proposed four configurations

Feature	Proposed Configuration-1	Proposed Configuration-2	Proposed Configuration-3	Proposed Configuration-4
Device current stress	**Very low**	**Very low**	Moderate	Moderate
Device voltage stress	Supply voltage	Supply voltage	Supply voltage	Supply voltage
Ripple in LED lamp	Small	**No ripple**	Small	Small
ZVS	**Yes**	**Yes**	Partial	**Yes**
Total output power	145W	87W	126W	110W
Peak efficiency	93.88%	**94.26%**	92.45%	93.2%
Circuit component count per lamp	**Low**	High	High	High
LED lamps	4	2	2	1
Wattage of all LED lamps	Same	Same	Different	Same
Rating of each lamp	36.25W	43.5W	Lamp-1=86W and lamp-2=40W	110W
Dimming	**Yes**	**Yes**	**Yes**	**Yes**
Independent dimming	No	No	**Yes**	-
Extension to multiple lamps	**Yes**	**Yes**	**Yes**	**Yes**
Current regulation	Yes	Yes	Yes	Yes
High power lighting applications	Suitable	Suitable	Suitable	Suitable

7.2 Scope for Future Work

The thesis work encourage with the scope for further research on following issues

1. The proposed configurations presented in this thesis work can be further explored and extended to other application.
2. Control techniques that suit LED based lighting applications can be further explored.
3. The proposed circuits can be investigated for solar photo voltaic (PV) fed lighting applications.
4. Development of LED drivers operated from utility supply.

References

[1] J. Zhang, L. Xu, X. Wu and Z. Qian, "A Precise Passive Current Balancing Method for Multioutput LED Drivers," *IEEE Transactions on Power Electronics*, vol. 26, no. 8, pp. 2149-2159, Aug. 2011.

[2] C. Zhao, X. Xie and S. Liu, "Multioutput LED Drivers With Precise Passive Current Balancing," *IEEE Transactions on Power Electronics*, vol. 28, no. 3, pp. 1438-1448, March 2013.

[3] C. Alessio, G. Stefano, and M. Vincenzo, "Materials to improve performance of discharge lamps," *IEEE Transactions on Power Electronics*, vol. 45, no. 5, pp. 1668–1672, Sep. / Oct. 2012.

[4] E. M. Sa Jr, C. S. Postiglione, R. S. Santiago, F. L. M. Antunes and A. J. Perin, "Self-oscillating Flyback Driver for Power LEDs", *IEEE Energy Conversion Congress and Exposition*, pp. 2827-2832, 2009.

[5] S. Li, H. Chen, S. Tan, S. Y. R. Hui and E. Waffenschmidt, "Critical design issues of retrofit light-emitting diode (LED) light bulb," *IEEE Applied Power Electronics Conference and Exposition - APEC 2014*, Fort Worth, TX, 2014, pp. 531-536.

[6] K. H. Loo, W. Lun, S. Tan, Y. M. Lai and C. K. Tse, "On Driving Techniques for LEDs: Toward a Generalized Methodology," *IEEE Transactions on Power Electronics*, vol. 24, no. 12, pp. 2967-2976, Dec. 2009.

[7] V. C. Bender, T. B. Marchesan and J. M. Alonso, "Solid-State Lighting: A Concise Review of the State of the Art on LED and OLED Modelling," *IEEE Industrial Electronics Magazine*, vol. 9, no. 2, pp. 6-16, June 2015.

[8] M. H. Crawford, "LEDs for Solid-State Lighting: Performance Challenges and Recent Advances," *IEEE Journal of Selected Topics in Quantum Electronics*, vol. 15, no. 4, pp. 1028-1040, July-Aug, 2009.

[9] S. Y. R. Hui and Y. X. Qin, "A general photo-electro-thermal theory for light emitting diode (LED) systems," *IEEE Transactions on Power Electronics*, vol. 24, no. 8, pp. 1967–1976, Aug. 2009.

[10] Vinod Kumar Khanna, "Fundamentals of Solid-State Lighting_ LEDs, OLEDs, and Their Applications in Illumination and Displays," *CRC Press*, 2014.

[11] W. Chen, S.N. Li, S.Y.R. Hui, "A comparative study on the circuit topologies for offline passive light-emitting diode drivers with long lifetime & high efficiency," *IEEE Energy Conversion Congress and Exposition*, Atlanta, GA, 2010, pp. 724-730.

[12] S. Y. Hui, Si Nan Li, Xue Hui Tao, Wu Chen, W. M. Ng, "A Novel Passive Offline LED Driver with Long Lifetime," *IEEE Transactions on Power Electronics*, vol. 25, no. 10, pp. 2665-2672, Oct. 2010.

[13] B. Lee, Hyunjae Kim, Chuntaek Rim, "Robust Passive LED Driver Compatible With Conventional Rapid-Start Ballast, "*IEEE Transactions on Power Electronics*, vol. 26, no. 12, pp. 3694-3706, Dec. 2011.

[14] J. M. Alonso, David Gacio, Antonio J. Calleja, Javier Ribas Emilio López Corominas, "A Study on LED Retrofit Solutions for Low-Voltage Halogen Cycle Lamps," *IEEE Transactions on Industry Applications*, vol. 48, no. 5, pp. 1673-1682, Sept.-Oct. 2012.

[15] J. Baek and S. Chae, "Single-Stage Buck-Derived LED Driver With Improved Efficiency and Power Factor Using Current Path Control Switches," *IEEE Transactions on Industrial Electronics*, vol. 64, no. 10, pp. 7852-7861, Oct. 2017.

[16] G. Tseng, K. Wu, H. Chiu and Y. Lo, "Single-stage high power-factor bridgeless AC-LED driver for lighting applications," *International Conference on Renewable Energy Research and Applications (ICRERA)*, Nagasaki, 2012, pp. 1-6.

[17] K. Modepalli and L. Parsa, "Lighting Up with a Dual-Purpose Driver: A Viable Option for a Light-Emitting Diode Driver for Visible Light Communication," *IEEE Industry Applications Magazine*, vol. 23, no. 2, pp. 51-61, March-April 2017.

[18] C. Cheng, C. Chang, T. Chung and F. Yang, "Design and Implementation of a Single-Stage Driver for Supplying an LED Street-Lighting Module With Power Factor Corrections," *IEEE Transactions on Power Electronics*, vol. 30, no. 2, pp. 956-966, Feb. 2015.

[19] Zhongming Ye, Fred Greenfeld and Zhixiang Liang, "Offline SEPIC converter to drive the high brightness white LED for lighting applications," *34th Annual Conference of IEEE Industrial Electronics*, Orlando, FL, 2008, pp. 1994-2000.

[20] F. Wang, L. Li, Y. Zhong and X. Shu, "Flyback-Based Three-Port Topologies for Electrolytic Capacitor-Less LED Drivers," *IEEE Transactions on Industrial Electronics*, vol. 64, no. 7, pp. 5818-5827, July 2017.

[21] A. Shrivastava, B. Singh and S. Pal, "A Novel Wall-Switched Step-Dimming Concept in LED Lighting Systems Using PFC Zeta Converter," *IEEE Transactions on Industrial Electronics*, vol. 62, no. 10, pp. 6272-6283, Oct. 2015.

[22] F. Sichirollo, J. M. Alonso and G. Spiazzi, "A Novel Double Integrated Buck Offline Power Supply for Solid-State Lighting Applications," *IEEE Transactions on Industry Applications*, vol. 51, no. 2, pp. 1268-1276, March-April 2015.

[23] D. G. Lamar, J. S. Zuniga, A. R. Alonso, M. R. Gonzalez and M. M. Hernando Alvarez, "A Very Simple Control Strategy for Power Factor Correctors Driving High-Brightness LEDs," *IEEE Transactions on Power Electronics*, vol. 24, no. 8, pp. 2032-2042, Aug. 2009.

[24] K. Zhou, Jian Guo Zhang, Subbaraya Yuvarajan, and Da Feng Weng, "Quasi-Active Power Factor Correction Circuit for HB LED Driver," *IEEE Transactions on Power Electronics*, vol. 23, no. 3, pp. 1410-1415, May 2008.

[25] G. Jane, Y. Lin, H. Chiu and Y. Lo, "Dimmable light-emitting diode driver with cascaded current regulator and voltage source," *IET Power Electronics*, vol. 8, no. 7, pp. 1305-1311, 7 2015.

[26] D. Camponogara, G. F. Ferreira, A. Campos, M. A. Dalla Costa and J. Garcia, "Offline LED Driver for Street Lighting With an Optimized Cascade Structure," *IEEE Transactions on Industry Applications*, vol. 49, no. 6, pp. 2437-2443, Nov.-Dec. 2013.

[27] F. Zhang, J. Ni and Y. Yu, "High Power Factor AC–DC LED Driver With Film Capacitors," *IEEE Transactions on Power Electronics*, vol. 28, no. 10, pp. 4831-4840, Oct. 2013.

[28] X. Qu, Siu-Chung Wong, and Chi K. Tse, "Noncascading Structure for Electronic Ballast Design for Multiple LED Lamps with Independent Brightness Control," *IEEE Transactions on Power Electronics*, vol. 25, no. 2, pp. 331-340, Feb. 2010.

[29] X. Wu, Jianyou Yang, Junming Zhang, and Zhaoming Qian, "Variable On-Time (VOT)-Controlled Critical Conduction Mode Buck PFC Converter for High-Input AC/DC HB-LED Lighting Applications," *IEEE Transactions on Power Electronics*, vol. 27, no. 11, pp. 4530-4539, Nov. 2012.

[30] U. Ramanjaneya Reddy and B. L. Narasimharaju, "Single-stage electrolytic capacitor less non-inverting buck-boost PFC based AC–DC ripple free LED driver," *IET Power Electronics*, vol. 10, no. 1, pp. 38-46, 2017.

[31] H. Kim, M. C. Choi, S. Kim and D. Jeong, "An AC–DC LED Driver With a Two-Parallel Inverted Buck Topology for Reducing the Light Flicker in Lighting Applications to Low-Risk Levels," *IEEE Transactions on Power Electronics*, vol. 32, no. 5, pp. 3879-3891, May 2017.

[32] S. Wang, X. Ruan, K. Yao, S. Tan, Y. Yang and Z. Ye, "A Flicker-Free Electrolytic Capacitor-Less AC–DC LED Driver," *IEEE Transactions on Power Electronics*, vol. 27, no. 11, pp. 4540-4548, Nov. 2012.

[33] M. Arias, D. G. Lamar, J. Sebastian, D. Balocco and A. A. Diallo, "High-Efficiency LED Driver Without Electrolytic Capacitor for Street Lighting," *IEEE Transactions on Industry Applications*, vol. 49, no. 1, pp. 127-137, Jan.-Feb. 2013.

[34] D. Camponogara, D. R. Vargas, M. A. Dalla Costa, J. M. Alonso, J. Garcia and T. Marchesan, "Capacitance Reduction With An Optimized Converter Connection Applied to LED Drivers," *IEEE Transactions on Industrial Electronics*, vol. 62, no. 1, pp. 184-192, Jan. 2015.

[35] D. G. Lamar, M. Arias, A. Rodriguez, J. Sebastian, A. Fernandez and J. A. Villarejo, "A sustained increase of input current distortion in active input current shapers to eliminate electrolytic capacitor for designing ac to dc HB-LED drivers for retrofit lamps applications," *IEEE Applied Power Electronics Conference and Exposition (APEC)*, Long Beach, CA, 2016, pp. 1823-1830.

[36] Q. Hu and R. Zane, "LED Driver Circuit with Series-Input-Connected Converter Cells Operating in Continuous Conduction Mode," *IEEE Transactions on Power Electronics*, vol. 25, no. 3, pp. 574-582, March 2010.

[37] H. van der Broeck, G. Sauerlander and M. Wendt, "Power driver topologies and control schemes for LEDs," *Twenty-Second Annual IEEE Applied Power Electronics Conference and Exposition*, Anaheim, CA, USA, 2007, pp. 1319-1325.

[38] Steve Winder, "Power Supplies for LED Driving" 2nd ed., *Newnes*, 2017.

[39] Y. Hu and M. M. Jovanovic, "LED Driver With Self-Adaptive Drive Voltage," *IEEE Transactions on Power Electronics*, vol. 23, no. 6, pp. 3116-3125, Nov. 2008.

[40] J. Garcia, A. J. Calleja, E. L. Corominas, D. G. Vaquero and L. Campa, "Interleaved Buck Converter for Fast PWM Dimming of High-Brightness LEDs," *IEEE Transactions on Power Electronics*, vol. 26, no. 9, pp. 2627-2636, Sept. 2011.

[41] W. Yu, J. Lai, H. Ma and C. Zheng, "High-Efficiency DC–DC Converter With Twin Bus for Dimmable LED Lighting," *IEEE Transactions on Power Electronics*, vol. 26, no. 8, pp. 2095-2100, Aug. 2011.

[42] A. Pollock, H. Pollock and C. Pollock, "High Efficiency LED Power Supply," *IEEE Journal of Emerging and Selected Topics in Power Electronics*, vol. 3, no. 3, pp. 617-623, Sept. 2015.

[43] K. I. Hwu and W. Z. Jiang, "Nonisolated Two-Phase Interleaved LED Driver With Capacitive Current Sharing," *IEEE Transactions on Power Electronics*, vol. 33, no. 3, pp. 2295-2306, March 2018.

[44] C. Zheng, W. Yu, J. Lai and H. Ma, "Single-switch three-level boost converter for PWM dimming LED lighting," *IEEE Energy Conversion Congress and Exposition*, Phoenix, AZ, 2011, pp. 2589-2596.

[45] P. Malcovati, M. Belloni, F. Gozzini, C. Bazzani and A. Baschirotto, "A 0.18-µm CMOS, 91%-Efficiency, 2-A Scalable Buck-Boost DC–DC Converter for LED Drivers," *IEEE Transactions on Power Electronics*, vol. 29, no. 10, pp. 5392-5398, Oct. 2014.

[46] M. Tahan and T. Hu, "Multiple String LED Driver With Flexible and High-Performance PWM Dimming Control," *IEEE Transactions on Power Electronics*, vol. 32, no. 12, pp. 9293-9306, Dec. 2017.

[47] Y. Wang, J. M. Alonso and X. Ruan, "A Review of LED Drivers and Related Technologies," *IEEE Transactions on Industrial Electronics*, vol. 64, no. 7, pp. 5754-5765, July 2017.

[48] Manuel Arias, Aitor Vazquez and Javier Sebastian (2012) "An Overview of the AC-DC and DC-DC Converters for LED Lighting Applications," *Automatika*, 53:2, 156-172, DOI: 10.7305/automatika.53-2.154.

[49] W. Thomas and J. Pforr, "Buck-boost converter topology for paralleling HB-LEDs using constant-power operation," *International Conference on Power Electronics and Drive Systems (PEDS)*, Taipei, 2009, pp. 568-573.

[50] S. Fan, S. Tseng, Y. Wu and J. Lee, "PV power system using buck/forward hybrid converters for LED Lighting," *IEEE Energy Conversion Congress and Exposition*, San Jose, CA, 2009, pp. 2584-2591.

[51] M. A. D. Costa, G. H. Costa, A. S. dos Santos, L. Schuch and J. R. Pinheiro, "A high efficiency autonomous street lighting system based on solar energy and LEDs," *Brazilian Power Electronics Conference*, Bonito-Mato Grosso do Sul, 2009, pp. 265-273.

[52] H. Wu and Y. Xing, "Families of Forward Converters Suitable for Wide Input Voltage Range Applications," *IEEE Transactions on Power Electronics*, vol. 29, no. 11, pp. 6006-6017, Nov. 2014.

[53] C. Brañas, F. J. Azcondo, R. Casanueva and F. J. Díaz, "Phase-controlled parallel-series (LCpCs) resonant converter to drive high-brightness power LEDs," *IECON 2011 - 37th Annual Conference of the IEEE Industrial Electronics Society*, Melbourne, VIC, 2011, pp. 2953-2957.

[54] E. Eloi dos Santos Filho, P. H. A. Miranda, E. M. Sa and F. L. M. Antunes, "A LED Driver With Switched Capacitor," *IEEE Transactions on Industry Applications*, vol. 50, no. 5, pp. 3046-3054, Sept.-Oct. 2014.

[55] Q. Luo, S. Zhi, C. Zou, B. Zhao and L. Zhou, "Analysis and design of a multi-channel constant current light-emitting diode driver based on high-frequency AC bus," *IET Power Electronics*, vol. 6, no. 9, pp. 1803-1811, November 2013.

[56] X. Chen, D. Huang, Q. Li and F. C. Lee, "Multichannel LED Driver With CLL Resonant Converter," *IEEE Journal of Emerging and Selected Topics in Power Electronics*, vol. 3, no. 3, pp. 589-598, Sept. 2015.

[57] U. Ramanjaneya Reddy and B. L. Narasimharaju, "A Cost-Effective Zero-Voltage Switching Dual-Output LED Driver," *IEEE Transactions on Power Electronics*, vol. 32, no. 10, pp. 7941-7953, Oct. 2017.

[58] X. Qu, S. Wong and C. K. Tse, "An Improved LCLC Current-Source-Output Multistring LED Driver With Capacitive Current Balancing," *IEEE Transactions on Power Electronics*, vol. 30, no. 10, pp. 5783-5791, Oct. 2015.

[59] J. M. Alonso, M. S. Perdigao, M. A. Dalla Costa, G. Martinez and R. Osorio, "Analysis and Experiments on a Single-Inductor Half-Bridge LED Driver With Magnetic Control," *IEEE Transactions on Power Electronics*, vol. 32, no. 12, pp. 9179-9190, Dec. 2017.

[60] J. Liu, J. Zeng, R. Hu and K. W. E. Cheng, "A Valley-Fill Driver With Current Balancing for Parallel LED Strings Used for High-Frequency AC Power Distribution of

Vehicle," *IEEE Transactions on Transportation Electrification*, vol. 3, no. 1, pp. 180-190, March 2017.

[61] J. Liu, W. Sun and J. Zeng, "Precise current sharing control for multi-channel LED driver based on switch-controlled capacitor," *IET Power Electron.*, vol. 10, no. 3, pp. 357-367, 3 10 2017.

[62] X. Chen, D. Huang, Q. Li and F. C. Lee, "Multichannel LED Driver With CLL Resonant Converter," *IEEE Journal of Emerging and Selected Topics in Power Electronics*, vol. 3, no. 3, pp. 589-598, Sept. 2015.

[63] J. W. Kim, J. P. Moon and G. W. Moon, "Duty-Ratio-Control-Aided LLC Converter for Current Balancing of Two-Channel LED Driver," *IEEE Trans. Industrial Electron.*, vol. 64, no. 2, pp. 1178-1184, Feb. 2017.

[64] W. Feng, F. C. Lee and P. Mattavelli, "Optimal Trajectory Control of LLC Resonant Converters for LED PWM Dimming," *IEEE Trans. Power Electron.*, vol. 29, no. 2, pp. 979-987, Feb. 2014.

[65] C. P. Henze, H. C. Martin, and D. W. Parsley, "Zero-voltage switching in high frequency power converters using pulse width modulation," *Proc. APEC*, pp. 33-40, Feb. 1988.

[66] Burdio JM, Canales F, Barbosa PM, Lee FC, "Comparison study of fixed-frequency control strategies for ZVS DC/DC series resonant converters," *IEEE Annual Power Electronics Specialists Conference*, 2001, pp. 427-432.

[67] W. A. Rodrigues, L. M. F. Morais, P. F. Donoso-Garcia, P. C. Cortizo, and S. I. Seleme JR, "Comparative analysis of power LEDs dimming methods," *Proc. COBEP*, pp. 378-383, Sep. 2011.

[68] E. Fred Schubert, Light-emitting diodes, 2nd ed., *Cambridge University Press*, 2006.

[69] G. Harbers, S. J. Bierhuizen and M. R. Krames, "Performance of High Power Light Emitting Diodes in Display Illumination Applications," *Journal of Display Technology*, vol. 3, no. 2, pp. 98-109, June 2007.

[70] Y. Yang, Z. Song and Y. Gao, "A White LED Driver Based on Dual Mode Switch Dimming," *Symposium on Photonics and Optoelectronics*, Wuhan, 2009, pp. 1-4.

[71] Xiaoru Xu and Xiaobo Wu, "High dimming ratio LED driver with fast transient boost converter," *IEEE Power Electronics Specialists Conference*, Rhodes, 2008, pp. 4192-4195.

[72] M. Doshi and R. Zane, "Control of Solid-State Lamps Using a Multiphase Pulsewidth Modulation Technique," *IEEE Transactions on Power Electronics*, vol. 25, no. 7, pp. 1894-1904, July 2010.

[73] I. Ashdown, "Extended parallel pulse code modulation of LEDs," *Proc. SPIE*, vol. 6337, pp. 63370W-1–63370W-10, Aug. 2006.

[74] C. Moo, Y. Chen and W. Yang, "An Efficient Driver for Dimmable LED Lighting," *IEEE Transactions on Power Electronics*, vol. 27, no. 11, pp. 4613-4618, Nov. 2012.

[75] W. Lun, K. H. Loo, S. Tan, Y. M. Lai and C. K. Tse, "Bilevel Current Driving Technique for LEDs," *IEEE Transactions on Power Electronics*, vol. 24, no. 12, pp. 2920-2932, Dec. 2009.

Publications

International Journals:

1. Kasi Ramakrishnareddy, Ch., Porpandiselvi, S., Vishwanathan, N.: "Soft Switched Full-Bridge LED Driver Configuration for Street Lighting Application" ***IET Power Electronics***, Vol. 11, No. 1, pp. 149-159, Jan. 2018. ***(Published)***

2. Kasi Ramakrishnareddy, Ch., Porpandiselvi, S., Vishwanathan, N.: "An Efficient Ripple Free LED Driver with Zero-Voltage Switching for Street Lighting Applications" ***European Power Electronics and Drives (Accepted for Publication).***

3. Kasi Ramakrishnareddy, Ch., Porpandiselvi, S., Vishwanathan, N., " A Three-leg Resonant Converter for Two Output LED Lighting Application with Independent Control" ***International Journal of Circuit Theory and Applications (Accepted for Publication).***

4. Kasi Ramakrishnareddy, Ch.; Porpandiselvi, S.; Vishwanathan, N.; " An Efficient Full-Bridge Resonant Converter for LED Lighting Application with Simple Current Control" ***IET Power Electronics (Communicated).***

Patent Filed:

1. Vishwanathan, N., Porpandiselvi, S., Ramakrishnareddy, K.: "Full-Bridge Soft Switched Driver for LED Based Street Lighting Application" ***Indian Patent Application, 201641038698 A***, 2016.